Institut for Bærende Konstruktioner og Materialer
Department of Structural Engineering and Materials
Danmarks Tekniske Universitet • Technical University of Denmark

BKM

New Production Processes, Materials and Calculation Techniques for Fiber Reinforced Concrete Pipes

Carsten Pedersen

Serie R No 14 1996

New Production Processes, Materials and Calculation Techniques

for

Fiber Reinforced Concrete Pipes

Carsten Pedersen

VTB - beton a/s
Eurotest aps
Department of Structural Engineering and Materials (BKM), Technical University of Denmark
and the Institute for Product Development (IPU)

Industrial Research Project, EF 481, supported by grants from the Danish Academy of Technical Sciences(ATV)

July 1996

New Production Processes, Materials and Calculation Techniques for Fiber Reinforced Concrete Pipes

Tryk:
LTT
Danmarks Tekniske Universitet
Lyngby
ISBN 87-7740-192-1
ISSN 1396-2167
Bogbinder:
H. Meyer, Bygning 101, DTU

PREFACE AND ACKNOWLEDGEMENTS

The work presented in this thesis has been carried out at VTB - beton a/s, Eurotest aps and at the Department of Structural Engineering and Material (BKM), Technical University of Denmark. The Institute for Product Development (IPU) has participated in the project as third party.
The thesis consists of a summary and five papers which can be read independently. Therefore some repetition may occur.

The project has been carried out as an Industrial Research Study, Ph.D, supported by grants from the Danish Academy of Technical Sciences (ATV).

The project was started on June 1, 1993 and ended on June 30, 1996.

The work was carried out under supervision of a group consisting of:

- Andreasen, J.P. (VTB)
- Byskov, E. (BKM)
- Gregersen, J.C. (IPU)
- Rasmussen, P. (Eurotest)
- Stang, H. (BKM)

E. Byskov was member of this group until April 20, 1995 when H. Stang took over his role as adviser, representing BKM.

From the beginning of the project and until October 3, 1995

- Krenchel, H. (BKM)
- Nielsen, A. (VTB)

participated in the project meetings.

Special thanks is given to H. Fredslund-Hansen for useful advice and for presentation of his idea for the project.
Besides the former mentioned, many people have contributed with help, advice and support during the project. I wish to express my thanks to all persons involved.

I thank my family and friends for their patience and support.

July 1996

Carsten Pedersen

CONTENTS

ABSTRACT

This project is a combination of developmental, experimental and modelling work and forms the basis for design and production of thin-walled, fiber reinforced concrete (FRC) pipes. The project incorporates material development, process techniques and structural design.

The project presents calculation methods relating to FRC pipes subjected to line load and earth pressure. The models take the stress-crack width relationship of the material into account. Very good agreement was observed with experimental data for unreinforced as well as for fiber reinforced pipes.

A technique for the extrusion of FRC profiles has been developed. During the process the material is dewatered. This has many obvious advantages. In the presence of excess water the material can be mixed. The degree of fiber reinforcement can be increased and the porosity of the hardened material can be reduced. Two experiments simulating the extrusion process have been developed. These experiments are useful for the composition of mixtures. Guidelines as to how the results of these experiments can form the basis for preparation of a full-scale extrusion are presented. An analytical model describing the experiments has been presented.

In this project the technique is applied in the manufacture of pipes with an inner diameter of 100 mm and a wall thickness of 10 mm. Degrees of reinforcement of between 1.5 vol.% and 5 vol.% of polypropylene fibers were achieved. The mechanical properties of the extruded pipes were tested. The experiments suggest that the mechanical properties are improved by this process compared with similar poured materials.

RESUME

Med en kombination af udviklings-, eksperimentelt- og modelleringsmæssigt arbejde er der i dette projekt skabt grundlag for design og produktion af tyndvæggede fiberarmerede beton(FRC) rør. Projektet kombinerer materialeudvikling, procesteknik og konstruktionsdesign.

Der er i projektet opstillet beregningsmodeller for FRC rør påvirket med linielast og jordtryk. Modellerne tager materialets spændings-revnevidderelation i regning. Meget god overensstemmelse med eksperimentelle data er observeret for både uarmerede og fiberarmerede rør.

Der er udviklet en proces til ekstrudering af FRC profiler. Ved processen afvandes materialet. Dette har en række åbenlyse fordele. Materialet kan blandes under vandoverskud. Fiberarmeringsgraden kan forøges og porøsiteten kan mindskes i det hærdede materiale. Der er udviklet to forsøg der modellerer ekstruderingsprocessen. Disse forsøg er anvendelige ved udvikling af recepter. Der gives retningslinier for, hvorledes disse forsøgsresultater finder anvendelse som forberedelse til fuld skala ekstrudering. En analytisk model til beskrivelse af forsøgene er opstillet.

Processen er i dette projekt anvendt til at producere rør med indvendig diameter 100 mm og vægtykkelse 10 mm. Armeringsgrader mellem 1.5 vol. % og 5 vol. % polypropylenfibre er opnået. De ekstruderede rør er testet for deres mekaniske egenskaber. Disse forsøg antyder, at der opnås forbedrede mekaniske egenskaber ved anvendelse af processen sammenlignet med tilsvarende blødstøbte materialer.

1. GENERAL INTRODUCTION

Our sewerage system is of vital importance to modern society. It improves standards of hygiene and eliminates the occurrence and spreading of disease. Without adequate drainage systems the considerable present-day manufacturing industry would be the cause of unpredictable environmental repercussions. Drainage systems are therefore of crucial importance to the wealth and welfare of modern society.

The sewerage system in Denmark is 55000 kilometres long and its value is estimated at 200 billion DKK. For many years a thorough renovation of the sewerage system has been discussed. This would amount to 35 billion DKK. See Pedersen[1]. A major part of the large pipes in the sewerage system are of unreinforced concrete or conventionally reinforced concrete.

At present manufacturers of concrete pipes are experiencing intensified competition from the plastics industry. Only a few years ago concrete pipes controlled the market, but today they have to compete with plastic pipes of increasingly large dimensions.

Main advantages of plastic pipes compared with concrete pipes:

- Significantly smaller dimensions making them lighter and more manageable at places of work, easier to transport and smaller machines.

- Smoother and stronger inner and outer surfaces.

- Greater flexibility, which results in less strain on underground pipes.

Main advantages of concrete pipes compared with plastic pipes:

- Concrete is considerably more environmentally friendly seen from a pollution and a resource point of view, especially when looking at the total life cycle of the pipes. See e.g. [2].

- Concrete is significantly less expensive and is manufactured almost exclusively from local raw materials.

In spite of the advantages of concrete pipes it is becoming increasingly difficult to compete with plastic pipes and the concrete industry is faced with a declining market share, a share being taken by the plastics industry. Within a few years' time it is very likely that a large part of the concrete pipe business will be forced to close down if new and improved products are not developed. Seen from an economic and an environmental viewpoint it is most regrettable to see the concrete industry losing market share.

The expected future investments urgently call for more future-orientated product development if the concrete pipe business is to keep abreast of competition from the plastic pipe business. In view of this, on June 1, 1993 VTB-beton a/s embarked upon a 3-year industrial research project in cooperation with the Department of Structural Engineering and Materials(BMK), former Department of Structural Engineering (ABK), the Technical University of Denmark (DTU) and the Institute for Product Development (IPU). The project has been supported by grants from the Academy of Technical Sciences (ATV). The main objective of the industrial research project has been to form the basis for determining dimensions and for manufacturing a completely new concrete pipe. The aim has been to manufacture a significantly thinner-walled fiber reinforced concrete (FRC) pipe, a much lighter and more flexible pipe. The flexible pipe reduces the earth pressure, which calculation-wise puts it between the traditional concrete pipe and the plastic pipe. The project focuses on:

- a calculation model for FRC pipes
- the development of a process technique
- the composition of pipe mixtures

All of these main studies are interdependent. Development of the process equipment presupposes knowledge of pipe dimensioning and of the composition and properties of the fresh material. A reliable pipe dimensioning depends on the knowledge of the mechanical properties of the hardened material which are influenced by the processing technique. The mechanical properties are determined by the composition of the fresh material and the process technique applied.

1.1 PIPE CALCULATION

Determination of the load-bearing capacity of unreinforced concrete pipes in soil is usually based on a calculation of the ultimate load on the basis of the concretes tensile strength in bending. By means of experiments the tensile strength in bending is monitored when the pipes are loaded until they break. The Danish code presupposes that the tensile strength in bending is a function of the pipes thickness and diameter. This is in accordance with practical experiences and with theoretical research carried out in Sweden in the eighties.

Based on the Swedish research this study contains calculation models for FRC pipes subjected to earth pressure and line load. The method is in accordance with the Danish code relating to unreinforced concrete pipes. The calculation model is described in chapter 2 of the Summary.

1.2 PROCESS TECHNIQUE AND PIPE MATERIAL

In Denmark unreinforced concrete pipes and conventional, reinforced concrete pipes are mostly manufactured by means of the so-called vibro-press process. By means of this process the pipes are cast vertically and the mould is removed immediately after casting. The finished pipe is stored vertically at the place of storage. Thygesen[3] demonstrated that with this

process it was possible to introduce up to 2.0 vol.% hooked end steel fibers (30 mm long and 0.5 mm in diameter). The pipes were 600 mm long with an inner diameter of 300 mm and a wall thickness of 40 mm.

Out of regard for the stability and the filling of the mould a thickness of less than 20-25 mm with the vibro-press process cannot be achieved.

The symmetrical shape of the pipes leads one to believe that it would be natural to apply a continuous process such as extrusion. When this project was initially embarked upon we tried to modify the well-known process for the extrusion of concrete floors. Various experiments took place with different mixtures in pipe moulds vibrated at high frequencies. However, we did not succeed in manufacturing stable thin-walled pipe profiles.

Later it was the aim to dewater the fresh concrete in order to achieve stable pipes. A number of minor experiments demonstrating the principle were carried out and they suggested that good mechanical properties were achievable. An extruder capable of extruding pipes with an inner diameter of 40 mm and a thickness of 5 mm was then constructed. The problem here was to overcome the friction blocking the conveyance of the consolidated specimen. This problem was solved by means of a moveable core. A patent has been applied for in respect of this process invention. During the course of the project pipes have been manufactured by means of this process with an inner diameter of 100 mm and a thickness of 10 mm.

In the development of pipe materials the following conditions must be taken into consideration:

- requirements to the material in regard to the manufacturing process
- material properties in the hardened stage

Full-scale experiments entail numerous man-hours and vast resources. For the project we therefore developed a model that tests the properties of the mixtures in relation to the process and the mechanical properties of the hardened material.

The manufacturing principle and the experiments are described in chapter 3 of the Summary.

2. CALCULATION OF FRC PIPES

It has been found that the mechanical behaviour of concrete pipes depends on the tensile load capacity across the cracks, the so-called stress-crack width relationship (e.g. Hansen and Thygesen[4]). Therefore, the stress-crack width relationship is of fundamental importance in terms of concrete pipes. In the present study, the empirical stress-crack width relationship proposed by Stang and Aarre[5], which fits a wide range of FRC materials very well, has been adopted for the description of fracture in FRC pipes. Other stress-crack width relationships can easily be implemented into the proposed structural models. This stress-crack width relationship

is used to obtain the generalized moment/axial force-rotation relationship to be implemented into the models for pipe calculations.

2.1 THE MOMENT-ROTATION RELATIONSHIP

The model for the generalized moment/axial force-rotation model is described in [6]:

> The Moment-Rotation Relationship with Implementation of Stress-Crack Width Relationship

The fibre reinforced concrete is assumed to be linear elastic in tension up to the ultimate tensile strength. When the tensile strength is reached, it is assumed that a single crack appears, whereas the rest of the cross section still behaves elastically. The model incorporates a layer - a crack band - which absorbs all deformation located in the crack zone. A similar assumption was made by Ulfkjær, Krenk and Brincker[7], who worked with a model for prediction of the behavior in bending of conventional unreinforced concrete beams.

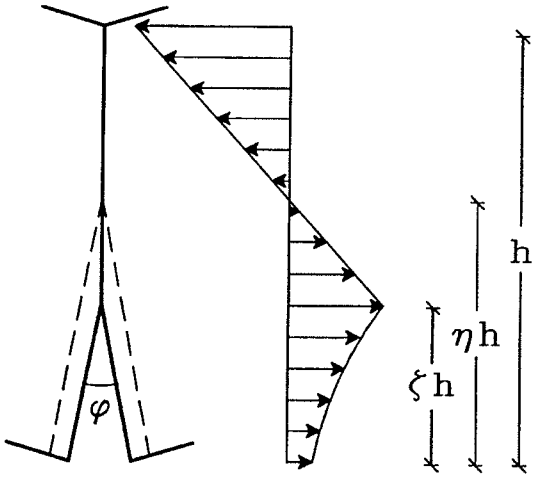

Figure 1. Distribution of normal stresses in the crack band section

Fig. 1 describes the distribution of stresses in a cross-section with depth h, φ being the rigid-body rotation. The resulting force of the fracture zone is determined by numerical integration of the stress-crack width relationship. Given φ and the axial force N, the position of the neutral axis can be determined through the equilibrium of forces at the cracked section. Hence the cross-sectional moment M relative to the center line is fully determined by φ and N:

$$M = M(\varphi, N) \tag{1}$$

2.2 CALCULATION OF FRC PIPES SUBJECTED TO LINE LOAD

The model for calculation of FRC pipes subjected to line load is described in the paper, [8]:

Calculation of FRC Pipes based on the Fictitious Crack Model

The models for pipe calculation presented are based on the assumption that a single crack appears when the tensile strength is reached, whereas the rest of the pipe still behaves elastically. Therefore, four single cracks are assumed to develop and a quarter of the cross section is modelled as a curved beam and two moment springs. The behavior of the springs is determined by equation (1). See Fig. 2.

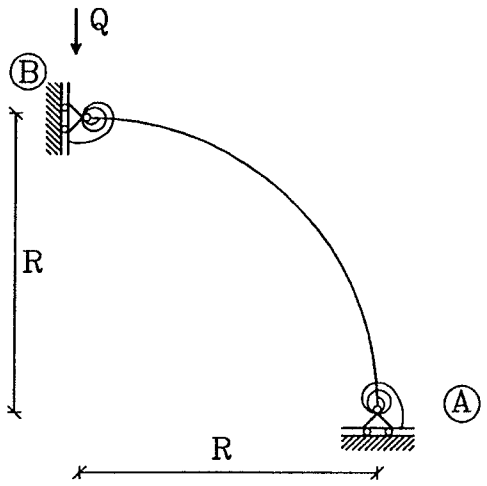

Figure 2. A quarter of the cross-section modelled as a curved beam

The deflection of points A and B is calculated as a sum of two terms: the deflection due to the elastic deformation of the pipe and the deflection due to the rigid-body rotation of the cracked pipe. See [8] for the set of equations. The idea of modelling the failure of concrete pipes by the formation of fictitious cracks was introduced by Gustafsson[9].

The results of the model calculation are corresponding values of load, crack mouth openings and deflections.

Results of the model have been compared with experimental results described by Thygesen[3], who investigated one pipe geometry (length = 600 mm, radius = 170 mm and wall-thickness = 40 mm) and five normal-strength concrete recipes: a plain concrete called 'PC OA00' and four FRCs called 'FRC OA05', 'FRC OA10', 'FRC OA15' and 'FRC OA20' with 0 vol.%, 0.5 vol.%, 1.0 vol.%, 1.5 vol.% and 2.0 vol.% of straight steel fibers respectively. Typical

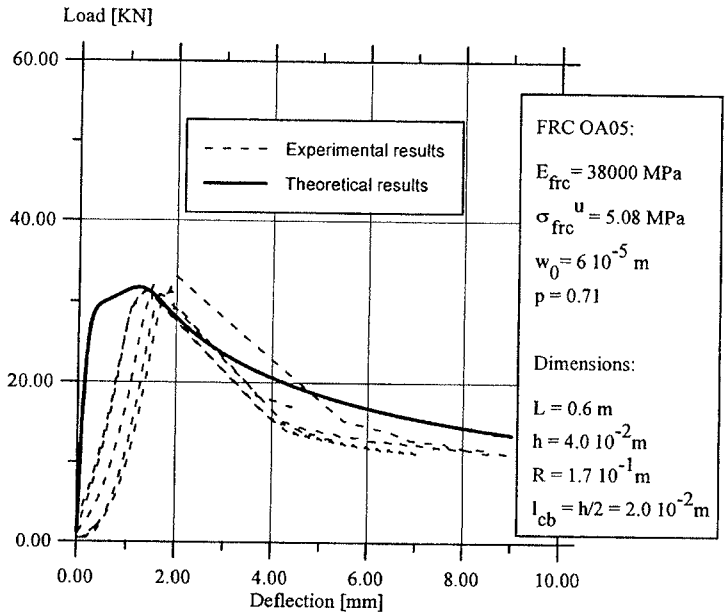

Figure 3. Load-deflection curves for pipes with 0.5 vol.% of steel fibers

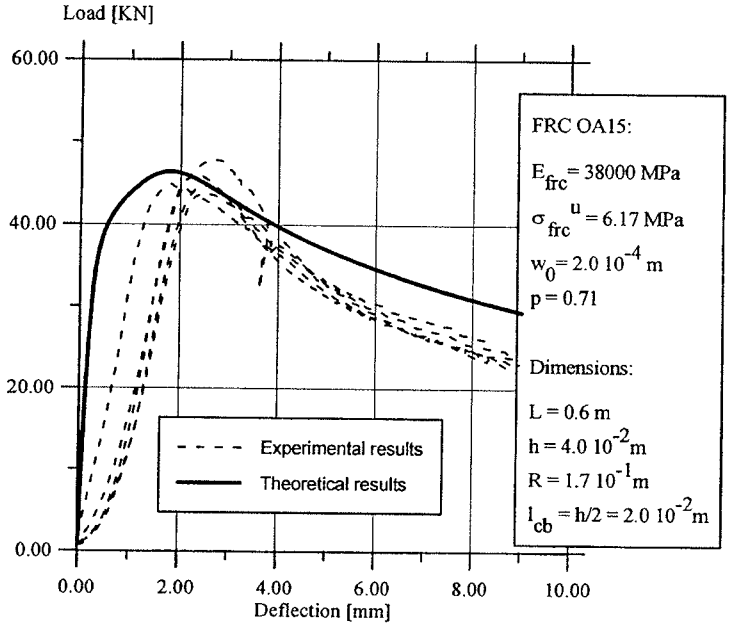

Figure 4. Load-deflection curves for pipes with 2.0 vol.% of steel fibers

examples of load-deflection curves for pipes reinforced with 0.5 vol.% and 2.0 vol.% are shown in Figs. 3 and 4 respectively. The stress-crack width relationship is characterized by the maximum stress σ^u_{frc}, the characteristic crack opening w_0 and the shape factor p. See [5]. The model prediction is shown with a fat line.

Furthermore, the results of the analytical model have been compared with the results of a large experimental study of unreinforced concrete pipes carried out at Eurotest aps. A normal-strength concrete recipe has been tested. All pipes were circular. The pipes were subjected to line load and the ultimate loads were measured. Details of each group of pipes are listed in Table 1, where d_i is the inside diameter, L is the length of the tested pipe section and h is the wall thickness.

d_i [mm]	L [mm]	h [mm]	Exp. results [KN]	Average of	Model prediction [KN]	Differences between experimental results and model prediction [%]
150	1330	40.5	98.4	6 tests	109.5	+11.3
200	1330	44.1	95.0	4 tests	95.7	+0.7
250	1330	49.1	88.7	6 tests	92.3	+4.1
250	1330	77.0	211.9	2 tests	203.4	-4.0
300	2105	57.6	175.4	16 tests	161.1	-8.2
300	2105	97.7	335.6	2 tests	406.6	+21.2
400	2355	75.2	245.2	30 tests	215.8	-12.0
400	2355	117.1	517.3	4 tests	471.1	-8.9
500	2355	92.9	267.2	16 tests	252.6	-5.5
500	2355	144.0	529.1	6 tests	542.0	+2.4
500	2355	83.1	217.4	12 tests	208.1	-4.3

Table 1. Comparison between experimental results and model prediction of the ultimate loads on unreinforced pipes (E_{frc} = 38 GPa, σ^u_{frc} = 4.81 MPa, $w_0 = 2\ 10^{-5}$ m and p = 0.71)

2.3 CALCULATION OF FRC PIPES SUBJECTED TO SOIL PRESSURE

A model for prediction of the mechanical behavior of plain concrete pipes and fiber reinforced concrete pipes subjected to soil pressure has been presented. The model is similar to the model described in section 2.2 - four single cracks are assumed to develop and a quarter of the pipe cross section is modelled as a curved beam and two moment springs. See Fig. 5. The

behaviour of the springs is determined by equation (1). The vertical soil pressure and the horizontal soil pressure, q and K_0q respectively, are uniformly distributed over the pipe diameter 2R.

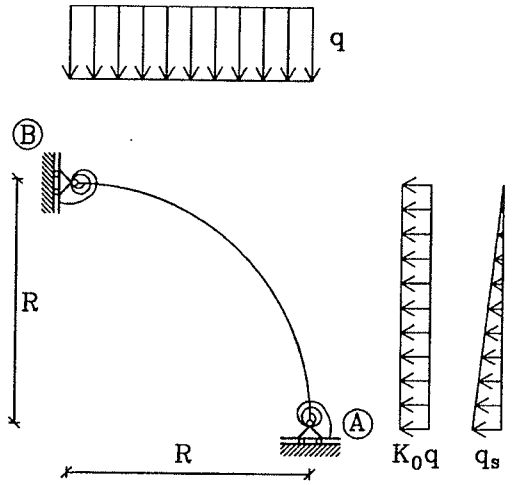

Figure 5. A quarter of the cross-section modelled as a curved beam

The ratio K_0 is known as the at-rest earth pressure coefficient. q_s is the soil reaction at point A due to the deflection of the pipe wall. The horizontal earth pressure caused by the reaction of the soil is assumed to be triangularly distributed and is determined on the basis of the deflection at point A and from the properties of the side fill.

The model for calculation of FRC pipes subjected to soil pressure is described in [10]:

FRC Pipes subjected to Earth Pressure, Design and Calculation.

The results of the analytical model have been compared with the results of the ultimate soil pressure, which are in accordance with the Danish Code of Practice for the Laying of Underground Rigid Pipelines of Concrete[11] for unreinforced concrete pipes with an inside diameters of 100, 300, 600 and 1000 mm. Examples of the results of the model are shown in Fig. 6 along with the maximum allowable vertical pressure from the Danish code (illustrated by straight lines). The internal diameter is 600 mm corresponding to the typical value of 84 mm wall thickness. Three load configurations are analysed: vertical soil pressure only, at-rest earth pressure only and at-rest earth pressure in combination with passive soil resistance.
The paper gives an example of how the model can be used in the design of pipes with an inside diameter of 200 mm. Fig. 7 shows the maximum allowable vertical pressure as a function of wall thickness for the different degrees of fiber reinforcement. For pipes with an

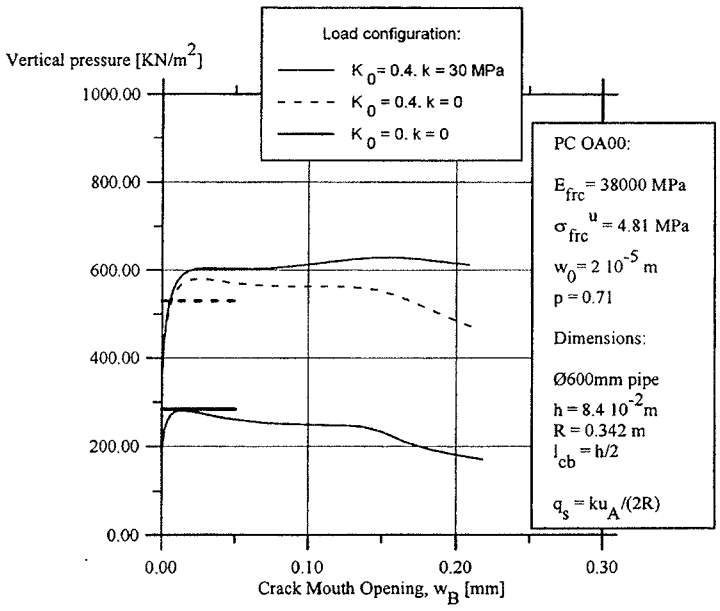

Figure 6. Comparison between the model and the Danish code

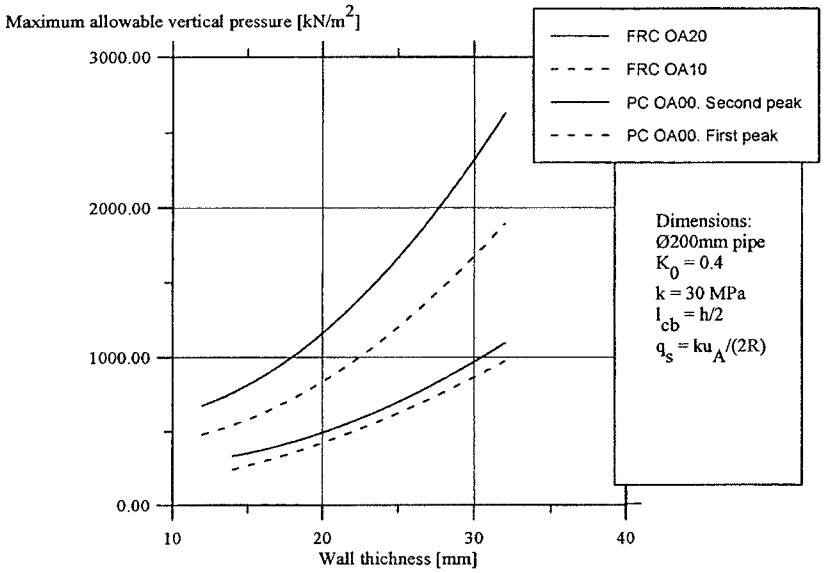

Figure 7. Maximum allowable pressure as a funktion of wall thickness

inside diameter of 200 mm a reduction to approximately 75% and 55% of the wall thickness can be obtained by a reinforcement of 1 vol.% and 2 vol.% of steel fibers, respectively.

3. FRC PIPES, PRODUCTION AND MATERIALS

During the course of this project a new technique for extrusion of FRC profiles has been developed. This technique is similar to the traditional extrusion technique but eliminates the problems related to the limitation in the design of mixtures for traditional extrusion. The production technique and the test results are described in [12]:

Extruded Fiber Reinforced Pipes

In the traditional extrusion technique it is necessary to use extra additions of water in the fresh mixture in order to achieve optimum material properties after extrusion - even higher additions of water than prescribed with regard to the requirement of stability of the extrudates, see e.g. Shao, Marikunte and Shah[13]. Furthermore the mechanical properties of the extruded material decline with increasing porosity, so it is preferred that the material has a low content of water - and hereby a low porosity.

The presented technique solves these problems. It is based on two simple principles:

- dewatering, to build up the fresh material into a stable mass with the required profile. Dewatering results in decreasing porosity and increasing degree of fiber reinforcement
- a simple mechanical operation to move the specimen forwards

The principle of the extrusion technique is illustrated in Fig. 8. Confinement pressure is applied to the material by the piston. In the draining section the core and the extruder pipe have pores, so that surplus liquid can pass through and be led away. The confinement pressure causes dewatering of the fresh material in the zone close to the draining section where the pipe of stable FRC material constitutes a filter which permits only water to pass. The length of the stable FRC pipe is increased as the water is squeezed out. To move the stable FRC pipe forwards the core is moved backwards and immediately after this forwards. When the core is moved backwards, the production pressure of the fresh material on the cross section of the stable FRC pipe combined with the frictional resistance between the FRC pipe and the extruder pipe, exceeds the frictional resistance between the FRC pipe and the core. Therefore the pipe of consolidated material will not be moved backwards with the core. When the core is moved forwards, the production pressure of the fresh material on the cross section of the FRC pipe combined with the frictional resistance between the FRC pipe and the core, exceeds the frictional resistance between the FRC pipe and the extruder pipe. Therefore the pipe of consolidated material will be moved forwards with the core. Hence this simple mechanical operation will cause the pipe of consolidated material to move one stroke length forwards. In that way more fresh material will be pressed forwards to the zone near the draining section.

The production pressure causes dewatering of this material as described above. By moving the core one stroke at adequate intervals a pipe of stable material will exit the section in front of the draining section.

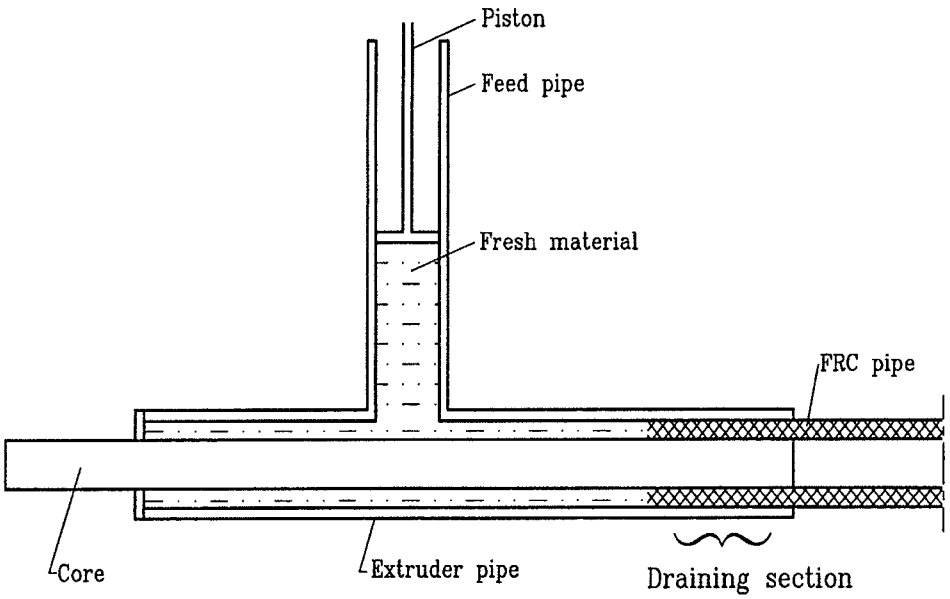

Figure 8. Plan for the extrusion principle developed in this study

By applying the production pressure and moving the core one stroke at adequate intervals the semi-continuous production process has been initiated. Guidelines for the design of the frictional section of the extruder are given in [12].

The present technique has been applied in the manufacture of FRC pipes with an inner and outer diameter of 100 mm and 120 mm respectively. A detailed description of the prototype extruder and the successful and unsuccessful extrusion tests performed is given in [12]. More than twenty recipes have been tested by use of the extruder, and almost ten recipes have been extruded successfully. A production pressure between 3.5 MPa and 15 MPa was used and output rates between 4 and 70 mm per minutes were obtained although no optimization of the output rate was achieved.

The extruded pipes were cut into 30 mm long test specimens. The specimens were subjected to line load at a cross-head speed of 0.1 mm/sec and corresponding values of line load and vertical and horizontal deflections were registered until a total vertical deflection of 8 mm was

reached. The deflections were measured on the interior of the specimens, using special fittings and two transducers. The fittings were attached directly to the inside of the specimens. The complete testing arrangement is shown in Fig. 9.

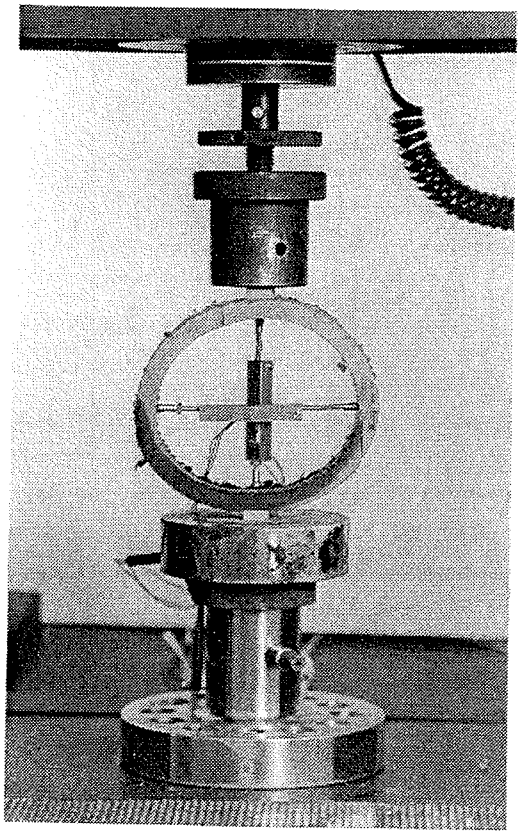

Figure 9. Testing arrangement

Examples of experimentally determined load-deflection curves for cement paste containing 0.5 vol.% of 3 mm polypropylene Crack-Stop fibers (diameter: 0.018 mm) combined with 2.0 vol.% of 3 mm polypropylene Krenit fibers (diameter: 0.100 mm) are shown in Fig. 10. This reinforcement of the fresh material results in approx. 0.75 vol.% of Crack-Stop fibers combined with approx. 3.0 vol.% of Krenit fibers in the extruded material. Fig. 10 also shows the theoretical load-deflection curves predicted for poured specimens with the same type and degree of fiber reinforcement as the extrudates (i.e. 0.75 vol.% of Crack-Stop fibers combined with 3.0 vol.% of Krenit fibers). The prediction of the load-deflection curves for the poured specimens is based on the model presented in section 2.2. Furthermore, Fig. 10 shows the predicted load-deflection curves, assuming improved bonding (x3) between fiber and matrix. The test results indicate that the stress-crack width relationship of the extruded material is improved compared to the stress-crack width relationship of similar traditionally

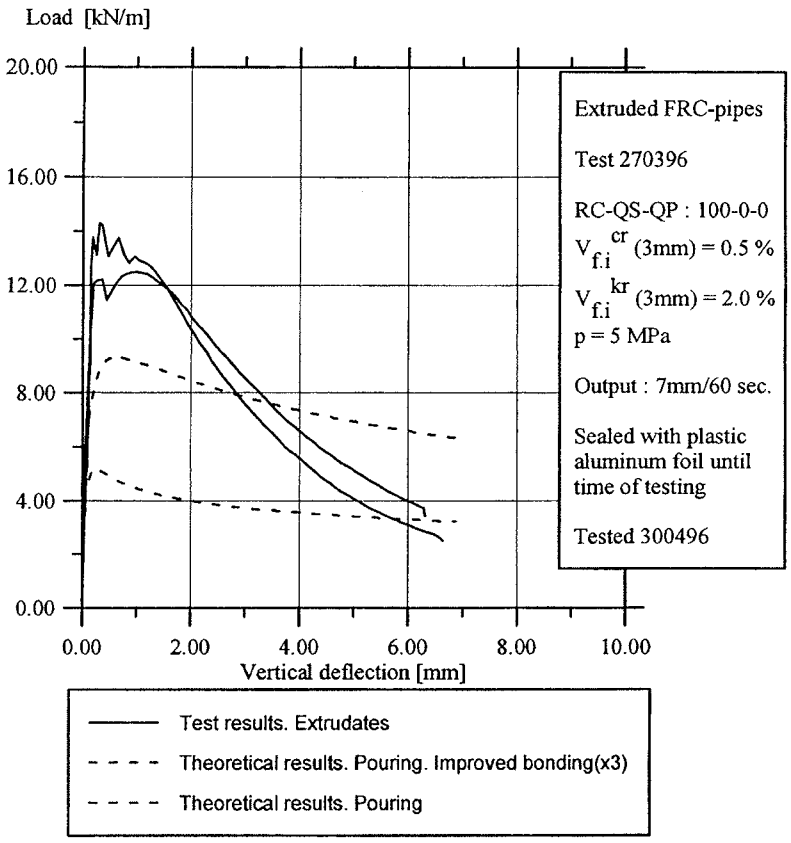

Figure 10. Load-deflection curves. Extruded FRC pipes.

cast materials. The improvement is interpreted as a positive effect of the extrusion process on the fiber-matrix bonding parametres.

Using a full-scale prototype extruder to test the extrudability of a new mixture and to measure the parameters of the process (e.g. the production pressure and the output rate) and the characteristics of the hardened specimens is expensive in terms of man-hours and raw materials. Furthermore full-scale tests require manual handling of heavy components. Therefore a simple consolidation test to predict the process parameters, the mechanical behaviour of the extruded material and the extrudability of a new mixture has been developed. The test set up to model the extrusion process is illustrated in Fig. 11. In this test, the slurry was poured into a special cylindrical mould, which consisted of a perforated pipe (inside diameter: 25 mm, length: 200 mm) and a piston (outside diameter: 25 mm) with a length of 200 mm. When the slurry had been poured into the perforated pipe, the piston were pushed into the

pipe. Then the mould containing the slurry was weighed in order to determine the exact quantity of slurry. The mould was then placed in a testing machine where pressure was put on the piston so that the material could consolidate and the water could slowly drain out.

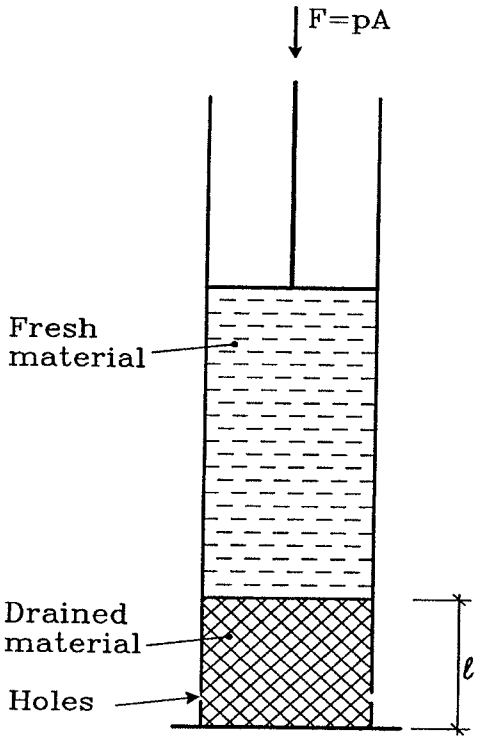

Figure 11. Model for describtion of the dewatering process

Corresponding values of time, confinement pressure and settlement of the piston were measured. Finally, the solid specimen was pressed out and examined (measured and weighed). By testing the solid specimens in three-point bending the mechanical behavior of a given recipe can be determined. The dimensions of the specimens are similar to those of the specimens used by Krenchel[14], who worked with a microfiller material, and by Dela and Stang[15], who worked with fracture energy of cement paste cylinders. More than 90 specimens have been tested in this way.

The test and the results obtained are described in [16]:

New Production Technique and Recipes For FRC Materials

Furthermore an analytical model describing the dewatering process, based on Darcy's law, is presented in [16].

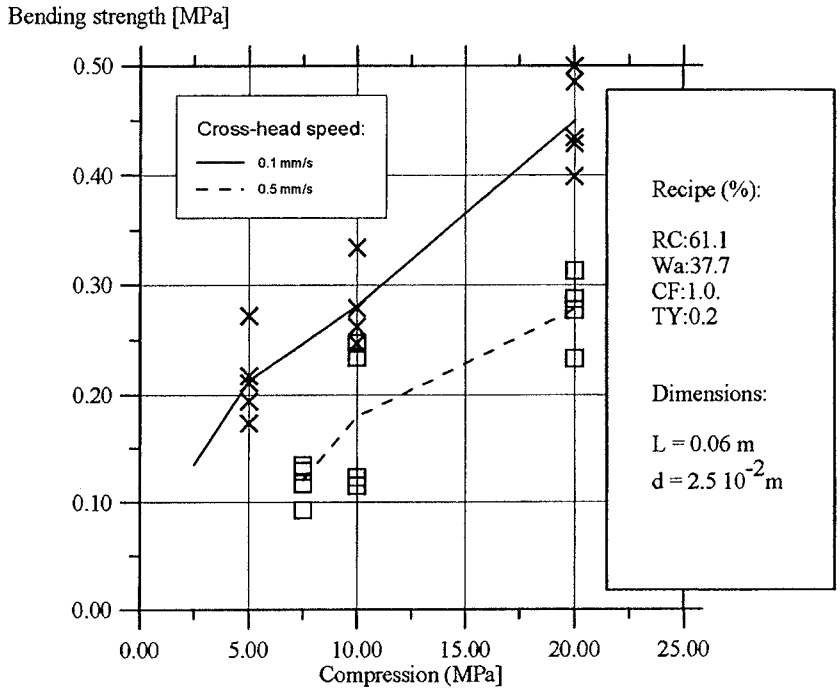

Figure 12. Bending strength approx. 90 min. after consolidation as a function of the final confinement pressure and cross-head speed

Fig. 12 shows an example of how the stability of the material (expressed by the bending strength approx. 90 min. after consolidation) is influenced by the cross-head speed and the final confinement pressure for a cement paste reinforced with 1.85 vol.% of 3 mm Crack-Stop fibers. Results from [16]. The confinement pressure was increased to 2.5, 5, 10 and 20 MPa at a cross-head speed of 0.1 mm/s. In this case 2.5 MPa was the minimum final confinement pressure at which stability of the specimens could be obtained. Furthermore the confinement pressure was increased to 7.5, 10 and 20 MPa respectively at a cross-head speed of 0.5 mm/s. In this case 7.5 MPa was the minimum final confinement pressure at which stability of the specimens could be obtained.

It is observed that the bending strength approx. 90 min. after consolidation increases as a function of the final confinement pressure and decreases as a function of the cross-head speed.

4. CONCLUSION

4.1 PIPE CALCULATION

During the coarse of this project a model based on the fictitious crack model for the moment/axial force-rotation relationship has been developed. The model is described by a set of simple equations which facilitate the study of complicated problems with a limited amount of data processing.
It has been shown how the relationship can be used on a structural level to describe the mechanical behaviour of pipes with no other reinforcement than fibers. Independently of pipe geometry and fibre volume concentration, very good agreement has been observed between the model prediction and the experimental data for pipes subjected to line load. However, the moment-rotation model can be used to describe the flexural behaviour and the formation of cracks in any structures.

It has been shown how the M-φ relationship can be used to describe the behaviour of FRC pipes subjected to soil pressure. The at-rest earth pressure and the reaction of the soil are taken into account. For the ultimate load on unreinforced concrete pipes good agreement has been observed between the model prediction and results which are in accordance with the Danish Code independently of pipe diameter.
It has been shown how the model can be used for material and structural optimization. The model indicates that for pipes with an inside diameter of 200 mm a reduction to approximately 75% and 55% of the wall thickness can be obtained by a reinforcement of 1 vol.% and 2 vol.% of steel fibers respectively (conventional pipe concrete).

Much more experimental work is needed in order to determine how the presented model is suited to describing the influence of the passive soil resistance that supports the pipe.

4.2 FRC PIPES, PRODUCTION AND MATERIALS

A new extrusion process has been presented. Powder material and fibers are mixed with an adequate amount of water. As an effect of the dewatering caused by application of pressure, the material builds up into a stable mass with the required profile. Therefore the process eliminates the problems related to the limitation in the design of mixtures for traditional extrusion. The test results indicate that the mechanical properties of the extrudates are improved by application of the process.
More work is needed in order to analyse how this separation effect is influenced by the mixture and by the design of the extruder.

The highest output rate observed in this study was 4 meters/hour. In industrial application of the extrusion process higher output rates can be obtained through integrated optimization of material and extruder.

A test set up to model the extrusion process and to predict the output rate of the process has been presented. However, much more work is needed in order to model how the production process is influenced by the composition of the material and by the parameters of the dewatering process.

5. FUTURE DEVELOPMENTS

All the necessary conditions for manufacture of an optimum fiber reinforced pipe are provided in this project. A complete set of models for:

- design
- manufacture of FRC pipes
- material composition

has been presented.

Extensive experimental research substantiating the calculation model for FRC pipes effected by earth pressure is, however, necessary. Only then will it be possible to evaluate whether or not the economical savings, as a result of the reduced wall thickness, will result in competitive FRC pipes and a subsequent product launch.

Extensive experimental work is called for in order to clarify how the output rate can be increased and how the inconvenient dewatering within the machine can be eliminated. The solution to these problems lies in the fundamental understanding of the process. The key to the optimum material composition and the extrusion design is an understanding of the fundamental conditions of the process.

However, the many new ingenious elements of the developed process make it feasible for the process to be applied in practise, if not for the manufacture of pipes, then for some other item.

6. REFERENCES

1. Pedersen, E.J. Fiber Reinforced Concrete Pipes. UNICON beton I/S. December 1992. In Danish.

2. Danish Concrete. February 1996, pp 10-13. In Danish.

3. Thygesen, E. Design of FRC Materials in Structures. Ph.D. thesis, Department of Structural Engineering, Technical University of Denmark, 1993. In Danish.

4. Hansen, S., and Thygesen, E. Fibre Reinforced Concrete Pipes. Report, Department of Structural Engineering, Technical University of Denmark, 1990. In Danish.

5. Stang, H., and Aarre, T. Evaluation of Crack Width in FRC with Conventional Reinforcement. 'Cem. Concr. Comp.', 14, 143-154, (1992).

6. Pedersen, C. The Moment-Rotation Relationship with implementation of Stress-Crack Width Relationships. Department of Structural Engineering, Technical University of Denmark, 1995.

7. Ulfkjær, J.P., Krenk, S., and Brincker, R. Analytical Model for Fictitious Crack Propagation in Concrete Beams. Journal of Engineering Mechanics, Vol. 121, No.1, January, 1995.

8. Pedersen, C. Calculation of FRC Pipes based on the Fictitious Crack Model. Department of Structural Engineering, Technical University of Denmark, 1995.

9. Gustafsson, P. J. Oarmerade Betonrörs Böjbrottlast och Ringbrottlast. Teoretiska beräkningsmetoder. Report TVBM-3012, Division of Building Materials, Univ. of Lund, Sweden. 1983. In Swedish.

10. Pedersen, C. FRC Pipes subjected to Earth Pressure, Design and Calculation. Department of Structural Engineering, Technical University of Denmark, 1995.

11. Dansk Ingeniørforening's Code of Practice for the Laying of Underground Rigid Pipelines of Concrete, etc, DS 437, Second Edition. Teknisk Forlag. 1986. In Danish.

12. Pedersen, C. Extruded Fiber Reinforced Pipes. Department of Structural Engineering, Technical University of Denmark, 1996.

13. Shao, Y., Marikunte, S., and Shah, S.P. Extruded Fiber Reinforced Composites. Concrete International, April 1995.

14. Krenchel, H. Microfiller Material for HPFRCC. Department of Structural Engineering, Technical University of Denmark, 1995.

15. Dela, B. F., and Stang, H. Determination of Fracture Energy of Cement Paste Cylinders in Three-Point Bending. Department of Structural Engineering, Technical University of Denmark, 1995.

16. Pedersen, C. New Production Technique and Recipes for FRC Materials. Department of Structural Engineering, Technical University of Denmark, 1996.

7. NOTATION

The following symbols are used in this summary

d_i	inside diameter
E_{frc}	Young's modulus of the FRC material
h	wall thickness
k	modulus of consolidation
K_0	at-rest earth pressure coefficient
l_{cb}	width of the crack band
L	length of pipe section
M	externally applied moment
N	axial force
p	shape factor
P	production pressure
q	vertical soil pressure
q_s	pressure at side of pipe caused by the change in horizontal diameter
Q	load on a quarter of the cross section of a pipe modelled as a curved beam
R	radius
u_A	deflection at point A
w_0	characteristic crack mouth opening
ζh	crack length
ηh	depth of the tensile zone
σ^u_{frc}	ultimate tensile strength of the FRC material
φ	rigid-body rotation

BKM REPORT NO. I3

THE MOMENT-ROTATION RELATIONSHIP WITH IMPLEMENTATION OF STRESS-CRACK WIDTH RELATIONSHIPS

By Carsten Pedersen[1]

ABSTRACT

A semi-analytical model for the flexural behavior of cement-based materials, based on the equilibrium of forces at a cracked section, is presented. The proposed model adopts the stress-crack width relationship to obtain the generalized moment/axial force-rotation relationship. The paper describes how the model can be used to obtain the load-displacement curves of concrete beams. A reasonable agreement has been observed between the model prediction and experimental data of both fibre reinforced concrete (FRC) beams and plain concrete beams subjected to three-point bending. Furthermore, results of the analytical model are shown to be in agreement with the numerical results of a model using finite element methods (FEM).

INTRODUCTION

The present paper deals with the flexural behavior of unreinforced cement-based materials and fiber composites. The flexural behavior is of vital importance for many practical applications such as pipes, slabs, roofing tiles and roadways.

It is necessary to apply nonlinear fracture mechanics for the description of fracture in unreinforced and reinforced concrete structures. Various models based on nonlinear fracture mechanics describe the softening behavior of unreinforced and reinforced concrete, e.g. the fictitious crack model (FCM) by Hillerborg, Modéer and Petersson(1), the crack band theory by Bazant and Oh(2), and the two parameter fracture model by Jenq and Shah(3). Describing concrete fracture by using fit for the softening curve of concrete has been carried out e.g. Stang and Aarre(4) and of Guinea, Planas and Elices(5). Micro-mechanical models have been developed by e.g. Li, Stang and Krenchel(6). In the present paper the model proposed by Stang and Aarre(4) will be adopted for prediction of the behavior in bending of structural members with no other reinforcement than fibers. Since a numerical integration scheme is implemented, other stress-crack width relationships can easily be implemented into the proposed structural model.

Few researchers have considered analytical methods based on the fictitious crack model for determination of the flexural behavior of concrete structures. Hillerborg et al.(1) combined the

---

[1] Industrial Ph.D. student, VTB-beton a/s, Dandyvej 11, DK-7100 Vejle, Denmark

FCM with finite element analysis for determination of the ultimate moment capacity of concrete beams subjected to pure bending. Chuang and Mai(7) proposed a model based on the crack band model. Ulfkjær, Brincker and Krenk(8) derived an analytical model for pure bending of concrete beams by assuming development of a fictitious crack in an elastic layer with a thickness proportional to the beam depth. A linear tension softening relation was assumed and no axial load was considered. Maalej and Li(9) developed an analytic model for the flexural strength of fiber reinforced cementitious composite beams subjected to pure bending. Here the authors adopted the analytic softening relations presented by Maalej, Li and Hashida(10) and by Li(11). However, this model does not consider axial load.
In this study, we adopt the FCM to develop a semi-analytic model for prediction of the flexural behavior of unreinforced concrete structures and fiber reinforced concrete structures subjected to bending and axial load. In this paper, the model is presented using an empirical softening relation that fits a wide range of experimental data very well. However, all other relationships can readily be introduced. The equilibrium of forces at a cracked section is determined by using a simple iteration technique and numerical integration of the softening relation. The model incorporates a layer that absorbs all deformation in the cracked zone. A similar assumption was made by Ulfkjær et al.(8). Given the complete uniaxial stress-crack width relationship, it is possible to predict the flexural behavior in moment-rotation and load-deflection relations.

ANALYTICAL CHARACTERIZATION OF FRC

The cement-based material is assumed to be linear elastic in tension up to maximum stress σ^{u}_{frc} with Young's modulus E_{frc}.
After the maximum stress has been reached, a discrete crack is formed in the material. This crack is characterized mechanically by the stress-crack width relationship. Stang and Aarre(4) have assumed the relationship to take the following simple form:

$$\sigma^{crk}_{frc} = f(w) = \frac{\sigma^{u}_{frc}}{1 + \left(\frac{w}{w_0}\right)^{p}} \qquad (1)$$

where σ^{crk}_{frc} denotes the stress transferred across the crack surfaces, w_0 represents a characteristic crack opening and p is a curve shape factor. Thus, the material is characterized by five material constants, three related to the pre-peak behavior: the elastic constants and the ultimate tensile strength, and two related to the post-peak behavior: the characteristic crack opening w_0 and the shape factor p. See (4) for full details.

MOMENT-ROTATION CURVE

Consider a short segment of a rectangular beam, with depth h as illustrated in Fig. 1. The beam is subjected to an external bending moment M per width of the beam and to an axial force N per width of the beam. The behavior of the material is assumed to be linear elastic

in tension up to maximum stress σ^u_{frc} with Young's modulus E_{frc}. When the ultimate tensile strength is reached, it is assumed that a single crack develops. Given the axial compressive force N, the moment M^{crk} at which a single crack develops is given by the theory of elasticity:

$$M^{crk} = \frac{2I}{h}\left(\frac{N}{A} + \sigma^u_{frc}\right) \tag{2}$$

where $I = h^3/12$ is the moment of inertia per width of the beam and $A = h$ is the cross-sectional area per width of the beam.

The fundamental idea of this model is to incorporate a layer - a crack band - which absorbs all deformation located in the crack zone.
The analysis of crack band behavior before a crack develops is performed according to the following equations. Consider a short segment of a rectangular FRC-beam, with depth h as illustrated in Fig. 2. The strain is assumed to be uniformly distributed along the axis of the beam over the crack band width l_{cb}. The relation between rotation φ and curvature κ is:

$$\kappa = \frac{\varphi}{l_{cb}} \tag{3}$$

According to the theory of elasticity the bending moment M is given by:

$$M = E_{frc} I \kappa \tag{4}$$

(2) and (3) give the relation between the bending moment and the rotation:

$$M = \frac{E_{frc} I}{l_{cb}} \varphi \tag{5}$$

Denoting the maximum compression stress σ_c and the maximum tensile stress σ_t, the following relationships describe the distribution of stress:

$$\sigma_c = \frac{N}{h} + \frac{hE_{frc}}{2l_{cb}} \varphi \tag{6}$$

$$\sigma_t = -\frac{N}{h} + \frac{hE_{frc}}{2l_{cb}} \varphi \tag{7}$$

When the ultimate tensile strength is reached, it is assumed that a single crack develops:

$$\sigma_t = \sigma^u_{frc} \tag{8}$$

Denoting the rotation by which a crack appears φ^{crk}, (7) and (8) give:

$$\varphi^{crk} = \frac{2l_{cb}}{hE_{frc}}\left(\frac{N}{h} + \sigma^u_{frc}\right) \tag{9}$$

In the elastic case, $\varphi \leq \varphi^{crk}$, the stress is proportional to the strain.

When the tensile strength is reached, it is assumed that a single crack develops at a maximum tensile stress σ^{u}_{frc} at the crack tip and a compressive stress σ_c at the cross section compressive side, whereas the rest of the beam still behaves elastically. Fig. 3 describes the distribution of stresses, where the post-peak tensile stress is a function of the crack width. It is assumed that the crack has a linear profile and that the rigid body rotation is related to the crack mouth opening w and the length ζh as follows:

$$\varphi = \frac{w}{\zeta h} \tag{10}$$

Therefore, the distribution of normal stresses within the fracture zone is given by (1). The resulting force per width of the fracture zone and the bending moment per width of the fracture zone relative to the crack tip, N_f and M_f respectively, can be obtained by integrating:

$$N_f = \frac{1}{\varphi} \int_0^w f(u)\, du \tag{11}$$

$$M_f = \frac{1}{\varphi^2} \int_0^w f(u)\, u\, du \tag{12}$$

With the given assumptions the depth ηh of the tensile zone may be related to the crack opening by:

$$\eta h = \frac{1}{\varphi} \left(\frac{\sigma^{u}_{frc}}{E_{frc}}\, l_{cb} + w\right) \tag{13}$$

where l_{cb} is the width of the crack band.
The resulting force per width of the compression zone is denoted N_c and the resulting force per width of the elastic tensile zone is denoted N_t:

$$N_c = \frac{\varphi\, E_{frc}\, (h - \eta h)^2}{2\, l_{cb}} \tag{14}$$

$$N_t = \frac{(\sigma^{u}_{frc})^2\, l_{cb}}{2\, \varphi\, E_{frc}} \tag{15}$$

Equation (14) describes how N_c is related to φ and η : $N_c(\varphi,\eta)$. Equation (15) describes how N_t is related to φ : $N_t(\varphi)$. Equation (11) describes how N_f is related to φ and w : $N_f(\varphi,w)$. For a given rotation φ, the equilibrium of the section is written in the following way in order to determine the position of the neutral axis:

$$N_c(\varphi,\eta) - N_t(\varphi) - N_f(\varphi,w) = N \quad (16)$$

The crack mouth opening w can be substituted from (13):

$$N_c(\varphi,\eta) - N_t(\varphi) - N_f(\varphi,\eta) = N \quad (17)$$

Given φ and N, the position of the neutral axis can be determined from (17). The cross-sectional moment relative to the center line becomes:

$$M = (\frac{1}{6}+\frac{1}{3}\eta)hN_c + (\frac{1}{2}-\frac{1}{3}\eta-\frac{2}{3}\zeta)hN_t + (\frac{1}{2}-\zeta)hN_f+M_f \quad (18)$$

The result of the calculation is corresponding values of rotation, stresses, crack mouth opening and bending moment. Hence, the complete moment-rotation relationship in the crack band is fully determined by φ and N:

$$M = M(\varphi,N) \quad (19)$$

CALCULATION PROCEDURE

The determination of the moment-rotation relationship for a given axial force is performed according to the following algorithm.
The starting point is zero rotation, $\varphi = 0$. The rotation is now increased in small steps. In the elastic case, $\varphi \leq \varphi^{crk}$, the moment and stresses can be obtained from equation (5)-(7).
When φ^{crk} is finally exceeded, it is assumed that a single crack appears. For each step of φ the solution of the nonlinear equilibrium equation (17) is determined by using a simple bisection iteration scheme. For each guess on η, w is determined from equation (13), N_f is determined by numerical integration of the softening relation (1) as outlined in equation (11), and N_c and N_t are determined from equations (14) and (15) respectively.
When the position of the neutral axis is determined as outlined above, the moment is calculated on the basis of equation (18), where M_f is determined numerically by equation (12). Ten steps are used throughout the present study in the numerical integrations (equations (11) and (12)).
The result of the calculation is corresponding values of rotation, stresses, crack mouth opening and bending moment.

FORCE-DISPLACEMENT CURVES

Consider a rectangular beam with depth h, length L subjected to three-point bending. In general, the deflection is calculated as a sum of two terms: $\delta = \delta_e + \delta_c$. δ_e is the elastic contribution and δ_c is the deflection due to rotation caused by crack formation in the crack band.

In the elastic case, $\varphi \leq \varphi^{crk}$, the deflection is given by $\delta = \delta_e$. According to the classical theory of elasticity δ_e is related to M and L as follows:

$$\delta = \delta_e = \frac{1}{12}\frac{ML^2}{E_{frc}I} = \frac{1}{12}\frac{\varphi L^2}{l_{cb}} \tag{20}$$

When a single crack has developed, $\varphi \geq \varphi^{crk}$, the deflection is given by $\delta = \delta_e + \delta_c$, where:

$$\delta_e = \frac{1}{12}\frac{ML^2}{E_{frc}I} = \frac{1}{12}\frac{M(\varphi,0)L^2}{E_{frc}I} \tag{21}$$

$$\delta_c = \frac{L}{4}(\varphi - \varphi^{crk}) \tag{22}$$

When $\varphi = \varphi^{crk}$, equations (20) and (22) are in accordance:

$$\delta = \frac{1}{12}\frac{M^{crk}L^2}{E_{frc}I} = \frac{1}{6}\frac{\sigma_{frc}^u L^2}{hE_{frc}} \tag{23}$$

RESULTS AND DISCUSSION

In this section, results of the semi-analytical model are compared with the experimental results described by Hansen and Stang(12) and with results of a detailed numerical model developed by Zhang and Stang(13). Furthermore, it is shown how the model prediction is influenced by the crack band width l_{cb} and by the external load N.

In figures 4 to 7 comparisons are shown between the results of the analytical model and the numerical results described by Zhang et al.(13) for beams subjected to three-point bending. The numerical model is based on the fictitious crack model with 21 nodes in the midsection. Rectangular elements were used. See (13) for full details. Results for one beam geometry (L = 400mm, h = b = 100mm) at five different crack band sizes for a typical, ordinary concrete and a typical fiber reinforced concrete are compared. The stress-crack opening relationships are shown in Fig. 8. The best agreement is obtained if the size of the crack band is one half of the beam depth, $l_{cb} = h/2$. A similar result was found by Ulfkjær et al.(8), who worked with a linear softening relation for conventional concrete. It is observed that the model determines the ultimate load very well and that the shapes of the load-crack length curves and of the crack length-crack mouth opening curves are almost identical.

The theoretical results according to equation (19) for the moment-rotation curves for different values of the external axial force are shown in figures 9 and 10 for the case h = 50 mm and $l_{cb} = h/2$. The axial loads are 0, 5 10^4, 10 10^4, and 20 10^4 N/m corresponding to compressive stresses of 0, 1, 2 and 4 MPa. The variation of M to axial load N as a function of φ for a typical ordinary concrete and a typical fiber reinforced concrete is shown in figures 9 and 10 respectively. The model prediction is shown only for crack widths from 0 mm to 0.30 mm (w_{max} = 0.30 mm), since this is the interval of primary interest in industrial applications of the

model. It is observed that $M(\varphi,N)$ increases as a function of N and that $M(\varphi,N)$ increases initially as a function of φ, reaches a maximum value and then starts to decrease as the rotation continues to increase.

In figures 10 to 12 the predicted load-deflection curves according to equations (20)-(23) are shown along with experimentally determined curves at age > 28 days for beams subjected to three-point bending. Experimentally measured by Hansen et al.(12). Beams with a span of 250 mm were subjected to three-point bending. Deflections at the middle were measured by using two standard Instron extensometers with a 25 mm gauge length. The extensometers were fitted on each side of the specimen. The average of the two extensometer signals was used as a measure for the deflection. The deflection was increased at a constant rate of 0.25 mm/min. Three normal-strength concrete recipes have been tested: a plain concrete called 'PC 7000' and two FRCs: one called 'FRC 9000' with 2 vol.% of polypropylene fibre and one called 'FRC 8500' with a combination of 1 vol.% of hooked steel fibers and 1 vol.% of pp fibers. See (12) for full details. The stress-crack width relationship has been determined experimentally by tensile tests, and the empirical σ-w relation based on equation (1) has been fitted using a least square technique. The experimental set-up used at the Department of Structural Engineering, TUD, is described in (4) and (12).
Reasonable good agreement with experimental results has been obtained. However, this does not apply to the initial part of the experimental curves. This part of the curves is affected by imperfect contact between specimen and bending fixture. It is clear that the model is well suited to describe the influence of fibre reinforcement on the ultimate load. This conclusion is further emphasized in Table 1, which show the observed and predicted ultimate loads.

CONCLUSION

The following conclusion can be drawn from this study:

A semi-analytical model based on the fictitious crack model for description of the flexural behavior of concrete structures has been presented. This model considers, if necessary, the axial load and the complete softening relation by using a simple numerical iteration technique. Application of the model in the design of FRC pipes will be shown in a subsequent paper. The model has to be calibrated in order to determine the single calibration factor, l_{cb}. Using $l_{cb} = h/2$ the model shows very good agreement with the results from a numerical model using finite element analysis.

The model is described by a set of simple equations. This opens up the possibility of studying complicated problems with a limited amount of data processing.
Reasonably good agreement with experimental results for the load-deflection curves of beams subjected to three-point bending has been obtained. In addition, the length and the CMOD of the fictitious crack have been obtained. The model is well suited to describe the influence of fibre reinforcement on bending strength.

ACKNOWLEDGEMENTS

The work presented in this paper has been carried out at the Department of Structural Engineering (ABK), Technical University of Denmark.
Carsten Pedersen's work has been carried out as an Industrial Research Study, Ph.D., supported by grants from the Danish Academy of Technical Sciences (ATV), VTB-beton a/s, Eurotest aps and the Institute for Product Development (IPU). The study is supervised by Dr. Henrik Stang (ABK), Manager Jens Peter Andreasen (VTB), Manager Poul Rasmussen (Eurotest) and M.Sc. Johan Christian Gregersen (IPU), whom Carsten Pedersen thanks for their inspiring instruction.
The author want to thank the staff at the Department of Structural Engineering for their help during the work.

REFERENCES

1. Hillerborg, A., Modéer, M., and Petersson, P. E. Analysis of crack formation and crack growth in concrete by means of fracture mechanics and finite elements. Cement and Concrete Research, Vol. 6, 773-782. 1976

2. Bazant, Z. P., and Oh, B. H. Crack Band theory for fracture of concrete. Mat. and Struct., Paris, France, Vol. 16, 155-177, 1983.

3. Jenq, Y. S., and Shah, S. P. Two parameter fracture model for concrete. Journal of Engineering Mechanics, Vol. 111, No. 10, 1985.

4. Stang, H. and Aarre, T. Evaluation of Crack Width in FRC with Conventional Reinforcement. 'Cem. Concr. Comp.', 14, 143-154, 1992.

5. Guinea, G. V., Planas, J., and Elices, M. A General Bilinear Fit for the Softening Curve of Concrete. Materials and Structures, 1994, 27, 99-105.

6. Li, V. C., Stang, H., and Krenchel, H. Micromechanics of Crack Bridging in Fiber Reinforced Concrete. Materials and Structures, 1993, 26, 486-494.

7. Chuang, T.-J., and Mai, Y.-W. Flexural Behavior of Strain-Softening Solids. Int. J. Solids and Struct., 25(12), 1427-1443, 1989.

8. Ulfkjær, J.P., Krenk, S., and Brincker, R. Analytical Model for Fictitious Crack Propagation in Concrete Beams. Journal of Engineering Mechanics, Vol. 121, No.1, January, 1995.

9. Maalej, M., and Li, V. C. Flexural Strength of Fiber Cementitious Composites. Department of Civil and Environmental Engineering, University of Michigan. May,

1993.

10. Maalej, M., Li, V. C., and Hashida, T. Effect of Fiber Rupture on Tensile Properties of Short Fiber Composites. Department of Civil and Environmental Engineering, University of Michigan. 1993.

11. Li, V. C. Postcrack Scaling Relations for Fiber Reinforced Cementitious Composites. Journal of Materials in Civil Engineering, 4(1), 41-57.

12. Hansen, S., and Stang, H. Experimentally Determined Mechanical Properties for Fiber Concrete. Report, Department of Structural Engineering, Technical University of Denmark, 1993. In Danish.

13. Zhang, J., and Stang, H. Model I Crack Growth in Plain and Fiber Reinforced Concrete Beams. Department of Structural Engineering, Technical University of Denmark, 1995. Under preparation.

NOTATION

The following symbols are used in this paper:

A	cross-sectional area
E_{frc}	Young's modulus of the FRC material
h	depth of a beam
I	moment of inertia
l_{cb}	width of the crack band
L	beam length
M	externally applied moment
M_f	bending moment per width of the fracture zone
M^{crk}	applied moment at which a single crack appears in the uncracked beam
N	externally applied force
N_c	resulting force per width of the compression zone
N_f	resulting force per width of the fracture zone
N_t	resulting force per width of the elastic tensile zone
p	shape factor
Q	load on beams in three point bending
w	crack mouth opening
w_0	characteristic crack mouth opening
δ	deflection
δ_c	deflection considering the crack as a hinge
δ_e	elastic deflection
ζh	crack length
ηh	depth of the tensile zone

σ_c	compressive stress
σ^{crk}_{frc}	stress within the fracture process zone, function of the crack width
σ^{u}_{frc}	ultimate tensile strength of the FRC-material
σ_t	tensile stress
κ	curvature
φ	rotation in the crack band
φ^{crk}	rotation by which a crack appears

TABLE CAPTION

Table 1 Comparison between experimental results and the model prediction for the ultimate load on beams subjected to three-point bending.

FIGURE CAPTIONS

Figure 1 Segment of a rectangular FRC beam

Figure 2 Crack band with a width of l_{cb}

Figure 3 Distribution of normal stresses in the crack band section

Figure 4 Comparison between the analytical model and the numerical model for beams subjected to three-point bending. Load as a function of crack length/h for a concrete similar to the mix 'PC 7000'. Numerical results from (13)

Figure 5 Comparison between the analytical model and the numerical model for beams subjected to three-point bending. Crack length/h as a function of crack mouth opening for a concrete similar to the mix 'PC 7000'. Numerical results from (13)

Figure 6 Comparison between the analytical model and the numerical model for beams subjected to three-point bending. Load as a function of crack length/h. Fiber concrete of the type 'FRC 8500'. Numerical results from (13)

Figure 7 Comparison between the analytical model and the numerical model for beams subjected to three-point bending. Crack length/h as a function of crack mouth opening. Fiber concrete of the type 'FRC 8500'. Numerical results from (13)

Figure 8 Stress-crack width relationships for a ordinary concrete and a typical fiber reinforced concrete

Table 1.

Recipe	σ_{frc}^{u} [MPa]	E_{frc} [MPa]	w_0 [m]	p	Exp. results [N]	Model prediction [N]
7000	3.71	31600	$2.18\ 10^{-5}$	1.274	2222 2225	2372
9000	4.01	22700	$1.63\ 10^{-4}$	0.381	2327 2335 2357	2460
8500	4.39	32900	$1.77\ 10^{-3}$	0.322	3489 3839 3959	3258

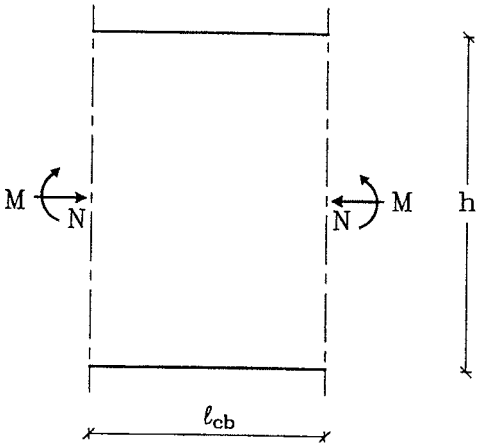

Figure 1

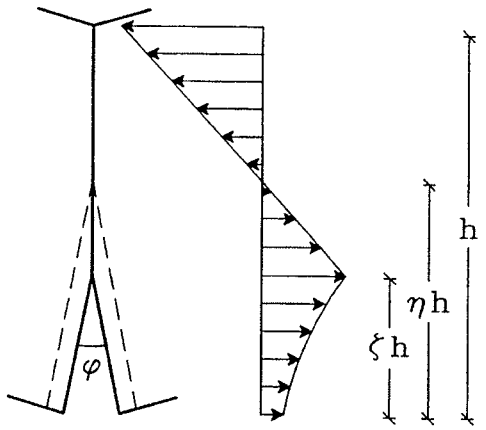

Figure 3

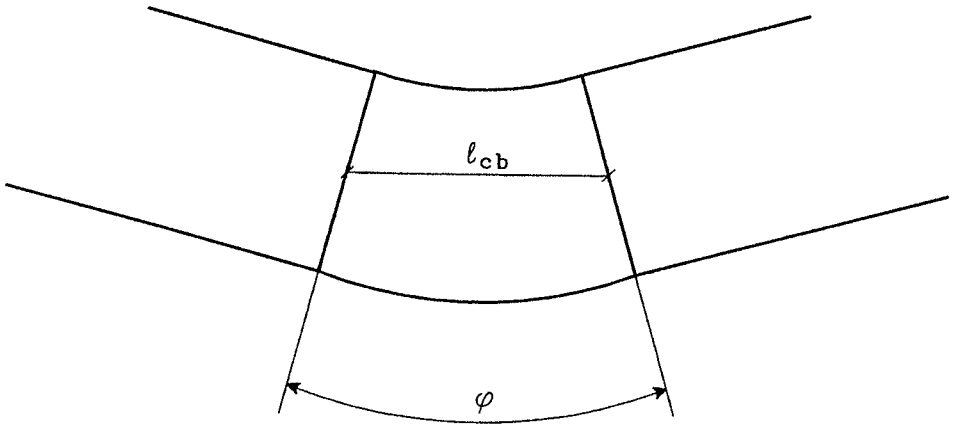

Figure 2

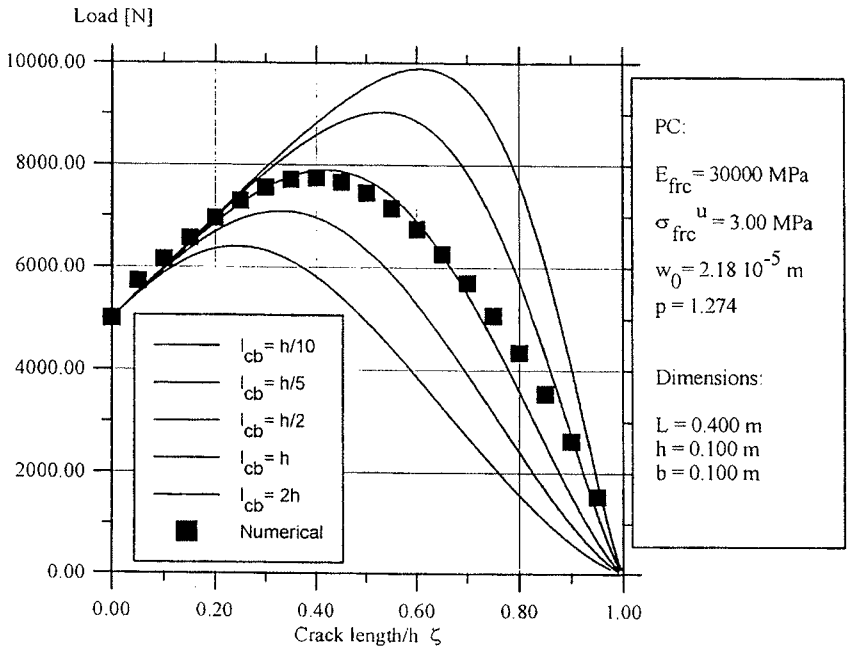

Figure 4

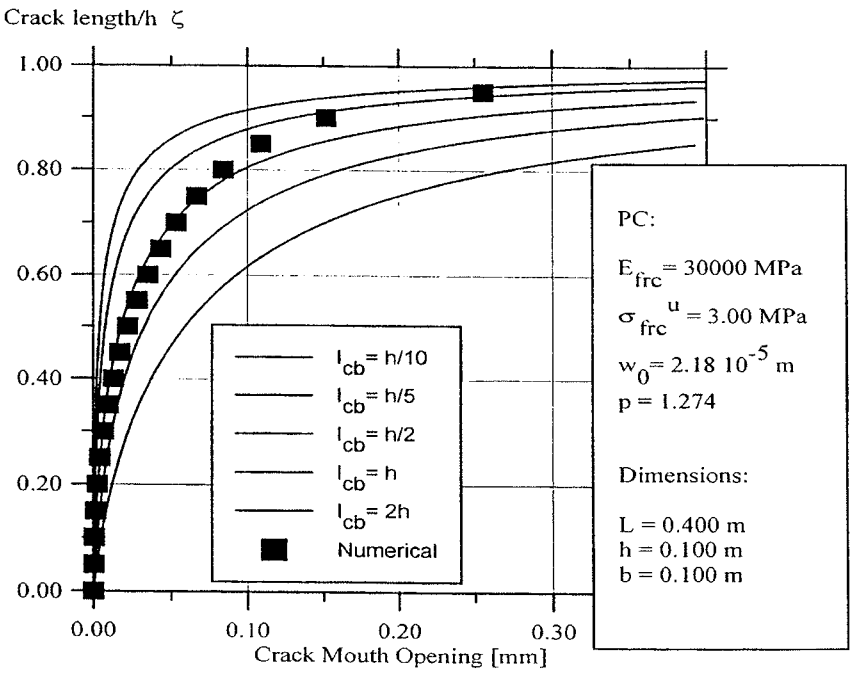

Figure 5

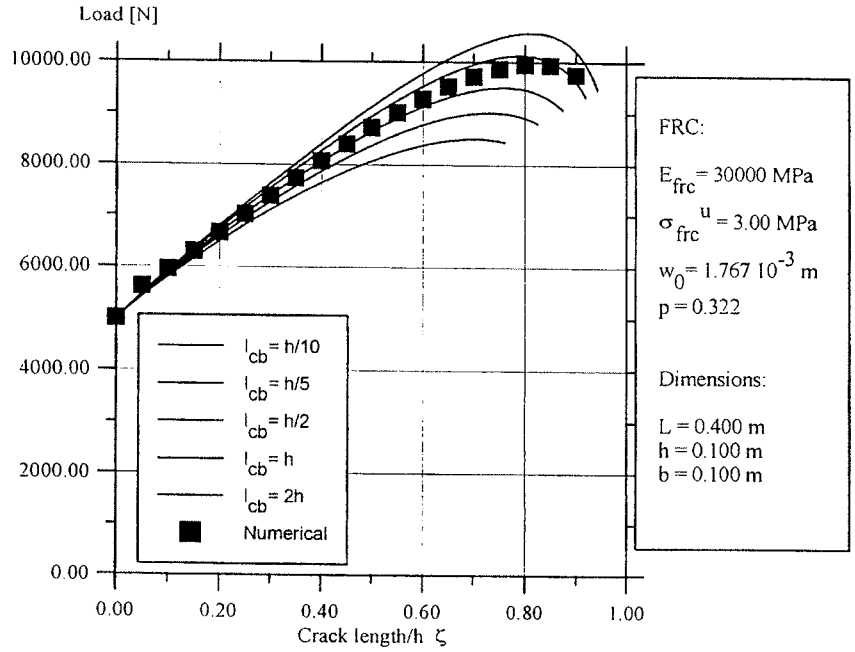

Figure 6

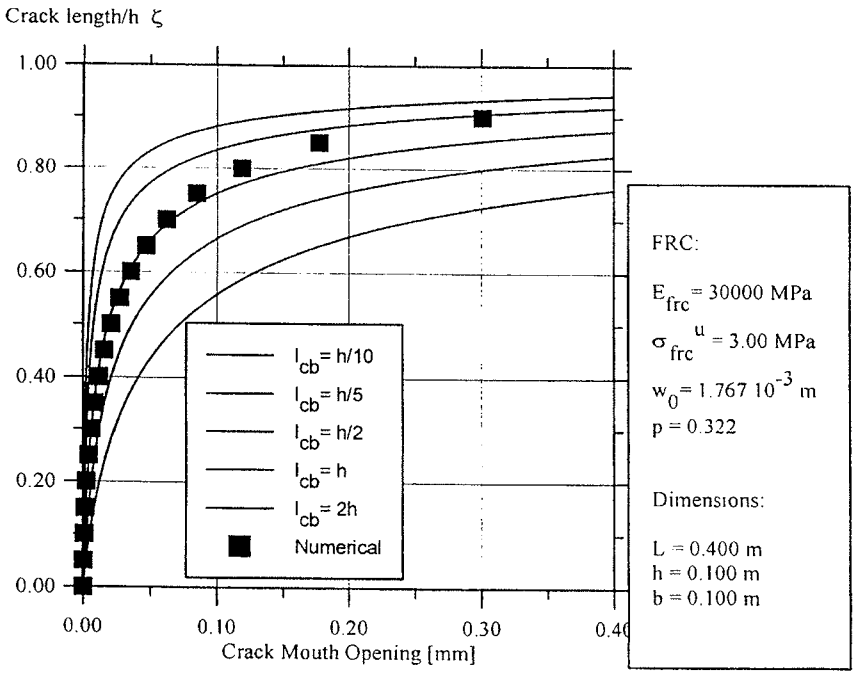

Figure 7

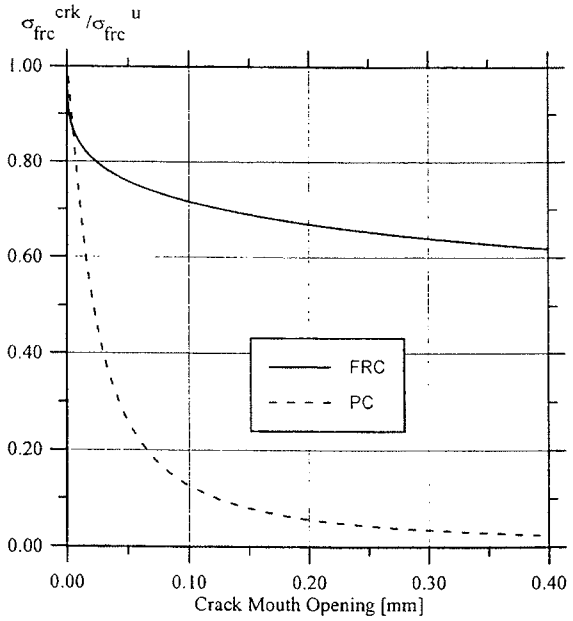

Figure 8

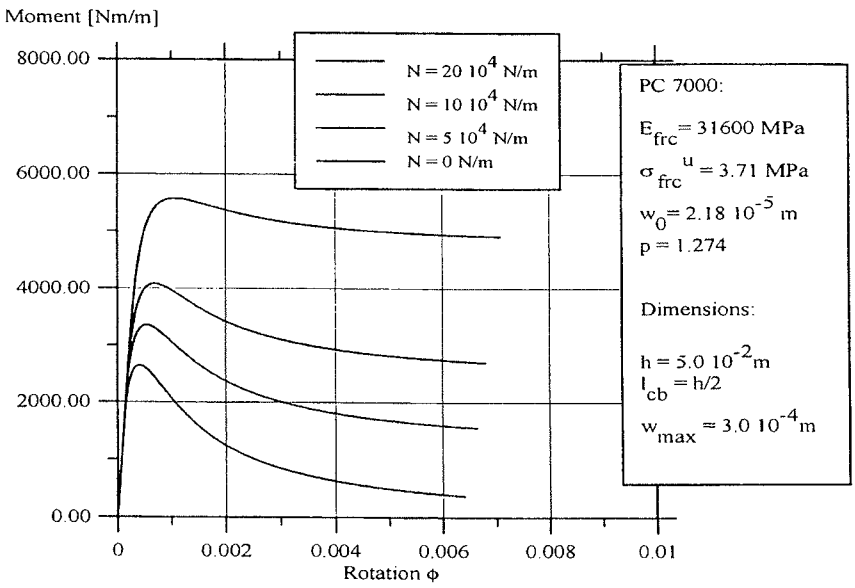

Figure 9

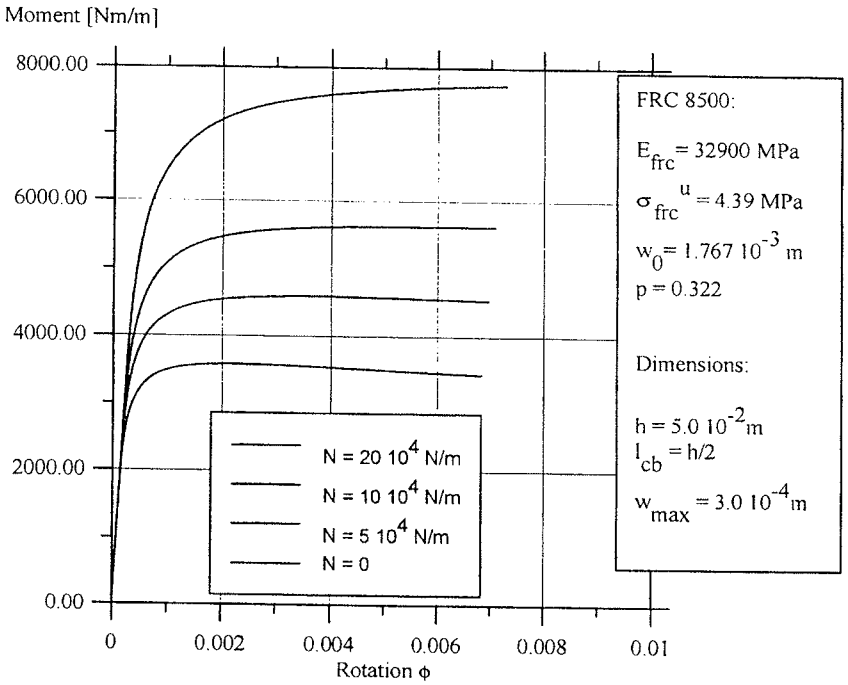

Figure 10

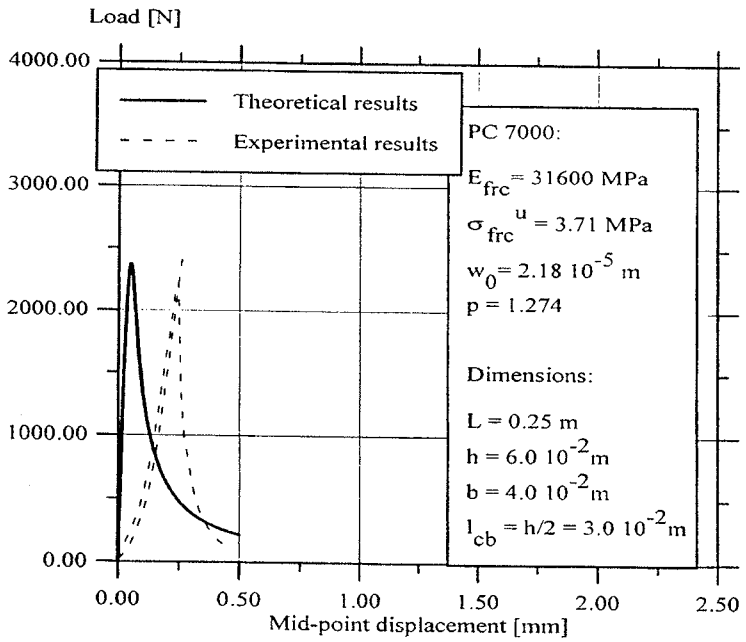

Figure 11

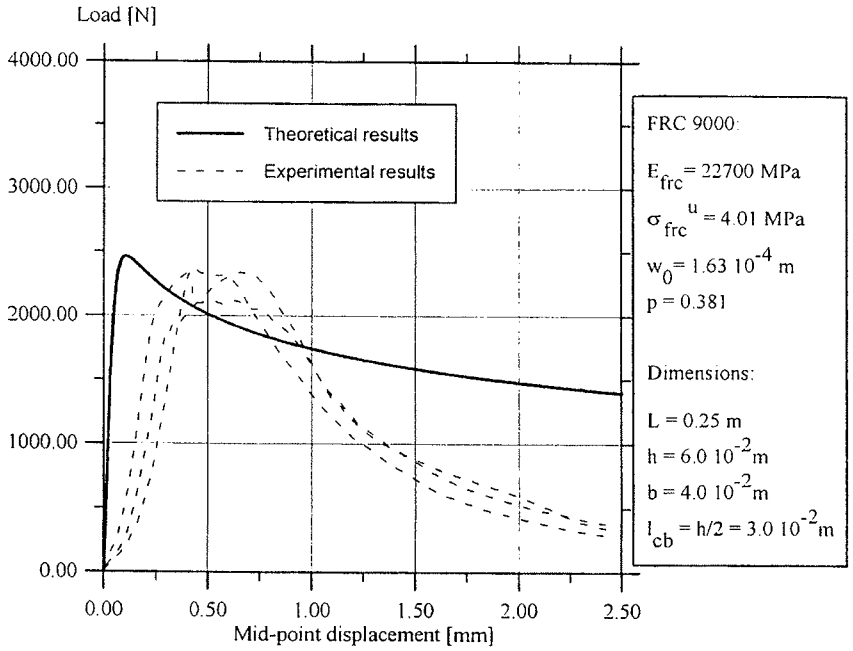

Figure 12

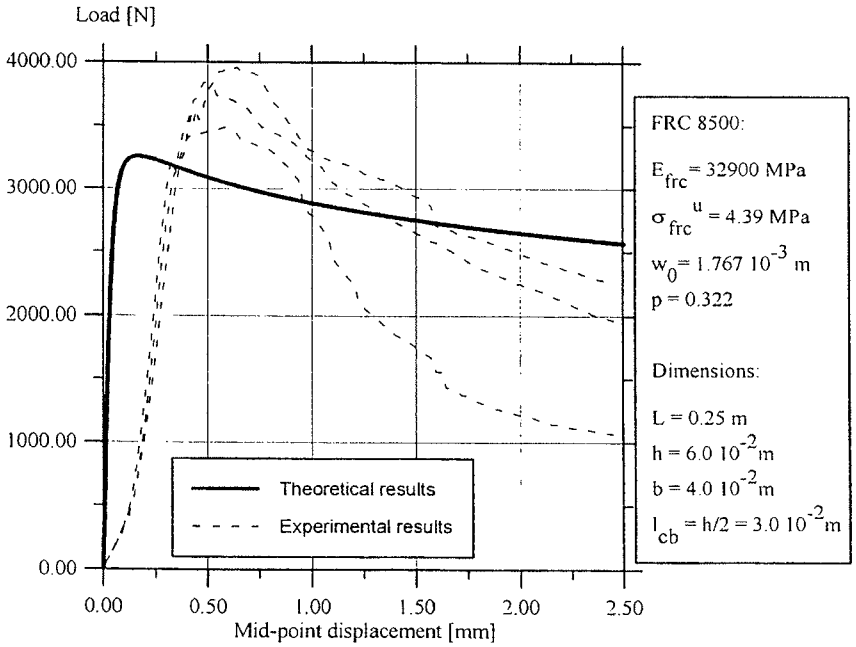

Figure 13

BKM REPORT NO. I4

CALCULATION OF FRC PIPES BASED ON THE FICTITIOUS CRACK MODEL

By Carsten Pedersen[1]

ABSTRACT

The present paper describes a model for prediction of the mechanical behavior of plain concrete pipes and fiber reinforced concrete (FRC) pipes. The paper describes implementation of a model for prediction of the moment-rotation relationship presented in previous work. This model is based on the fictitious crack model (FCM). Therefore, this paper represents an example of how the moment-rotation relationship can be used on a structural level. Very good agreement has been observed between the model prediction and experimental data relating to FRC pipes and unreinforced pipes subjected to line load. Furthermore, good agreement has been obtained with the results of a model using finite element analysis.

INTRODUCTION

The present paper deals with analyses of the mechanical behavior of unreinforced concrete pipes and concrete pipes with no other reinforcement than fibers. Concrete pipes are produced in series and the production of pipes constitutes a considerable part of the total consumption of concrete. The costs caused by failures are not to be considered as negligible. Pedersen(1) estimates the value of the Danish sewage pipelines and the cost of needed repairs at about 200 billion Danish kroner and 35 billion Danish kroner respectively (1992 prices). In spite of this, strength design has, for many years, been done almost exclusively on an empirical basis and has been based on previous practical experiences.

Theoretical strength analysis of unreinforced concrete pipes has, with a few exceptions, been based on the linear elastic brittle model. However, it has been proved that there is a discrepancy between this conventional theory and experimental results. It seems that the assumption of the linear elastic brittle behavior of the material can be questioned. This conclusion was made by Gustafsson(2), who worked with fracture analysis of unreinforced concrete pipes.

It has been found that the mechanical behavior of concrete pipes depends on the tensile load capacity across the cracks, the so-called stress-crack width relationship (e.g. Hansen and Thygesen(3)). For this reason the stress-crack width relationship is of fundamental importance in terms of concrete pipes and it is necessary to apply nonlinear fracture

---

[1] Industrial Ph.D. student, VTB-beton a/s, Dandyvej 11, DK-7100 Vejle, Denmark

mechanics for the description of fracture in concrete pipes with no other reinforcement than fibers. A similar result was obtained by Gustafsson(4), who worked with unreinforced concrete pipes and by Hansen et al.(3), who worked with FRC pipes.
The model presented in this paper is based on the assumption that a single crack appears when the tensile strength is reached, whereas the rest of the pipe still behaves elastically. Therefore, four single cracks are assumed to be developed. A similar result was found by Hansen et al.(3) when measuring the curvature of specimens after failure. Few researchers have considered analytical methods based on nonlinear elastic fracture mechanical models for describing fracture in concrete pipes. The idea of modeling the failure of concrete pipes by the formation of fictitious cracks was introduced by Gustafsson(4). A simplified bi-linear tension softening relation was used and no reinforcement was considered. Thygesen(5) combined the FCM with finite element analysis to determine the ultimate load capacity of reinforced and unreinforced concrete pipes.
In this study, we adopt the moment-rotation relationship proposed by Pedersen(6) to develop a semi-analytic model for prediction of the mechanical behavior of pipes with no other reinforcement than fibers. Given the complete uniaxial stress-crack width relation, it is possible to predict the load-deflection behavior of pipes subjected to line load.
Furthermore, this paper represents an example of how the moment-rotation relationship can be used on a structural level and it attempts to show that structures can be developed provided that the materials are characterized in a way that can be applied in structural calculations.

ANALYTICAL CHARACTERIZATION OF FRC

The fibre reinforced concrete is assumed to be linear elastic in tension up to a maximum stress of σ^{u}_{frc} with Young's modulus E_{frc}.
After the maximum stress has been reached, a discrete crack develops in the material. This crack is characterized mechanically by the stress-crack width relationship. Stang and Aarre(7) have assumed the relationship to take the following simple form:

$$\sigma^{crk}_{frc} = f(w) = \frac{\sigma^{u}_{frc}}{1 + \left(\frac{w}{w_0}\right)^{p}} \qquad (1)$$

where σ^{crk}_{frc} denotes the stress transferred across the crack surfaces, w_0 represents a characteristic crack opening and p is a curve shape factor. Thus, the FRC material is characterized by five material constants, three of which are related to the pre-peak behavior: the elastic constants and the ultimate tensile strength, and two of which are related to the post-peak behavior: the characteristic crack opening w_0 and the shape factor p. See (7) for full details.

MOMENT-ROTATION RELATIONSHIP

The model for prediction of the behavior in bending of fiber reinforced concrete elements adopted here was developed by Pedersen(6). The model represents implementation of the σ-w relationship(1) for fiber concrete and is similar to a model for prediction of the behavior in bending of conventional unreinforced concrete beams proposed by Ulfkjær, Krenk and Brincker(8).

The fundamental idea of this model is to incorporate a layer - a crack band - which absorbs all deformation located in the crack zone. The strain is uniformly distributed over the crack band width l_{cb}. The value $l_{cb} = h/2$ is used throughout the present study and is in accordance with the results from reference (6).

When the tensile strength is reached, it is assumed that a single crack appears, whereas the rest of the element still behaves elastically with a maximum tensile stress of σ^u_{frc} at the crack tip and a compressive stress of σ_c at the cross section compressive side. Fig. 1 describes the distribution of stresses at the cracked section, where the post-peak tensile stress is a function of the crack width. It is assumed that the crack has a linear profile and that the rigid-body rotation is related to the crack mouth opening w and the length ζh as follows:

$$\varphi = \frac{w}{\zeta h} \tag{2}$$

Given φ and the axial force N, the position of the neutral axis can be determined through the equilibrium of forces at the cracked section. The resulting force of the fracture zone is determined by numerical integration of the softening relation. Hence the cross-sectional moment M relative to the center line is fully determined by φ and N:

$$M = M(\varphi,N) \tag{3}$$

The moment-rotation relationship is obtained and the result of the calculation is corresponding values of rotation, forces, stresses, crack mouth opening and bending moment. See reference (6) for full details.

FORCE-DEFLECTION CURVES, PIPES

Geometrical parameters are defined in Fig. 2. The shape of the cross section of the pipe is described by radius R and wall thickness h. The pipe is subjected to a line load of 2Q per pipe length.

A quarter of the cross section is modelled as a curved beam and two moment springs. The bending moment per pipe length is related to the angle α by:

$$M(\alpha) = RQ\sin\alpha - M_B \tag{4}$$

where M_B is the bending moment at the pipe top-point B. Fig. 3. The rotation β due to the elastic deformation can be obtained by integrating:

$$\beta = \frac{R}{E_{frc}I}\int_0^{\frac{\pi}{2}} (RQ\sin\alpha - M_B)\, d\alpha = \frac{R}{E_{frc}I}\left(RQ - \frac{\pi}{2}M_B\right) \tag{5}$$

where $I = h^3/12$ is the moment of inertia per length of the pipe wall. The equilibrium of the section gives:

$$M_A + M_B = RQ \tag{6}$$

Until a single crack appears at the top-point, the solution is given by the theory of elasticity and the pipe is modelled as shown in Fig. 4. The geometrical equation is given by:

$$\beta = 0 \tag{7}$$

The bending moments per length of the pipe wall at points A and B, respectively can be calculated from:

$$M_A = \frac{2QR}{\pi} \tag{8}$$

$$M_B = QR\,(1 - \frac{2}{\pi}) \tag{9}$$

When a single crack appears at the top-point B, the pipe is modelled as shown in Fig. 5. The geometrical equation is given by:

$$\frac{1}{2}\,(\varphi_B - \varphi_B^{crk}) = \beta = \frac{R}{E_{frc}I}\,(RQ - \frac{\pi}{2}M_B) \tag{10}$$

This leads to:

$$Q = \frac{\pi}{2R}M_B + \frac{E_{frc}I}{2R^2}(\varphi_B - \varphi_B^{crk}) \tag{11}$$

where φ_B^{crk} is the rotation due to the elastic deformation of the crack band. According to previous work (6) φ_B^{crk} is given by:

$$\varphi_B^{crk} = \frac{2l_{cb}\sigma_{frc}^u}{hE_{frc}} \tag{12}$$

See reference (6) for full details.
The bending moments can be calculated from:

$$M_A = RQ - M_B \tag{13}$$

$$M_B = M_B(\varphi_B, 0) \tag{14}$$

When a single crack appears at point A, the pipe is modelled as shown in Fig. 6. The geometrical equation is given by:

$$\frac{1}{2}\,(\varphi_B - \varphi_B^{crk}) = \beta + \frac{1}{2}\,(\varphi_A - \varphi_A^{crk}) = \frac{R}{E_{frc}I}\,(RQ - \frac{\pi}{2}M_B) + \frac{1}{2}\,(\varphi_A - \varphi_A^{crk}) \tag{15}$$

This leads to:

$$Q = \frac{\pi}{2R}M_B + \frac{E_{frc}I}{2R^2}(\varphi_B - \varphi_B^{crk} - \varphi_A + \varphi_A^{crk}) \quad (16)$$

where φ_A^{crk} is the rotation due to the elastic deformation of the crack band. According to reference (6) φ_A^{crk} can be obtained from:

$$\varphi_A^{crk} = \frac{2l_{cb}}{hE_{frc}}(\frac{Q}{h} + \sigma_{frc}^u) \quad (17)$$

See (6) for full details.
The bending moments can be calculated from:

$$M_A = RQ - M_B = M_A(\varphi_A, Q) \quad (18)$$

$$M_B = M_B(\varphi_B, 0) \quad (19)$$

The deflection is calculated as a sum of two terms : the deflection due to the elastic deformation of the pipe and the deflection due to the rigid-body rotation of the cracked pipe. The deflection u_A^e at point A due to the elastic deformation is given by:

$$u_A^e = \frac{R^2}{E_{frc}I}(M_B(1 - \frac{\pi}{2}) + \frac{1}{2}RQ) \quad if \quad \varphi_A \le \varphi_A^{crk} \quad (20)$$

$$u_A^e = \frac{R^2}{E_{frc}I}(M_B(1 - \frac{\pi}{2}) + \frac{1}{2}RQ) + \frac{1}{2}R(\varphi_A - \varphi_A^{crk}) \quad if \quad \varphi_A \ge \varphi_A^{crk} \quad (21)$$

or:

$$u_A^e = \frac{R^2}{E_{frc}I}(M_B - \frac{1}{2}RQ) \quad if \quad \varphi_B \le \varphi_B^{crk} \quad (22)$$

$$u_A^e = \frac{R^2}{E_{frc}I}(M_B - \frac{1}{2}RQ) + \frac{1}{2}R(\varphi_B - \varphi_B^{crk}) \quad if \quad \varphi_B \ge \varphi_B^{crk} \quad (23)$$

The deflection u_B^e at point B due to the elastic deformation is given by:

$$u_B^e = \frac{R^2}{E_{frc}I}(\frac{\pi}{4}RQ - M_B) \quad if \quad \varphi_A \le \varphi_A^{crk} \quad (24)$$

$$u_B^e = \frac{R^2}{E_{frc}I}(\frac{\pi}{4}RQ - M_B) + \frac{1}{2}R(\varphi_A - \varphi_A^{crk}) \quad if \quad \varphi_A \ge \varphi_A^{crk} \quad (25)$$

or:

$$u_B^e = \frac{R^2}{E_{frc}I}\left(M_B\left(\frac{\pi}{2} - 1\right) + RQ\left(\frac{\pi}{4} - 1\right)\right) \quad if \quad \varphi_B \le \varphi_B^{crk} \tag{26}$$

$$u_B^e = \frac{R^2}{E_{frc}I}\left(M_B\left(\frac{\pi}{2} - 1\right) + RQ\left(\frac{\pi}{4} - 1\right)\right) + \frac{1}{2}R(\varphi_B - \varphi_B^{crk}) \quad if \quad \varphi_B \ge \varphi_B^{crk} \tag{27}$$

The curvature is not taken into account.

The deflections u_A^c and u_B^c at points A and B, respectively due to the rigid-body rotation of the curved beam are given by Fig. 7:

$$u_A^c = u_B^c = 0 \quad if \quad \varphi_B \le \varphi_B^{crk} \tag{28}$$

$$u_A^c = u_B^c = \frac{1}{2}R(\varphi_B - \varphi_B^{crk}) \quad if \quad \varphi_A \le \varphi_A^{crk} \quad and \quad \varphi_B \ge \varphi_B^{crk} \tag{29}$$

$$u_A^c = u_B^c = \frac{1}{2}R(\varphi_A - \varphi_A^{crk}) + \frac{1}{2}R(\varphi_B - \varphi_B^{crk}) \quad if \quad \varphi_A \ge \varphi_A^{crk} \tag{30}$$

CALCULATION PROCEDURE

The determination of the force-deflection relationship is performed according to the following algorithm.

The starting point is zero rotation, $\varphi_A = \varphi_B = 0$. The rotation φ_B is increased in small steps. In the elastic case, $\varphi_B \le \varphi_B^{crk}$, the load Q can be obtained from equations (6), (8) and (9). When φ_B^{crk} given by equation (12) is finally exceeded, it is assumed that a single crack appears at point B. The moment M_B is determined from the moment-rotation relationship given by equation (14). The load Q and the moment M_A are calculated from equations (11) and (8) respectively. Given M_A, the rotation φ_A is determined from the M-φ relation. When φ_A^{crk} given by equation (17) is finally exceeded, it is assumed that a single crack appears at point A. The moment M_B is calculated from the moment-rotation relationship given by equation (19). The solution of the nonlinear equilibrium equation (18) is determined by using a simple bisection iteration scheme. For each guess on φ_A, Q and φ_A^{crk} are determined from equations (16) and (17).

When corresponding values of load, rotations and bending moments are determined as outlined above, the deflections can be obtained from equations (20)-(30).

RESULTS AND DISCUSSION

Results of the semi-analytical model have been compared with experimental results described by Thygesen(5), who investigated one pipe geometry (L = 600mm, R = 170mm

and h = 40mm) and five normal-strength concrete recipes: a plain concrete called 'PC OA00' and four FRCs called 'FRC OA05', 'FRC OA10', 'FRC OA15' and 'FRC OA20' with 0 vol.%, 0.5 vol.%, 1.0 vol.%, 1.5 vol.% and 2.0 vol.% of straight steel fibers respectively. The test specimens were subjected to line load through steelbands, and corresponding values of load, horizontal deflection and vertical deflection were measured. The stress-crack width relationship was determined experimentally by tensile tests and the empirical σ-w relation based on equation (1) was fitted using a least square technique. The experimental setup used at the Department of Structural Engineering, TUD, is described in (7) and (9). The material parameters describing the tensile behavior of the 5 different FRC materials are summarized in Table 1. Examples of experimental results at age 28 days for the stress-crack opening relationship are shown in Fig. 8 and 9 for recipes FRC OA05 and FRC OA20 respectively. The fitting of the analytical expression (1) is also shown in these figures along with the relationship used by Thygesen(5) for numerical modelling. See (5) for full details. Figures 8 and 9 from reference (5).

Table 1 shows comparison between experimental results, numerical results and model prediction of the ultimate load. The numerical model is based on the fictitious crack model with 30 elements in a quarter of the cross section and 8 nodes per element. See (5) for full details. It is clear that the model is well suited for describing the influence of fibre reinforcement on the ultimate load. This conclusion is further emphasized in Table 2, which shows a comparison between experimental results and numerical results and between experimental results and model prediction of the differences between ultimate loads.

Fig. 10 shows the theoretical prediction of the load-deflection behavior, mix 'PC OA00'. Fig. 11 to 14 shows the predicted load-deflection curves along with the experimentally determined curves for pipes subjected to standard tests for recipes 'FRC OA05', 'FRC OA10', 'FRC OA15' and 'FRC OA20' respectively. It is observed that the model determines the load-deflection curves very well and that the ultimate loads are practically identical. Therefore, the model describes the influence of fibre reinforcement on the load-deflection behavior very well.

The results of the analytical model have been compared with the results of a large experimental investigation carried out at Eurotest aps. A normal-strength concrete recipe similar to recipe 'PC 0A00' has been tested. Unfortunately no stress-crack width relationship has been determined experimentally. Therefore, the parameters measured by Thygesen(5) for recipes 'PC 0A00' are used in the present study for model prediction (E_{frc} = 38000 MPa, σ_{frc}^{u} = 4.81 MPa, $w_0 = 2\ 10^{-5}$m and p = 0.71). All pipes were circular and the wall thickness of each pipe was measured at four different spots. The pipes were subjected to line load through steelbands and the ultimate loads were measured. Details of each group of pipes are listed in Table 3, where h is the average wall thickness and L is the length of the pipe section. It appears from Table 3 that the ultimate loads are well predicted regardless of inside diameter and wall thickness.

CONCLUSION

Based on the work described here, the following conclusion can be drawn:

It has been shown how the M-φ relationship can be used on a structural level to describe the behavior of structures with no other reinforcement than fibers.

The model can be used as an analytical design tool for material and structural optimization.

Using the proposed model, it is possible to determine the load-deflection behavior of pipes subjected to line load. Independently of pipe geometry and fibre volume concentration, very good agreement has been observed between the model prediction and experimental data.

ACKNOWLEDGEMENTS

The work presented in this paper has been carried out at the Department of Structural Engineering (ABK), Technical University of Denmark.
Carsten Pedersen's work has been carried out as an Industrial Research Study, Ph.D. supported by grants from the Danish Academy of Technical Sciences (ATV), VTB-beton a/s, Eurotest aps and the Institute for Product Development (IPU). The study is supervised by Dr. Henrik Stang (ABK), Manager Jens Peter Andreasen (VTB), Manager Poul Rasmussen (Eurotest) and M.Sc. Johan Christian Gregersen (IPU), whom Carsten Pedersen thanks for their inspiring instruction.
The author want to thank the staff at the Department of Structural Engineering for their help during the work.

REFERENCES

1. Pedersen, E.J. Fiber reinforced concrete pipes. UNICON beton I/S. December 1992. In Danish.

2. Gustafsson, P. J. Fracture Mechanics Studies of Non-yielding Materials like Concrete. Modelling of Tensile Fracture and Applied Strength Analysis. Report TVBM-1007, thesis, Division of Building Materials, Univ. of Lund, Sweden. 1985.

3. Hansen, S., and Thygesen, E. Fibre Reinforced Concrete Pipes. Report, Department of Structural Engineering, Technical University of Denmark, 1990. In Danish.

4. Gustafsson, P. J. Oarmerade betonrörs böjbrottlast och ringbrottlast. Teoretiska beräkningsmetoder. Report TVBM-3012, Division of Building Materials, Univ. of Lund, Sweden. 1983. In Swedish.

5. Thygesen, E. Design of FRC materials in structures. Ph.D. thesis, Department of Structural Engineering, Technical University of Denmark, 1993. In Danish.

6. Pedersen, C. The moment-rotation relationship with implementation of stress-crack width relationships. Department of Structural Engineering, Technical University of

Denmark, 1995.

7. Stang, H., and Aarre, T. Evaluation of Crack Width in FRC with Conventional Reinforcement. 'Cem. Concr. Comp.', 14, 143-154, (1992).

8. Ulfkjær, J.P., Krenk, S., and Brincker, R. Analytical Model for Fictitious Crack Propagation in Concrete Beams. Journal of Engineering Mechanics, Vol. 121, No.1, January, 1995.

9. Hansen, S., and Stang, H. Experimentally Determined Mechanical Properties for Fiber Concrete. Report, Department of Structural Engineering, Technical University of Denmark, 1993. In Danish.

NOTATION

The following symbols are used in this paper

d_i	inside diameter
E_{frc}	Young's modulus of the FRC material
h	wall thickness
I	moment of inertia
l_{cb}	width of the crack band
L	length of pipe section
M	externally applied moment
M_A	moment at point A
M_B	moment at point B
p	shape factor
Q	load on a quarter of the cross section of a pipe modelled as a curved beam
R	radius
u_A	deflection at point A
u_B	deflection at point B
u_A^c	deflection at point A due to the rigid-body rotation
u_A^e	deflection at point A due to elastic deformation
u_B^c	deflection at point B due to the rigid-body rotation
u_B^e	deflection at point A due to elastic deformation
w	crack mouth opening
w_0	characteristic crack mouth opening
α	angle from pipe top-point
β	rotation due to elastic deformation
ζh	crack length
ηh	depth of the tensile zone
σ_c	compressive stress
σ^{crk}_{frc}	stress within the fracture process zone, function of the crack width

σ^{u}_{frc} ultimate tensile strength of the FRC material
φ rigid-body rotation
φ_A rigid-body rotation at point A
φ_B rigid-body rotation at point B
φ^{crk} rotation by which a crack appears
φ^{crk}_{A} rotation by which a crack appears at point A
φ^{crk}_{B} rotation by which a crack appears at point B

TABLE CAPTIONS

Table 1 Comparison between experimental results, numerical results and model prediction of the ultimate load on pipes subjected to line load. Experimental results and numerical results of reference (5).

Table 2 Comparison between experimental results, numerical results and model prediction of the differences between ultimate loads on pipes subjected to line load. Experimental results and numerical results of (5).

Table 3 Comparison between experimental results and model prediction of the ultimate loads on pipes subjected to line load.

FIGURE CAPTIONS

Figure 1 Distribution of normal stresses in the crack band section. Figure from reference (6)

Figure 2 Geometry of pipe cross section. Shape after failure caused by line load 2Q is indicated by the dotted figure

Figure 3 Equilibrium of forces at a quarter of the cross section

Figure 4 A quarter of the cross section modelled as a curved beam until a single crack is formed at the top-point B

Figure 5 A quarter of the cross section modelled as a curved beam when a single crack is formed at the top-point B and until a crack appears at point A

Figure 6 A quarter of the cross section modelled as a curved beam when single cracks have appeared at points A and B

Figure 7 The deflections u_A^c and u_B^c at points A and B, respectively, due to the rigid-body rotation

Figure 8 Experimentally determined stress-crack width relationship with the fitted analytical expression(1). In this figure the expression used by Thygesen(5) for numerical modelling is also shown (LUSAS). Mix 'FRC OA05'. Figure from reference (5)

Figure 9 Experimentally determined stress-crack width relationship with the fitted analytical expression(1). In this figure the expression used by Thygesen(5) for numerical modelling is also shown (LUSAS). Mix 'FRC OA20'. Figure from reference (5)

Figure 10 Theoretical predictions of the load-deflection behavior of a pipe subjected to line load, mix'FRC OA00'

Figure 11 Comparison between experimental results and theoretical predictions of the load-deflection behavior of a pipe subjected to line load, mix 'FRC OA05'. Experimental results from (5)

Figure 12 Comparison between experimental results and theoretical predictions of the load-deflection behavior of a pipe subjected to line load, mix 'FRC OA10'. Experimental results from (5)

Figure 13 Comparison between experimental results and theoretical predictions of the load-deflection behavior of a pipe subjected to line load, mix 'FRC OA15'. Experimental results from (5)

Figure 14 Comparison between experimental results and theoretical predictions of the load-deflection behavior of a pipe subjected to line load, mix 'FRC OA20'. Experimental results from (5)

Table 1.

Recipe	σ_{frc}^{u} [MPa]	E_{frc} [MPa]	w_0 [m]	p	Exp. results [KN]	Numerical results [KN]	Model prediction [KN]
OA00	4.81	38000	$2.0\ 10^{-5}$	0.71	24.5	28.7	23.7
OA05	5.08	38000	$6.0\ 10^{-5}$	0.71	31.9	37.1	31.7
OA10	5.72	38000	$1.5\ 10^{-4}$	0.72	37.2	47.8	41.6
OA15	6.17	38000	$2.0\ 10^{-4}$	0.71	45.4	55.0	46.4
OA20	6.39	38000	$3.8\ 10^{-4}$	1.04	55.3	67.3	56.5

Table 2.

Recipe	Differences between experimental results and numerical results [%]	Differences between experimental results and model prediction [%]
OA00	+17	-3.3
OA05	+16	-0.6
OA10	+28	+12
OA15	+21	+2.2
OA20	+22	+2.2

Table 3.

d_i [mm]	L [mm]	h [mm]	Exp. results [KN]	Average of	Model prediction [KN]	Differences between experimental results and model prediction [%]
150	1330	40.5	98.4	6 tests	109.5	+11.3
200	1330	44.1	95.0	4 tests	95.7	+0.7
250	1330	49.1	88.7	6 tests	92.3	+4.1
250	1330	77.0	211.9	2 tests	203.4	-4.0
300	2105	57.6	175.4	16 tests	161.1	-8.2
300	2105	97.7	335.6	2 tests	406.6	+21.2
400	2355	75.2	245.2	30 tests	215.8	-12.0
400	2355	117.1	517.3	4 tests	471.1	-8.9
500	2355	92.9	267.2	16 tests	252.6	-5.5
500	2355	144.0	529.1	6 tests	542.0	+2.4
500	2355	83.1	217.4	12 tests	208.1	-4.3

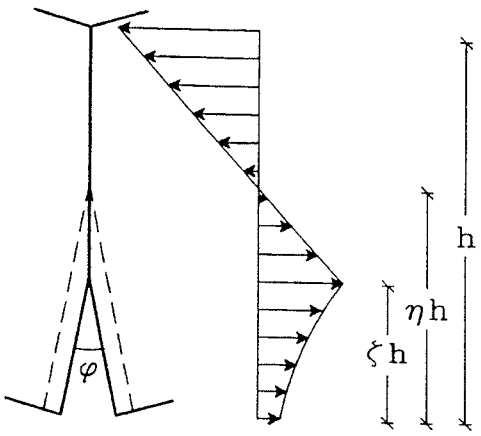

Figure 1

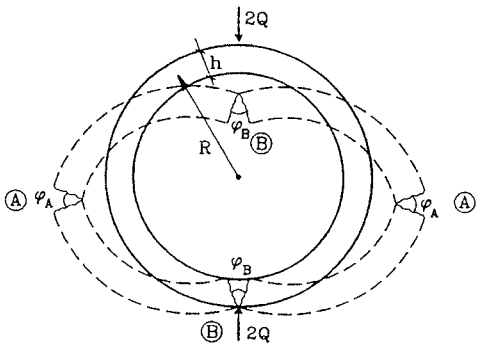

Figure 2

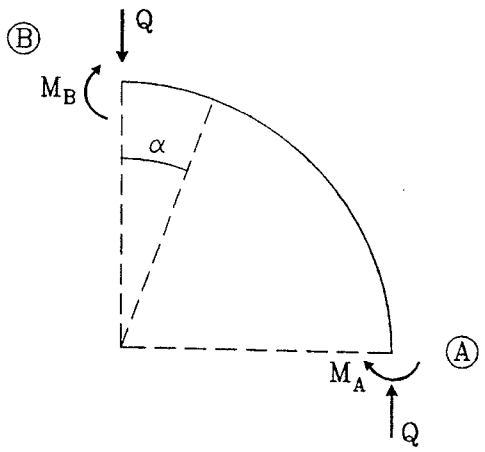

Figure 3

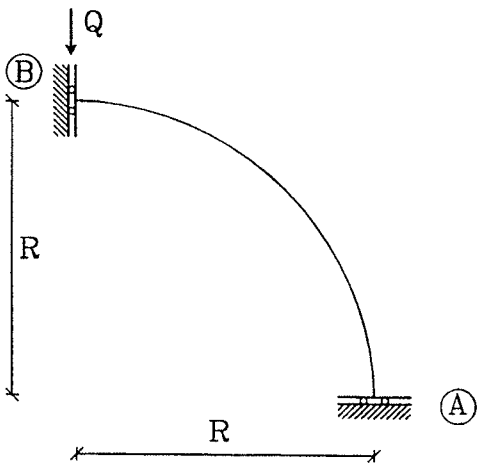

Figure 4

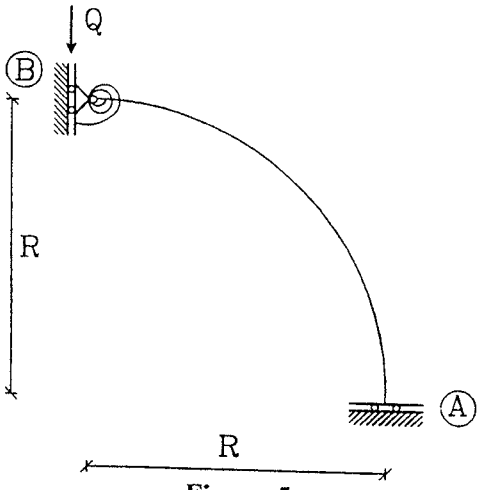

Figure 5

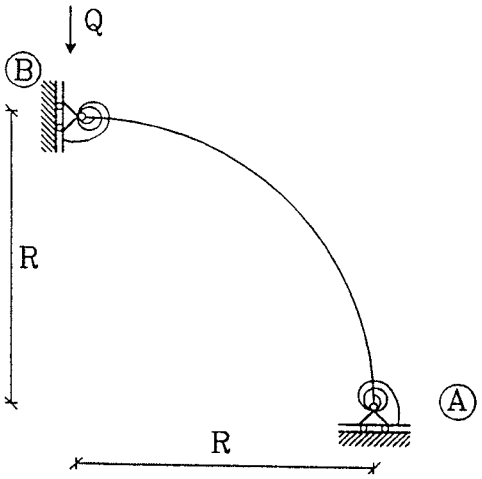

Figure 6

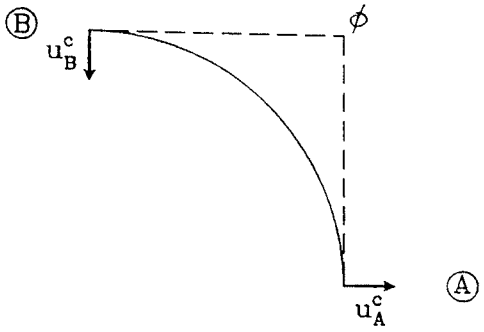

Figure 7

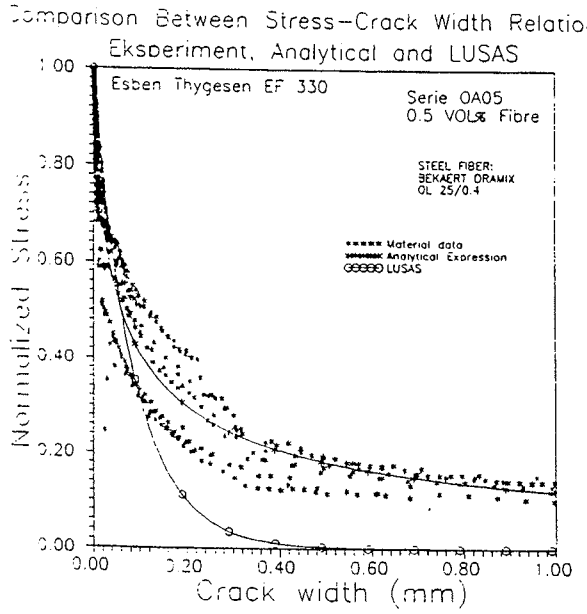

Figure 8

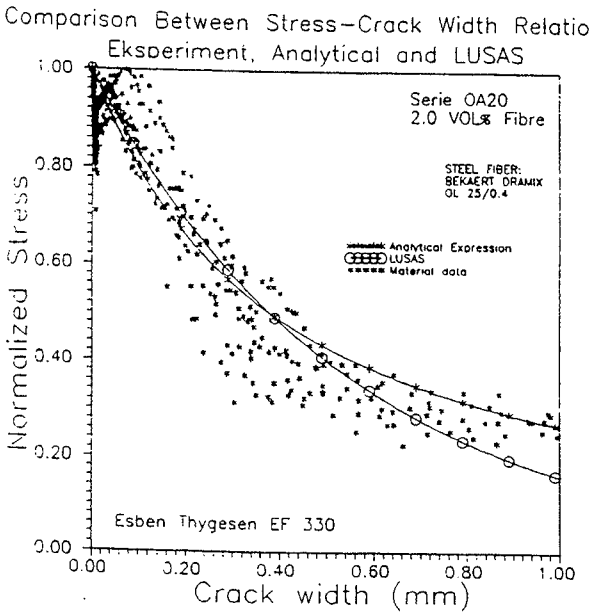

Figure 9

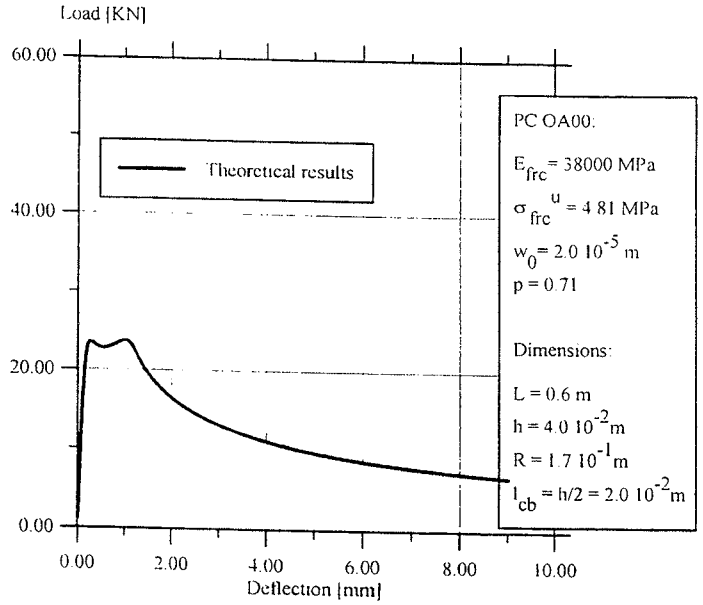

Figure 10

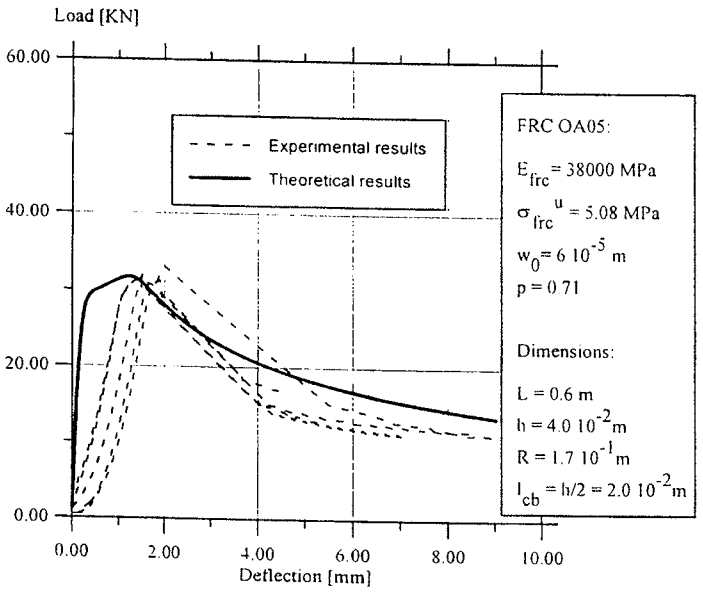

Figure 11

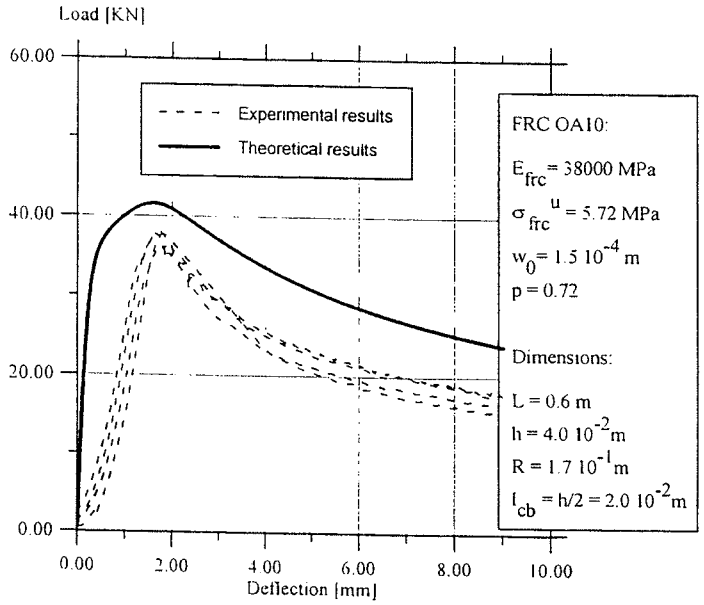

Figure 12

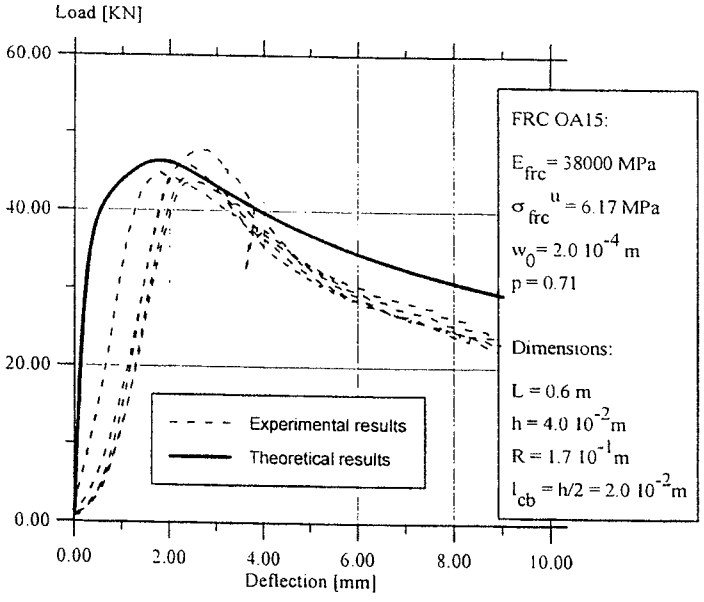

Figure 13

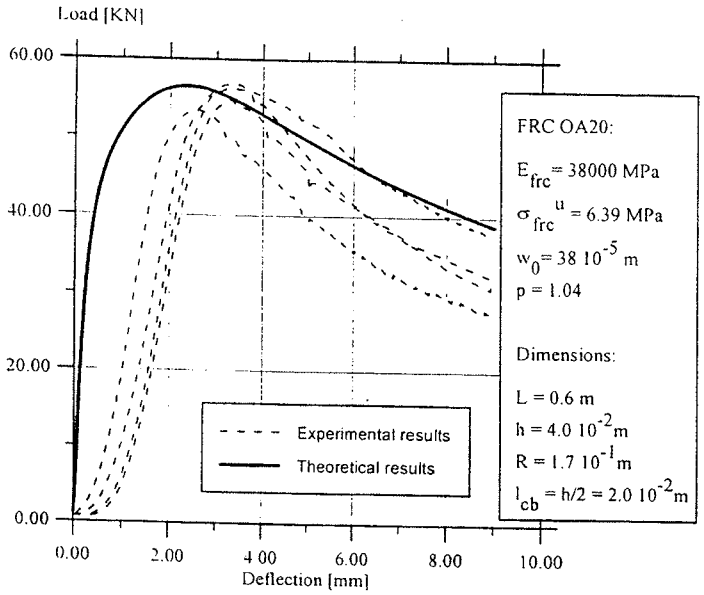
Load [KN]
60.00
40.00
20.00
0.00
0.00
2.00
4.00
6.00
8.00
10.00
Deflection [mm]
Experimental results
Theoretical results
FRC OA20:
E_{frc} = 38000 MPa
σ_{frc}^{u} = 6.39 MPa
w_0 = 38 10^{-5} m
p = 1.04
Dimensions:
L = 0.6 m
h = 4.0 10^{-2}m
R = 1.7 10^{-1}m
l_{cb} = h/2 = 2.0 10^{-2}m

Figure 14

FRC PIPES SUBJECTED TO EARTH PRESSURE, DESIGN AND CALCULATION

By Carsten Pedersen[1]

ABSTRACT

The present paper describes a model for prediction of the mechanical behavior of plain concrete pipes and fiber reinforced concrete (FRC) pipes subjected to earth pressure. The proposed model adopts the generalized moment/axial force-rotation relationship presented in previous work. This relationship is based on the fictitious crack model (FCM). Independently of inside diameter, good agreement has been observed between the model prediction relating to unreinforced concrete pipes and results which are in accordance with the Danish Code of Practice. The paper shows how the model can be used to set up analytical design tools for FRC pipes.

INTRODUCTION

The present paper deals with analyses of the mechanical behavior of unreinforced concrete pipes and fiber reinforced concrete pipes subjected to earth pressure.
Few researchers have considered analytical methods to determine the load capacity of concrete pipes in the serviceability limit state. Marston(1) proposed a theory for loads on underground conduits based on a large experimental program. Spangler(2) derived an empirical equation for prediction of the deflection of circular underground pipes. However, these models do not consider nonlinear fracture mechanics for the describtion of the ultimate load capacity.
It has been found that the mechanical behavior of concrete pipes depends on the tensile load capacity across the cracks, the so-called stress-crack width relationship (e.g. Hansen and Thygesen(3)). For this reason the stress-crack width relationship is of fundamental importance where concrete pipes are concerned and it is necessary to apply nonlinear fracture mechanics for the description of fracture in concrete pipes with no other reinforcement than fibers. A similar result was obtained by Gustafsson(4), who worked with unreinforced concrete pipes and by Hansen et al.(3), who worked with FRC pipes.
The model presented in this paper is based on the assumption that a single crack appears when the tensile strength is reached, whereas the rest of the pipe still behaves elastically. Therefore, four single cracks are assumed to be developed. A similar result was found by Hansen et al.(3) when measuring the curvature of specimens after failure.

---

[1] Industrial Ph.D. student, VTB-beton a/s, Dandyvej 11, DK-7100 Vejle, Denmark

The idea of modeling the failure of concrete pipes by the formation of fictitious cracks was introduced by Gustafsson(4). A simplified bi-linear tension softening relation was used and no reinforcement was considered. Thygesen(5) combined the fictitious crack model (FCM) with finite element analysis for determination of the ultimate load capacity of reinforced and unreinforced concrete pipes subjected to line load. Pedersen(6) adopted the moment/axial force-rotation relationship to derive a semi-analytic model for prediction of the mechanical behavior of FRC pipes subjected to line load. The moment/axial force-rotation relationship was based on the complete uniaxial stress-crack width relationship. See Pedersen(7).
In this study, we adopt the moment/axial force-rotation relationship to derive a semi-analytic model for prediction of the mechanical behavior of FRC pipes subjected to earth pressure. The at-rest earth pressure and the soil reaction are taken into account. Given the complete uniaxial stress-crack width relationship, it is possible to predict corresponding values of load, deflection and crack mouth opening.
The results of the analytical model are compared with results which are in accordance with the Danish Code of Practice for the Laying of Underground Rigid Pipelines of Concrete(8). Futhermore, the paper shows how a design and an optimization tool can be established by using the proposed model.

ANALYTICAL CHARACTERIZATION OF FRC

The fibre reinforced concrete is assumed to be linear elastic in tension up a to maximum stress of σ^{u}_{frc} with Young's modulus E_{frc}.
After the maximum stress has been reached, a discrete crack develops in the material. This crack is characterized mechanically by the stress-crack width relationship. Stang and Aarre(9) have assumed the relationship to take the following simple form:

$$\sigma^{crk}_{frc} = f(w) = \frac{\sigma^{u}_{frc}}{1 + (\frac{w}{w_0})^{p}} \qquad (1)$$

where σ^{crk}_{frc} denotes the stress transferred across the crack surfaces, w_0 represents a characteristic crack opening and p is a curve shape factor. Thus, the FRC material is characterized by five material constants, three of which are related to the pre-peak behavior: the elastic constants and the ultimate tensile strength, and two of which are related to the post-peak behavior: the characteristic crack opening w_0 and the shape factor p. See (9) for full details.

MOMENT-ROTATION RELATIONSHIP

The model for prediction of the behavior in bending of fiber reinforced concrete elements adopted here was developed by Pedersen(7). The model represents an implementation of the σ-w relationship(1) for fiber reinforced concrete similar to a model for prediction of the behavior in bending of conventional unreinforced concrete beams proposed by Ulfkjær, Krenk and Brincker(10).

The fundamental idea of this model is to incorporate a layer - a crack band - which absorbs all deformation located in the crack zone. The strain is uniformly distributed over the crack band width l_{cb}. The value $l_{cb} = h/2$ is used throughout the present study and is according to the results of reference(7).
When the tensile strength is reached, it is assumed that a single crack appears, whereas the rest of the element still behaves elastically with a maximum tensile stress of σ^u_{frc} at the crack tip and a compressive stress of σ_c at the cross section compressive side. Fig. 1 describes the distribution of stresses at the cracked section, where the post-peak tensile stress is a function of the crack width. It is assumed that the crack has a linear profile and that the rigid-body rotation is related to the crack mouth opening w and the length ζh as follows:

$$\varphi = \frac{w}{\zeta h} \tag{2}$$

Given φ and the axial force N, the position of the neutral axis can be determined through the equilibrium of forces at the cracked section. The resulting force of the fracture zone is determined by numerical integration of the softening relation. Hence the cross-sectional moment M relative to the center line is fully determined by φ and N:

$$M = M(\varphi, N) \tag{3}$$

The moment-rotation relationship is obtained and the result of the calculation is corresponding values of rotation, forces, stresses, crack mouth opening and bending moment. See reference (7) for full details.
The moment-rotation relationship (3) was adopted by Pedersen(6) to create a semi-analytic model forprediction of the mechanical behavior of pipes subjected to line load. See (6) for full details.

AT-REST EARTH PRESSURE

The at-rest earth pressure coefficient K_0 is defined as the ratio between horizontal and vertical stresses. Under the assumption of linear elasticity, K_0 may be considered constant and related to the Poisson's ratio of the soil. Experimental data suggest that K_0 is related to the angle of soil friction φ_s by:

$$K_0 = 1 - \sin\varphi_s \tag{4}$$

see e.g. Hansen(11).
According to the Danish Code of Practice for Foundation Engineering(12) the typical values of φ_s are between 15° and 35°, which correspond to values of K_0 between 0.43 and 0.74. The value of $K_0 = 0.40$ is used throughout the present study.

SOIL REACTION

To measure the modulus of soil reaction, Watkins and Nielson(13) constructed a device which simulated the side of a pipe being forced into the side fill. Watkins and Nielson(13)

have shown the modulus of soil reaction E' to be related to the horizontal earth pressure q_s and the change in the horizontal pipe diameter $2u_A$:

$$E' = \frac{q_s}{\frac{u_A}{R}} \tag{5}$$

where R is the radius of the pipe.
Nielson(14) found that the modulus of soil reaction(5) is sensitive to the value of Poisson's ratio and recommended a value of k/4 for design work, where k is the modulus of consolidation. However, no at-rest earth pressure was considered.
Based on literature studies a value of 2k/3 was found by Christensen(15), who worked with buckling of soil-surrounded pipes. Christensen(16) considered k/2 to be a conservative value. This value is used throughout the present study. By this adoption the horizontal earth pressure is related to the deflection by:

$$q_s = \frac{k}{2R} u_A \tag{6}$$

According to the Danish Code of Practice for Foundation Engineering(12) the typical values of k are larger than 30 MPa for intact sand deposits and compressed sand. The value of k = 30 MPa is used throughout the present study.

FORCE-DEFLECTION CURVES

Geometrical parameters are defined in figure 2. In the serviceability limit state the load is modelled as shown in figures 2-4. The vertical soil pressure and the horizontal soil pressure, q and K_0q respectively, are uniformly distributed over the pipe diameter 2R. The ratio K_0 is known as the at-rest earth pressure coefficient. q_s is the soil reaction at point A due to the deflection of the pipe wall, u_A. The horizontal earth pressure caused by the soil reaction is assumed to be triangularly distributed as shown in figures 2-4. q_s is determined from relation (6). However, all other relationships can readily be introduced.

A quarter of the cross-section is modelled as a curved beam and two moment springs. The bending moment per pipe length is related to the angle α by:

$$M(\alpha) = \frac{1}{2} qR^2(1 - K_0)\sin^2\alpha - \frac{1}{6} q_s R^2(2 - 3\cos^2\alpha + \cos^3\alpha) - M_B \tag{7}$$

where M_B is the bending moment at the pipe top-point B. See figure 5. The rotation β due to the elastic deformation can be obtained by integrating:

$$\beta = \frac{R}{E_{frc} I} \int_0^{\frac{\pi}{2}} M(\alpha) = \frac{R\pi}{2E_{frc} I} \left(\frac{1}{4} qR^2(1 - K_0) - \frac{1}{3} q_s R^2\left(\frac{1}{4} + \frac{2}{3\pi}\right) - M_B\right) \tag{8}$$

where $I = h^3/12$ is the moment of inertia per length of the pipe wall. The equillibrium of the section gives:

$$M_A + M_B = \frac{1}{2}qR^2(1 - K_0) - \frac{1}{3}q_sR^2 \tag{9}$$

Until a single crack appears at the top-point, the solution is given by the theory of elasticity and the pipe is modelled as shown in figure 2. The geometrical equation is:

$$\beta = 0 \tag{10}$$

When a single crack appears at the top-point B, the pipe is modelled as shown in figure 3. The geometrical equation is:

$$\frac{1}{2}(\varphi_B - \varphi_B^{crk}) = \beta \tag{11}$$

where φ_B^{crk} is the rotation due to the elastic deformation of the crack band. According to Pedersen(6), φ_B^{crk} is given by:

$$\varphi_B^{crk} = \frac{2l_{cb}}{hE_{frc}}\left(\frac{R(K_0q + \frac{1}{2}q_s)}{h} + \sigma_{frc}^u\right) \tag{12}$$

See (6) for full details.
The bending moment can be calculated from equation (3) where:

$$M_B = M_B(\varphi_B, R(K_0q + \frac{1}{2}q_s)) \tag{13}$$

When a single crack appears at the point A, the pipe is modelled as shown in figure 4. The geometrical equation is:

$$\frac{1}{2}(\varphi_B - \varphi_B^{crk}) = \beta + \frac{1}{2}(\varphi_A - \varphi_A^{crk}) \tag{14}$$

where φ_A^{crk} is the rotation due to the elastic deformation of the crack band. According to (6), φ_A^{crk} can be obtained from:

$$\varphi_A^{crk} = \frac{2l_{cb}}{hE_{frc}}\left(\frac{Rq}{h} + \sigma_{frc}^u\right) \tag{15}$$

See (6) for full details.
The bending moments can be calculated from:

$$M_A = M_A(\varphi_A, Rq) \tag{16}$$

$$M_B = M_B(\varphi_B, R(K_0 q + \frac{1}{2}q_s)) \quad (17)$$

The deflection is calculated as a sum of two terms : the deflection due to the elastic deformation of the pipe and the deflection due to the rigid-body rotation of the cracked pipe. The deflection u_A^e at point A due to the elastic deformation is given by:

$$u_A^e = \frac{R^2}{E_{frc}I}(M_B(1-\frac{\pi}{2}) + \frac{1}{2}qR^2(1-K_0)(\frac{\pi}{4}-\frac{1}{3}) - \frac{1}{6}q_sR^2(\frac{\pi}{16}+\frac{2}{3})) \text{ if } \varphi_A \le \varphi_A^{crk} \quad (18)$$

$$u_A^e = \frac{R^2}{E_{frc}I}(M_B(1-\frac{\pi}{2})+\frac{1}{2}qR^2(1-K_0)(\frac{\pi}{4}-\frac{1}{3})-\frac{1}{6}q_sR^2(\frac{\pi}{16}+\frac{2}{3}))+\frac{1}{2}R(\varphi_A-\varphi_A^{crk}) \text{ if } \varphi_A \ge \varphi_A^{cr} \quad (19)$$

or:

$$u_A^e = \frac{R^2}{E_{frc}I}(M_B - \frac{1}{6}qR^2(1 - K_0) + \frac{\pi}{32}q_sR^2) \quad \text{if} \quad \varphi_B \le \varphi_B^{crk} \quad (20)$$

$$u_A^e = \frac{R^2}{E_{frc}I}(M_B - \frac{1}{6}qR^2(1 - K_0) + \frac{\pi}{32}q_sR^2) + \frac{1}{2}R(\varphi_B - \varphi_B^{crk}) \quad \text{if} \quad \varphi_B \ge \varphi_B^{crk} \quad (21)$$

The deflection u_B^e at point B due to the elastic deformation is given by:

$$u_B^e = \frac{R^2}{E_{frc}I}(\frac{1}{3}qR^2(1 - K_0) - \frac{5}{24}q_sR^2 - M_B) \quad \text{if} \quad \varphi_A \le \varphi_A^{crk} \quad (22)$$

$$u_B^e = \frac{R^2}{E_{frc}I}(\frac{1}{3}qR^2(1 - K_0) - \frac{5}{24}q_sR^2 - M_B) + \frac{1}{2}R(\varphi_A - \varphi_A^{crk}) \quad \text{if} \quad \varphi_A \ge \varphi_A^{crk} \quad (23)$$

or:

$$u_B^e = \frac{R^2}{E_{frc}I}(M_B(\frac{\pi}{2} - 1) + qR^2(1 - K_0)(\frac{1}{3} - \frac{\pi}{8}) + q_sR^2(\frac{\pi}{24} - \frac{7}{72})) \text{ if } \varphi_B \le \varphi_B^{crk} \quad (24)$$

$$u_B^e = \frac{R^2}{E_{frc}I}(M_B(\frac{\pi}{2}-1)+qR^2(1-K_0)(\frac{1}{3}-\frac{\pi}{8})+q_sR^2(\frac{\pi}{24}-\frac{7}{72}))+\frac{1}{2}R(\varphi_B-\varphi_B^{crk}) \text{ if } \varphi_B \ge \varphi_B^{crk} \quad (25)$$

The deflections u_A^c and u_B^c at points A and B,respectively due to the rigid-body rotation of the curved beam are given by figure 6:

$$u_A^c = u_B^c = 0 \quad if \quad \varphi_B \leq \varphi_B^{crk} \tag{26}$$

$$u_A^c = u_B^c = \frac{1}{2}R(\varphi_B - \varphi_B^{crk}) \quad if \quad \varphi_A \leq \varphi_A^{crk} \quad and \quad \varphi_B \geq \varphi_B^{crk} \tag{27}$$

$$u_A^c = u_B^c = \frac{1}{2}R(\varphi_A - \varphi_A^{crk}) + \frac{1}{2}R(\varphi_B - \varphi_B^{crk}) \quad if \quad \varphi_A \geq \varphi_A^{crk} \tag{28}$$

CALCULATION PROCEDURE

The determination of the force-deflection relationship is now performed according to the following algorithm.
The starting point is zero rotation, $\varphi_A = \varphi_B = 0$. The rotation φ_B is increased in small steps. The solution of the nonlinear equilibrium equation(9) is determined by using a simple bisection iteration scheme where M_A and M_B is determined on the basis of (16) and (17). For each guess on q_s, φ_A and q are determined from the geometrical equations (10), (11) and (14) by iteration. When corresponding values of loads and rotations are determined as outlined above, the deflections can be obtained from equations (18)-(28). It is checked whether the relation (6) is obtained. Thus, adjusting q_s involves a double bisection iteration scheme: for each guess on φ_A, a new solution for q has to be obtained by using the geometrical equations.

THE DANISH CODE OF PRACTICE

In this section, the results of the analytical model are compared with results which are in accordance with the Danish Code of Practice for the Laying of Underground Rigid Pipelines of Concrete(8). Referring to the Danish Code(8) the ultimate soil pressure is the pressure which results in a tensile stress equal to the stress according to the ultimate test load. The stress is determined by the theory of elasticity.
Corresponding values of test load, tensile stress and maximum vertical soil pressure according to the Danish Code are shown in Table 1. The ultimate test load Q is predicted by a model presented in previous work for a plain normal-strength concrete called 'PC OA00'. This recipe is described by Thygesen(5). The model for prediction of line load behavior is similar to the model presented in this paper. Independently of pipe geometry and fibre volume concentration, this model shows very good agreement with experimental data. See Pedersen(6) for full details.
In figures 7 to 10 theoretical results are shown along with the maximum load q from Table 1. The internal diameters are 100, 300, 600 and 1000 mm corresponding to typical values of 24, 44, 84 and 131 mm of wall thickness. Three load configurations are investigated: only vertical soil pressure ($K_0 = 0$, $k = 0$), only at-rest earth pressure ($K_0 = 0.4$, $k = 0$) and at-rest earth pressure in combination with passive soil resistance ($K_0 = 0.4$, $k = 30$ MPa). Independently of inside diameter, good agreement has been observed between the model

prediction and results which are in accordance with the Danish Code(8)

MAXIMUM ALLOWABLE CRACK OPENING

Determination of the maximum allowable crack mouth opening for pipes subjected to soil pressure is performed according to the following (conservative) approach.
In the serviceability limit state the pipe must be secured against failure caused by any redistribution of soil pressure. Since the line load (test load) is the most disadvantageous load for the pipe cross section, the maximum allowable crack opening for any given pipe cross section ought to be determined from the test load-crack mouth opening curve. When the peak of the test load-crack mouth opening curve is reached, additional loads result in failure of the pipe. Hence the crack mouth opening according to the peak of the test load-crack mouth opening curve is the maximum allowable crack opening in the serviceability limit state.

DESIGN OF FRC PIPES

The model and the design approach presented above now constitute a complete design tool, which can be used when prescribing pipe geometry and fiber reinforcement.
This section represents an example of how this procedure can be used in the design of pipes with an inside diameter of 200mm.

Examples of load-crack mouth opening curves are shown in figures 11 and 12 for recipes 'PC OA00' and 'FRC OA20' respectively. 'FRC OA20' is a fiber reinforced concrete with 2.0 vol.% of straight steel fibers. This recipe is described by Thygesen(5). The inside diameter is d_i = 200mm. Curves for different values of wall thickness are shown. It is observed that the maximum allowable crack mouth openings are approximately 0.01mm and 0.07mm according to the first and second peaks respectively for recipe 'PC OA00'. For recipe 'FRC OA20' the maximum allowable crack mouth openings are approximately 0.14mm.
Examples of vertical pressure-crack mouth opening curves are shown in figures 13 and 14 for recipes 'PC OA00' and 'FRC OA20' for different values of wall thickness. According to the maximum allowable crack opening, the maximum allowable vertical pressure can be determined as a function of wall thickness h.
The maximum allowable vertical pressure as a function of wall thickness is shown in figure 15 for different degrees of fiber reinforcement. 'FRC OA10' is a fiber reinforced concrete with 1.0 vol.% of straight steel fibers. For pipes with an inside diameter of 200mm a reduction to approximately 75% and 55% of the wall thickness can be obtained by a reinforcement of 1 vol.% and 2 vol.% of steel fibers, respectively.

CONCLUSION

Based on the work described here the following conclusion can be drawn:

It has been shown how the M-φ relationship can be used to describe the behavior of FRC pipes subjected to earth pressure. The at-rest earth pressure and the soil reaction are taken into account.

The presented model can be used for material and structural optimization.

For unreinforced concrete pipes good agreement has been observed between the model prediction and results which are in accordance with the Danish Code independently of pipe diameter.

The model indicates that for pipes with an inside diameter of 200 mm a reduction to approximately 75% and 55% of the wall thickness can be obtained by a reinforcement of 1 vol.% and 2 vol.% of steel fibers respectively.

ACKNOWLEDGEMENTS

The work presented in this paper has been carried out at the Department of Structural Engineering (ABK), Technical University of Denmark.
Carsten Pedersen's work has been carried out as an Industrial Research Study, Ph.D. supported by grants from the Danish Academy of Technical Sciences (ATV), VTB-beton a/s, Eurotest aps and the Institute for Product Development (IPU). The study is supervised by Dr. Henrik Stang (ABK), Manager Jens Peter Andreasen (VTB), Manager Poul Rasmussen (Eurotest) and M.Sc. Johan Christian Gregersen (IPU), whom Carsten Pedersen thanks for their inspiring instruction.
The author want to thank the staff at the Department of Structural Engineering for their help during the work.

REFERENCES

1. Marston, A. The Theory of External Loads on Closed Conduits in the Light of the Latest Experiments. Bulletin No. 96, Iowa Eng. Experiment Station, Ames, Iowa, 1930.

2. Sprangler, M. G. The Structural Design of Flexible Culverts. Bulletin No. 153. Iowa Eng. Experiment Station, Ames, Iowa, 1942.

3. Hansen, S., and Thygesen, E. Fibre Reinforced Concrete Pipes. Report, Department of Structural Engineering, Technical University of Denmark, 1990. In Danish.

4. Gustafsson, P. J. Oarmerade betonrörs böjbrottlast och ringbrottlast. Teoretiska beräkningsmetoder. Report TVBM-3012, Division of Building Materials, Univ. of Lund, Sweden. 1983. In Swedish.

5. Thygesen, E. Design of FRC Materials in Structures. Ph.D. thesis, Department of Structural Engineering, Technical University of Denmark, 1993. In Danish.

6. Pedersen, C. Calculation of FRC pipes based on the fictitious crack model. Department of Structural Engineering, Technical University of Denmark, 1995.

7. Pedersen, C. The moment-rotation relationship with implementation of stress-crack width relationships. Department of Structural Engineering, Technical University of Denmark, 1995.

8. Dansk Ingeniørforening's Code of Practice for the Laying of Underground Rigid Pipelines of Concrete, etc, DS 437, Second Edition. Teknisk Forlag. 1986. In Danish.

9. Stang, H., and Aarre, T. Evaluation of Crack Width in FRC with Conventional Reinforcement. 'Cem. Concr. Comp.', 14, 143-154, (1992).

10. Ulfkjær, J.P., Krenk, S., and Brincker, R. Analytical Model for Fictitious Crack Propagation in Concrete Beams. Journal of Engineering Mechanics, Vol. 121, No.1, January, 1995.

11. Hansen, B. Advanced Theoretical Soil Mechanics. Technical University of Denmark. February, 1993.

12. Dansk Ingeniørforening's Code of Practice for Foundation Engineering, DS 415. 3rd ed. Teknisk Forlag. 1984. In Danish.

13. Watkins, R.K., and Nielson, F.D. Development and Use of the Modpares Device in Predicting the Deflection of Flexible Conduits Embedded in Soil. Publ. by ASCE Pipeline Crossing Committee in ASCE Pipe Line Journal, Jan. 1964.

14. Nielson, F.D. Modulus of Soil Reaction as Determined from Triaxial Shear Test. New Mexico State University. Highway Research Record, 46th Annual Meeting. 1966.

15. Christensen, N.H. Elastic instability of pipes subjected to earth pressure. The Danish Geotechnical Institute. 1969. In Danish.

16. Christensen, N.H. Internal paper. The Danish Geotechnical Institute. 1993. In Danish.

NOTATION

The following symbols are used in this paper

d_i	inside diameter
E'	modulus of soil reaction
E_{frc}	Young's modulus of the FRC-material
h	wall thickness
I	moment of inertia
k	modulus of consolidation
K_0	at-rest earth pressure coefficient
l_{cb}	width of the crack band
M	externally applied moment
M_A	moment at point A
M_B	moment at point B
N	axial force
p	shape factor
q	vertical soil pressure
q_s	pressure at side of pipe caused by the change in horizontal diameter
Q	line load on pipe subjected to test load
R	radius of pipe
u_A	deflection at point A. $u_A = u_A^e + u_A^c$
u_B	deflection at point B. $u_B = u_B^e + u_B^c$
u_A^c	deflection at point A due to the rigid-body rotation
u_A^e	deflection at point A due to elastic deformation
u_B^c	deflection at point B due to the rigid-body rotation
u_B^e	deflection at point A due to elastic deformation
w	crack mouth opening
w_0	characteristic crack mouth opening
α	angle from pipe top-point
β	rotation due to elastic deformation
ζh	crack length
ηh	depth of the tensile zone
σ_c	compressive stress
σ^{crk}_{frc}	stress within the fracture process zone, function of the crack width
σ^{u}_{frc}	ultimate tensile strength of the FRC material
σ_t	tensile stress
φ	rigid-body rotation
φ_A	rigid-body rotation at point A
φ_B	rigid body rotation at point B
φ_s	angle of friction of soil
φ^{crk}	rotation by which a crack appears
φ^{crk}_A	rotation by which a crack appears at point A
φ^{crk}_B	rotation by which a crack appears at point B

TABLE CAPTIONS

Table 1 — Corresponding values of Q, σ_t and q according to the Danish Code(8)

FIGURE CAPTIONS

Figure 1 — Distribution of normal stresses in the crack band section. Figure from reference (7)

Figure 2 — A quarter of the cross section modelled as a curved beam until a single crack is formed at top-point B

Figure 3 — A quarter of the cross section modelled as a curved beam when a single crack is formed at top-point B and until a crack appears at point A

Figure 4 — A quarter of the cross section modelled as a curved beam when single cracks have appeared at points A and B

Figure 5 — Equilibrium of forces at a quarter of the cross section

Figure 6 — The deflections u_A^c and u_B^c at points A and B, respectively, due to the rigid-body rotation

Figure 7 — Comparison between the analytical model and results which are in accordance with the Danish Code of Practice for the Laying of Underground Rigid Pipelines of Concrete(8). Unreinforced pipes, d_i = 100 mm

Figure 8 — Comparison between the analytical model and results which are in accordance with the Danish Code of Practice for the Laying of Underground Rigid Pipelines of Concrete(8). Unreinforced pipes, d_i = 300 mm

Figure 9 — Comparison between the analytical model and results which are in accordance with the Danish Code of Practice for the Laying of Underground Rigid Pipelines of Concrete(8). Unreinforced pipes, d_i = 600 mm

Figure 10 — Comparison between the analytical model and results which are in accordance with the Danish Code of Practice for the Laying of Underground Rigid Pipelines of Concrete(8). Unreinforced pipes,

Table 1.

d_i [mm]	h [mm]	Q [kN/m][2]	σ_t [MPa][3]	K_0	q [kN/m^2][4]
100	24	48.8	10.03	0	1002
100	24	48.8	10.03	0.4	2017
300	44	47.0	7.97	0	347.9
300	44	47.0	7.97	0.4	654.3
600	84	76.2	7.05	0	283.7
600	84	76.2	7.05	0.4	530.7
1000	131	104.4	6.57	0	235.1
1000	131	104.4	6.57	0.4	436.7

[2]According to ref(5). Plain concrete: σ^u_{frc} = 4.81 MPa, $w_0 = 2\ 10^{-5}$ and p = 0.71

[3]Tensile stress according to Q. Determined by the theory of elasticity

[4]Vertical soil pressure which results in tensile stress equal to σ_t. Determined by the theory of elasticity

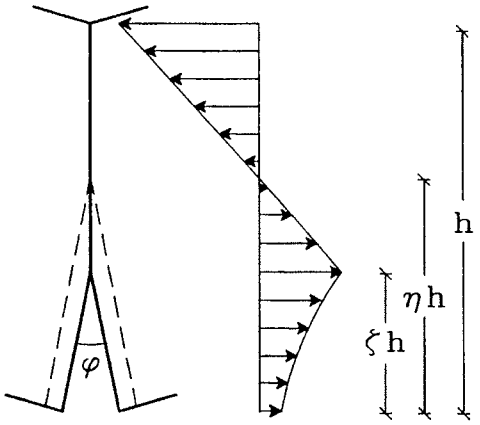

Figure 1

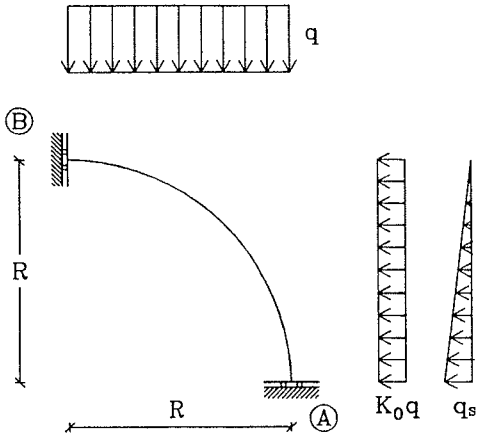

Figure 2

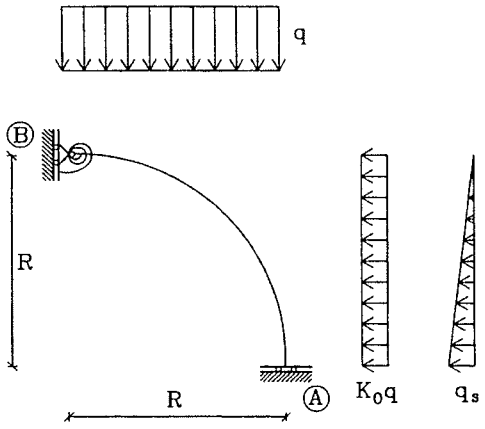

Figure 3

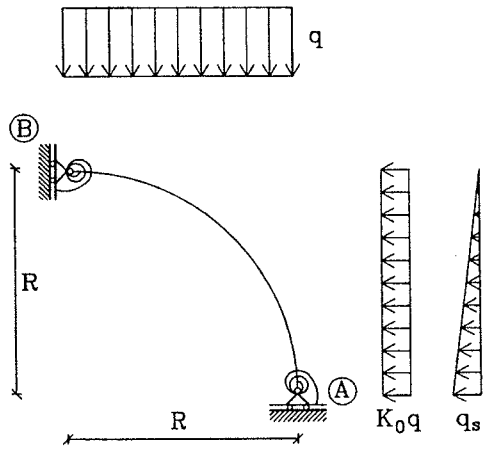

Figure 4

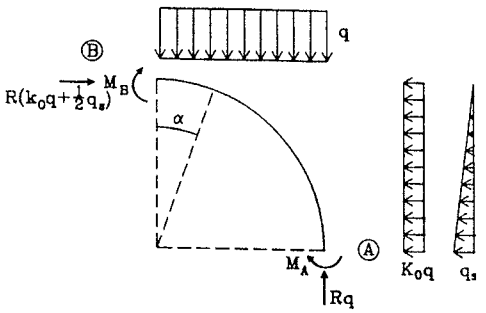

Figure 5

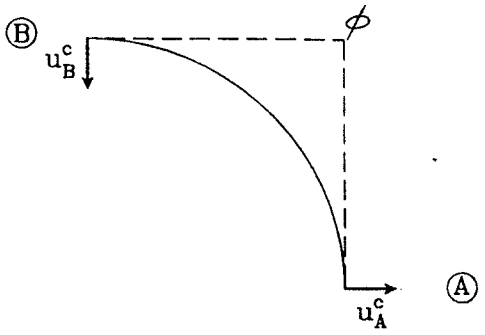

Figure 6

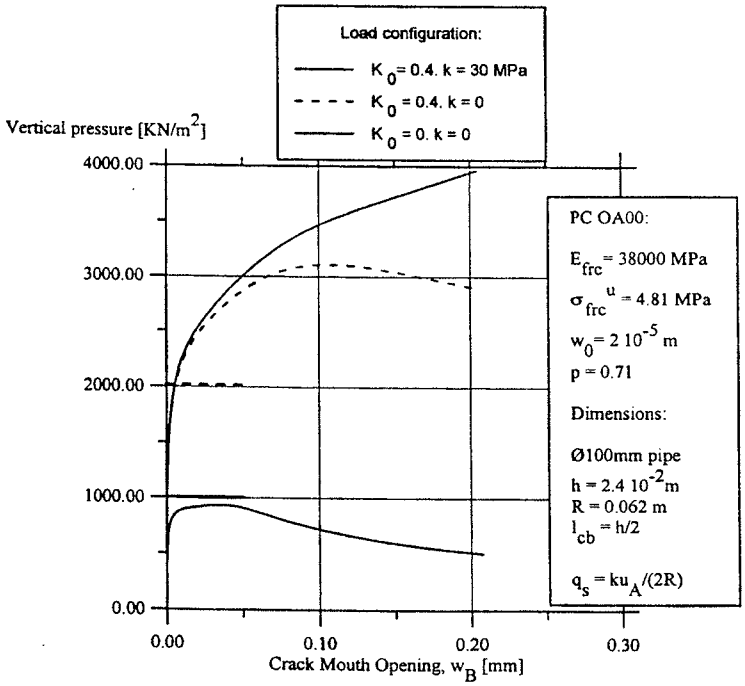

Figure 7

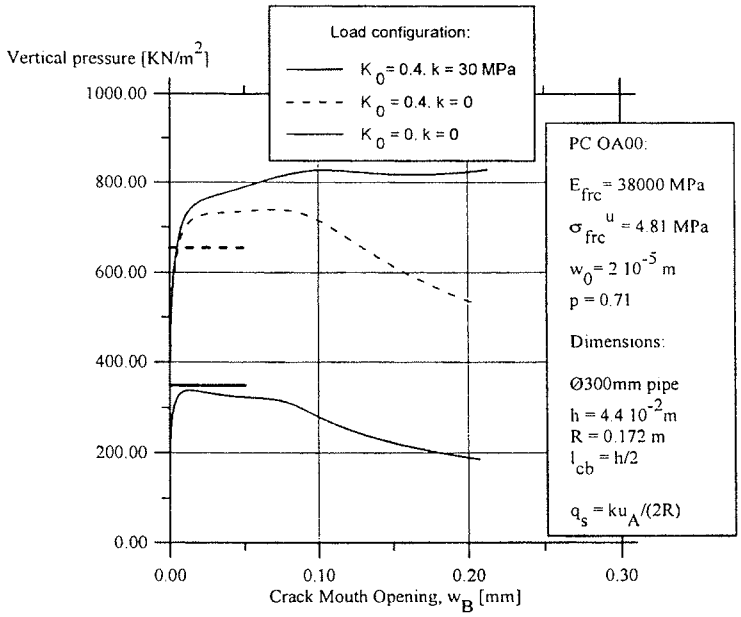

Figure 8

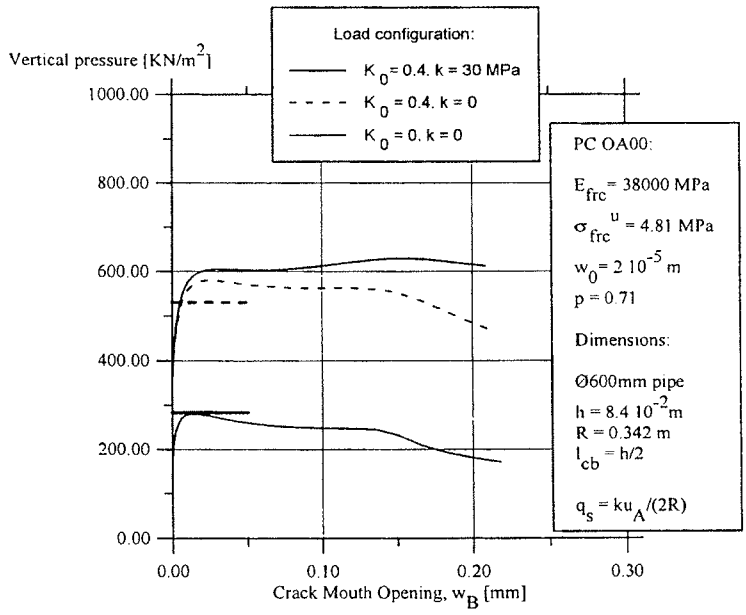

Figure 9

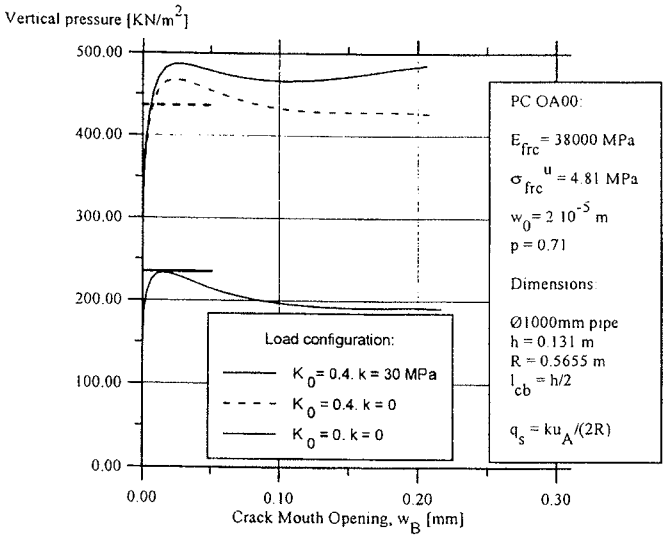

Figure 10

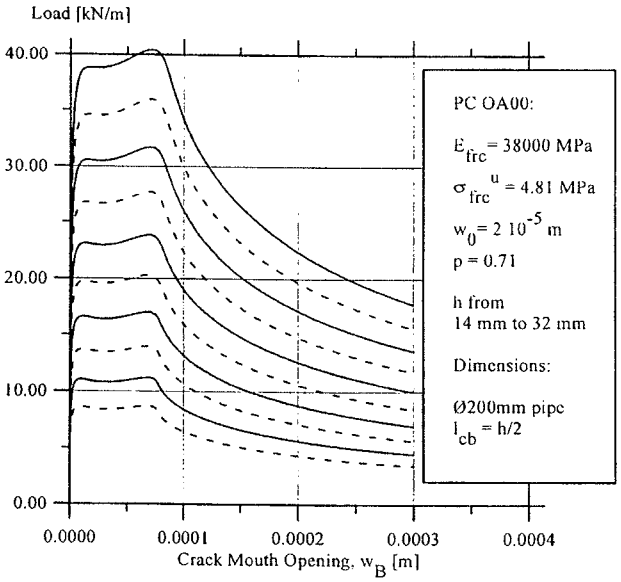

Figure 11

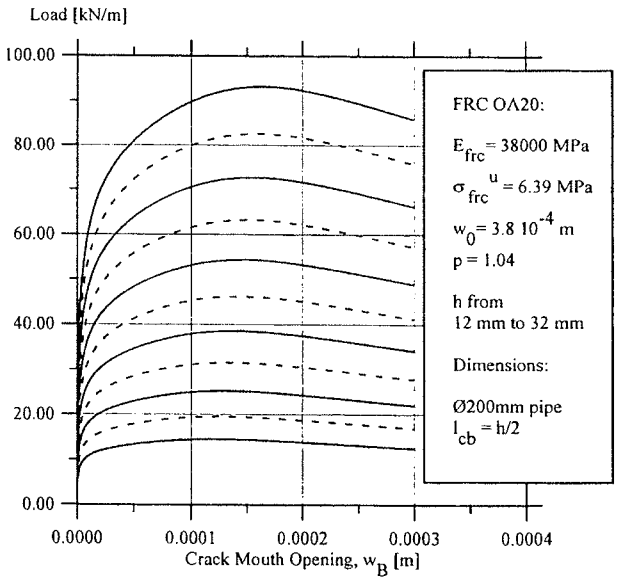

Figure 12

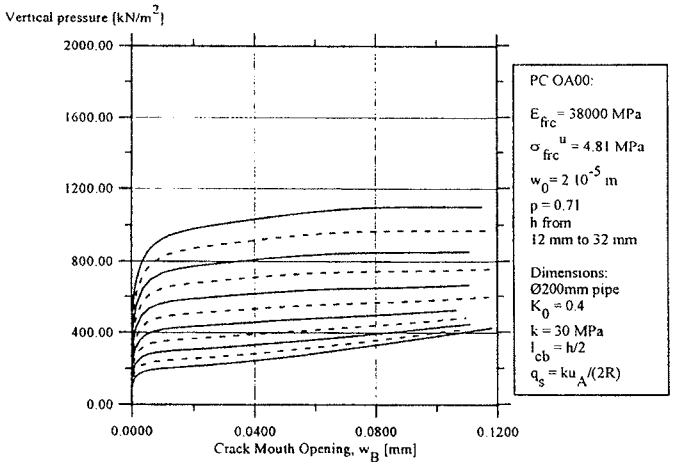

Figure 13

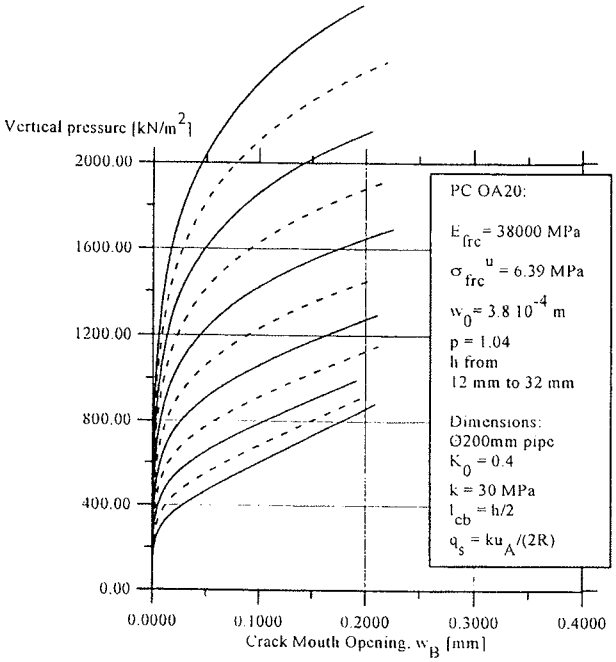

Figure 14

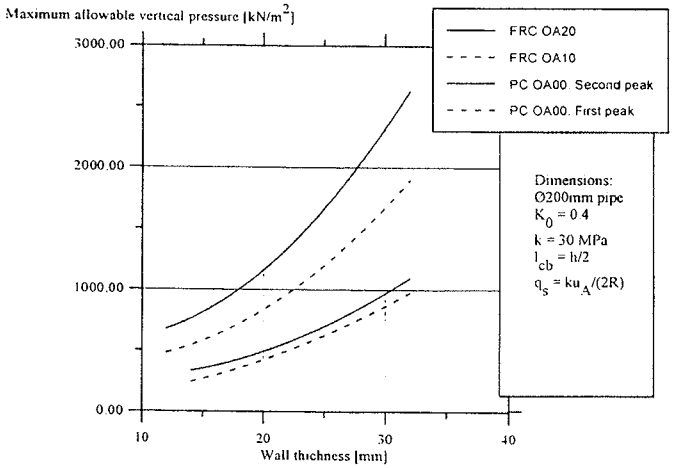

Figure 15

BKM REPORT NO. I6

NEW PRODUCTION TECHNIQUE AND RECIPES FOR FRC MATERIALS

By Carsten Pedersen[1]

ABSTRACT

A new technique for production of fiber reinforced concrete (FRC) profiles has been in the process of development in Denmark during the past two years. This manufacturing process is similar to the well-known extrusion technique. This paper describes two simple tests which model the new process. These tests are intended to investigate the extrudability of new mixtures and the material properties which can be obtained. The paper furthermore presents a model for description of the extrusion process and for prediction of the output rate of the process.

INTRODUCTION

During the past two years, a new technique for production of FRC profiles has been in the process of development in Denmark at VTB-beton a/s, the Department of Structural Engineering, the Technical University of Denmark and the Institute for Product Development. This manufacturing process is similar to the well-known extrusion technique, see e.g. Shao, Marikunte and Shah(1). Like extrusion, this new process is an economical mass-production method.

The success of traditional extrusion depends on the mixture, see e.g. Thygesen(2). The liquid phase and the cementitious constituents must not separate under application of pressure. When subjected to pressure the mixture must be plastic enough to flow into the die cross section, yet rigid enough to resist deformation after it exits the die. The mixture must not stick to the die and must yield a smooth surface after extrusion. These requirements significantly limit the composition of mixtures for extrusion.

This new manufacturing process resolves these problems. Fibers and powder material are mixed with an appropriate amount of water. The water is then drained out by this new technique, which is based on a simple mechanical operation. The driving force which causes water to flow is a confinement pressure. When applying pressure the material instantaneously builds up into a stable mass with the required profile. See Pedersen(3) for full details.

In this study we adopt Darcy's law to derive a simple model for the dewatering process. On the basis of some simple tests the model predicts the output rate of the extrusion process for a given confinement pressure and a given recipe. Reasonable agreement has been observed

---

[1] Industrial Ph.D. student, VTB-beton a/s, Dandyvej 11, DK-7100 Vejle, Denmark

between the model prediction and experimental data for FRC recipes, see(3).
This paper describes two simple consolidation tests which model the dewatering process used in the new manufacturing technique. The aim of these tests is to form the basis of the full scale extrusion tests, see ref(3).
The first of these tests is intended to investigate:

- the extrudability of new mixtures. The mixtures must be rigid enough to resist deformation and must yield a smooth surface after extrusion.
- how the material properties are influenced by the dewatering process parameters (confinement pressure and confinement time).

The second of these tests is intended to investigate:

- how the dewatering process (confinement pressure and confinement time) and the output rate are influenced by the content of admixtures.
- how the presented analytical model can be used to predict the output rate of the extrusion process independently of the production pressure.

Furthermore this test series has been developed to gain qualitative experience with the production technique.

MIXING PROCEDURE

A series of cylindrical FRC specimens was manufactured as described in the section below and tested in the laboratory. The diameter of all specimens was 25 mm and a length of 80-100 mm was aimed at for all the specimens. The dimensions of the specimens are similar to those of the specimens used by Krenchel(4), who worked with a microfiller material and by Dela and Stang(5), who worked with fracture energy of cement paste cylinders.

Firstly the Crack-Stop fibers were mixed with the powder material and Tylose powder and were dispersed by high gravity shaking. Then the powder material was mixed with water using a 1 litre Braun "food processor". By weight the water-dry material ratio was typically 2:3. After two minutes of mixing, Krenit fibers were added continuously over the next two minutes of mixing.

TEST SETUP AND PROCEDURE

In the former test, the slurry was poured into a special cylindrical mould, which consisted of a perforated pipe (inside diameter: 25 mm, length: 200 mm) and two pistons (outside diameter: 25 mm) with a length of 50 mm and 200 mm, respectively, the former being placed on a foot. See figure 1.
When the slurry had been poured into the perforated pipe, the two pistons were pushed into the pipe from both ends. Then the mould containing the slurry was weighed to determine the

exact quantity of slurry. The mould was then placed in a 10 kN Instron testing machine (type: 6022) where pressure was put on the 200 mm piston so that the material could consolidate and water drain out slowly. See figure 2. Corresponding values of time, confinement pressure and settlement of the piston were measured. Finally, the solid specimen was pressed out and examined (measured and weighed). See figure 3.

The test procedure and test equipment used in the second test was similar to the procedure and equipment described in the section above, except that the pipe mould was perforated only in the bottom. See figure 4.

TESTING FRC SPECIMENS

Three-point bending tests were carried out over a span of 60 mm at a cross-head speed of 0.02 mm/s. Load and deflection were measured until a total mid-span deflection of 2.5 mm was reached. Each test took about 2 minutes. See figure 5. The ultimate bending strength, σ_b is determined from the load at peak point. $\sigma_b = M/W$.
All tests were carried out in a 10 kN Instron closed-loop testing machine (type: 6022) with two Instron extensometers (type 2620-602).

The variables in the test programme were type of matrix material, fibre volume concentration, cross-head speed in the process of consolidating, and final confinement pressure.

A total of 93 specimens were made to cover this programme as shown in Tables 1-4.

MATRIX

The basic powder material was ordinary Danish rapid-hardening Portland cement (RC, grain density: $\gamma_k = 3.15$, median particle size: $d_{50/50} \sim 14$ μm). This cement was combined with five different types of material: Silica powder (Elkem Silica: ES, $\gamma_k = 2.17$, $d_{50/50} \sim 1\text{-}5$ μm), quartz powder (QS, $\gamma_k = 2.62$, $d_{50/50} \sim 24$ μm), beach sand (BS, $\gamma_k = 2.20$, $d_{max} \sim 250$ μm) and ordinary Danish fly ash (FA, $\gamma_k = 2.20$, $d_{50/50} \sim 50$ μm)

In the present study methylhydroxyethylcellulose(MHEC) is used to increase the viscosity of the mixing water. The MHEC used in this study is produced by the German company Hoechst under the name Tylose FL15002, see ref(6). Tylose was used by Thygesen(2) and Strabo et al.(7), who worked with traditional extrusion of fiber reinforced concrete.
The content of Tylose FL15002 was based on tests which aimed at optimizing the amount of Tylose in the actual mix. The Tylose-water-ratio by weight was typically: 0.20% - 0.53%.

FIBERS

The fibers used were polypropylene Crack-Stop fibers and polypropylene Krenit fibers. The polypropylene fibers are produced in Denmark by Cemfiber, see ref(8) and (9). The

polypropylene Krenit fibers were of a special type, with improved bonding. The properties of the fibers are listed in Table 5.

MODEL, DEWATERING PROCESS

In this section, a simple analytical model for description of the dewatering process is presented. Based on the second of the simple consolidation tests described above, this model is intended to determine how the output rate of the extrusion process is influenced by the mixture (e.g. the content of Tylose) and the production (confinement) pressure.

Consider an amount of drained material with cross-sectional area A and length l in contact with cement paste subjected to confinement pressure p. See figure 4. It is assumed that the minimum distance which a water particle must flow is equal to the length of the drained material l. This condition is called single drainage. It is assumed that the water flow dV/dt is proportional to the build-up of stable material Adl/dt:

$$\frac{dV}{dt} = \beta A \frac{dl}{dt} \tag{1}$$

where t is the elapsed time and β is a proportionality constant. The driving force which causes water to flow is the drop in pressure p. The quantity of water flowing past the cross-sectional area A may be expressed by the formula:

$$\frac{dV}{dt} = \alpha A \frac{p}{l} \tag{2}$$

where l is the distance over which the drop in pressure occurs and α is a proportionality constant. The expression is known as Darcy's law. See e.g. Spangler and Handy(10).
Substituting dv/dt from (1) in (2), the following equation is obtained:

$$l \frac{dl}{dt} = \frac{\alpha}{\beta} p \tag{3}$$

The problem of solving the differential equation (3) is separated into two different cases.
In the first case, the confinement pressure is increased linearly p(t) = at. Hence, the solution is given by:

$$l = \sqrt{l_0^2 + \frac{a\alpha}{\beta} t^2}, \quad p(t) = at \tag{4}$$

where l_0 is the initial length of the drained material.
In the second case, the confinement pressure is constant p(t) = p. Hence:

$$l = \sqrt{l_0^2 + \frac{p\alpha}{2\beta} t}, \quad p(t) = p \tag{5}$$

EXPERIMENTAL RESULTS AND DISCUSSION

To investigate how the material properties are influenced by confinement pressure and confinement time a series of specimens was manufactured and tested as described above. A total of 93 specimens were made in this way to cover the programme as shown in Tables 1-4. Details of fiber volume concentration, length of specimens and bending strengths are shown for the recipes tested in this programme. The bending strength was measured after approximately 2 minutes and after 90 minutes to estimate the degree of stability of the extruded material (expressed by the bending strength). To estimate the material properties of the hardened specimens the bending strength was measured after 7 days. The specimens were placed in a normal moist curing chamber (20^0C, 95% RH) until the time of testing.

Tables 1 and 2 show how the stability of the material (expressed by the bending strength after 2 min. and after 90 min.) is influenced by the cross-head speed and the final confinement pressure for a cement paste reinforced with 1.85 vol-% of 3mm Crack-Stop fibers. For the experimental results shown in Table 1 the confinement pressure was increased to 2.5, 5, 10 and 20 MPa respectively at a cross-head speed of 0.1 mm/s. In this case 2.5 MPa was the minimal final confinement pressure at which stability of the specimens could be obtained. For the experimental results shown in Table 2 the confinement pressure was increased to 7.5, 10 and 20 MPa respectively at a cross-head speed of 0.5 mm/s. In this case 7.5 MPa was the minimal final confinement pressure at which stability of the specimens could be obtained. The calculation of the porosity is based on the weight of the specimens after dehydration (105^0C for about 3 days), the length of the specimens and the assumption that no powder material is lost during the consolidation process.

In figure 6 the bending strength approx. 90 min. after consolidation is shown as a function of the final confinement pressure and cross-head speed. Results from Tables 1 and 2. It is observed that the bending strength increases as a function of the final confinement pressure and decreases as a function of the cross-head speed.

Figure 7 shows the bending strength as a function of the porosity. Results from tables 1 and 2. It is observed that the bending strength decreases as a function of the porosity.

Table 1 shows that the bending strength after 2 min. is approx. 50% of the bending strength after 90 min. Typical examples of experimental values of bending stress as a function of mid-point displacement are shown in figure 8. In this case the confinement pressure was increased to 20 MPa at a cross-head speed of 0.1 mm/s and the specimens were tested after approx. 90 min. Figure 9 shows the bending stress as a function of the mid-point displacement for specimens tested after 7 days.

Tables 3 and 4 show how the bending strength and the porosity are influenced by the composition of the matrix. The reinforcement is 6 mm Krenit special fine combined with 3 mm Crack-Stop fibers. It is observed that the highest bending strength is obtained with a

matrix containing cement combined with 13 weight-% of silica, quarts and fly ash. Furthermore these results indicate that with the test equipment used in this programme stability of the specimens can be obtained if about 40% of the powder material is cement combined with equal parts of silica, quartz and fly ash.

To investigate how the dewatering process (time, pressure, settlement) is influenced by the content of Tylose a series of tests was performed. See figure 4.
The confinement pressure was increased linearly from 0 MPa to 10 MPa within 2 minutes and held at 10 MPa for 2 minutes. Examples of corresponding values of confinement pressure and settlement are shown in figures 10 to 14. Examples of corresponding values of settlement and time are shown in figures 15 to 19. The content of Tylose is 0.00, 0.05, 0.10, 0.20, and 0.40 % of the cement weight respectively. The recipe was cement paste with a water-cement-ratio by weight of 0.44 reinforced with 2.3 vol. % of 3mm Crack-Stop fibers. The settlement s is proportional to the amounts of water drained out of the test specimens:

$$s = \frac{V}{A} \tag{6}$$

Given $l_0 = 0$, equation (1), (4) and (6) give the following expression for the inclination of the s-t curve caused by the confinement pressure p(t) = at:

$$\frac{ds}{dt} = \sqrt{a\alpha\beta} \tag{7}$$

where β is mainly influenced by the content of water. Given β, α can be obtained from equation (7):

$$\alpha = \frac{1}{a\beta}\left(\frac{ds}{dt}\right)^2 \tag{8}$$

where ds/dt is determined as the inclination of the s-t curve caused by the confinement pressure p(t) = at. It is assumed that $\beta = 0.3$ for the recipes used in this study.
Corresponding values of ds/dt and α are shown in Table 6 for the tests shown in figures 10-19. Table 6 also shows the length of the drained material and the length of the drained material determined by equations (4), (5), (7) and (8). The content of Tylose is 0.00, 0.05, 0.10, 0.20, and 0.40 % of the cement weight. Reasonably good agreement with experimental results is obtained. Application of this model in the extrusion of FRC pipes will be shown in a subsequent paper(3).

CONCLUSION

Based on the work described here the following conclusion can be drawn:

An analytical model for description of a new extrusion process has been presented. Reasonably good agreement with experimental results has been obtained for the recipes tested in this programme.

With the test equipment used in this programme, stability of the specimens can be obtained if about 40% of the powder material is cement combined with equal parts of silica, quarts and fly ash. Stability of the specimens can be obtained if about 50% of the powder material is cement combined with equal parts of silica, quartz sand, fly ash and beach sand.

More work and experience are needed to investigate how the production process is influenced by the composition of the material and by the parameters of the dewatering process.

ACKNOWLEDGEMENTS

The work presented in this paper has been carried out at the Department of Structural Engineering (ABK), Technical University of Denmark.
Carsten Pedersen's work has been carried out as an Industrial Research Study, Ph.D. supported by grants from the Danish Academy of Technical Sciences (ATV), VTB-beton a/s, Eurotest aps and the Institute for Product Development (IPU). The study is supervised by Dr. Henrik Stang (ABK), Manager Jens Peter Andreasen (VTB), Manager Poul Rasmussen (Eurotest) and M.Sc. Johan Christian Gregersen (IPU), whom Carsten Pedersen thanks for their inspiring instruction.
The author want to thank the staff at the Department of Structural Engineering for their help during the work.

REFERENCES

1. Shao, Y., Marikunte, S., and Shah, S.P. Extruded Fiber Reinforced Composites. Concrete International, April 1995.

2. Thygesen, E. Design of FRC materials in structures. Ph.D. thesis, Department of Structural Engineering, Technical University of Denmark, 1993. In Danish.

3. Pedersen, C. Extruded Fiber reinforced pipes. Department of Structural Engineering, Technical University of Denmark, 1996.

4. Krenchel, H. Microfiller Material for HPFRCC. Department of Structural Engineering, Technical University of Denmark, 1995.

5. Dela, B. F., and Stang, H. Determination of Fracture Energy of Cement Paste Cylinders in 3 Point Bending. Department of Structural Engineering, Technical University of Denmark, 1995.

6. Tylose. Hoechst Limited Company, D-6230 Frankfurt am Main 80. 1995. In German.

7. Strabo, F., Clauson-Kaas, N.F., Just Andersen, P. and Thaulow, N. Extrusion of Fiber reinforced Concrete. Technological Institute, Denmark. 1987. In Danish.

8. Specification paper. Crack-Stop fibers. Cemfiber A/S, DK-8800 Varde, Denmark. November 1994.

9. Specification paper. Krenit fibers. Cemfiber A/S, DK-8800 Varde, Denmark. November 1994.

10. Spangler, M.G., and Handy, R.H. Soil Engineering. Third Edition. Iowa State University. Intext Educational Publishers. 1973.

NOTATION

The following symbols are used in this paper

a	see equation (4)
A	cross-sectional area of drained material
d	diameter of test specimens
$d_{50/50}$	median particle size
d_f	diameter of fiber
E_f	Young's modulus of the fiber material
I	moment of inertia
l_0	initial length of drained material
l	length of drained material
L	length of test specimens
L_f	length of fiber
M	bending moment at peak point
p	confinement pressure
s	settlement
t	elapsed time
V	amounts of drained material
W	section modulus
α	see equation (2)
β	see equation (1)
γ_k	grain density
γ_f	density of fiber material
σ_b	ultimate bending strength

TABLE CAPTIONS

Table 1 Corresponding values of final confinement pressure, length of specimens, vol-% of fibers, porosity obtained and bending strength for specimens consolidated at a cross-head speed of 0.1 mm/s.

Table 2 Corresponding values of final confinement pressure, length of

specimens, vol-% of fibers, porosity obtained and bending strength for specimens consolidated at a cross-head speed of 0.5 mm/s.

Table 3 Corresponding values of length of specimens, vol-% of fibers, porosity obtained and bending strength for specimens consolidated to 20 MPa at a cross-head speed of 0.1 mm/s.

Table 4 Corresponding values of length of specimens, vol-% of fibers, porosity obtained and bending strength for specimens consolidated to 20 MPa at a cross-head speed of 0.1 mm/s.

Table 5 Properties of fibers

Table 6 Corresponding values of ds/dt, α and l as a function of the content of Tylose.

FIGURE CAPTIONS

Figure 1 The special cylindrical mould. This mould consist of a perforated pipe (inside diameter: 25 mm, length: 200 mm) and two pistons (outside diameter: 25 mm) with a length of 50 mm and 200 mm, respectively, the former placed on a foot

Figure 2 Consolidation of the FRC material

Figure 3 Pressing out the solid specimens

Figure 4 Model for description of the dewatering process

Figure 5 Three-point bending test

Figure 6 Bending strength approx. 90 min. after consolidation as a function of the final confinement pressure and cross-head speed

Figure 7 Bending strength as a function of porosity

Figure 8 Experimental values of bending stress as a function of mid-point displacement. Tested after 90 min

Figure 9 Experimental values of bending stress as a function of mid-point displacement. Tested after 7 days

Figure 10 Confinement pressure as a function of settlement. Tylose 0.00% of

Table 1.

Recipe, RC-ES-QS-FA-BS (weight-%) : 100/0/0/0/0
Vol-% of Crack-Stop fibre(3mm) : 1.85
Cross-head speed(mm/s) : 0.1

Final confinement pressure (MPa)	2.5	5	5	10	20	20
Length of specimens (mm)	73 96 85 94	85 86 71 82 84	94.5 101.5 93 91.5	68 81 66 67	78 77 81 80 83	89.5 74.8 93.5 77.5 77.0
Vol-% obtained of Crack-Stop fibre	2.76 2.69 2.62 2.58	2.88 2.93 2.89 2.90 2.85	2.79 2.79 2.80 2.80	3.14 3.08 3.07 3.16	3.19 3.22 3.27 3.29 3.26	3.16 3.05 3.13 3.16 3.11
Porosity obtained (%)	47.5 48.0 50.9 51.8	44.5 43.8 44.0 44.5 45.1	47.3 46.7 47.0 46.4	40.8 42.3 43.5 42.8	39.2 39.2 39.2 38.0 39.0	40.7 43.1 42.0 40.8 41.9
σ_b (after 2 minutes) (MPa)			0.07 0.11 0.11 0.07			0.23 0.19 0.37 0.27 0.26
σ_b (after ~90 minutes) (MPa)	0.15 0.13 0.16 0.11	0.27 0.19 0.17 0.21 0.22		0.26 0.33 0.25 0.28	0.40 0.43 0.49 0.43 0.50	

Table 2.

Recipe, RC-ES-QS-FA-BS (weight-%) : 100/0/0/0/0
Vol-% of Crack-Stop fibre(3mm) : 1.85
Cross-head speed(mm/s) : 0.5

Final confinement pressure (MPa)	7.5	10	20
Length of specimens (mm)	105 100 102 99 112	90 76 82 99	80 72 80
Vol-% obtained of Crack-Stop fibre	2.64 2.62 2.69 2.72 2.69	2.95 2.91 2.82 2.83	3.13 3.07 3.14
Porosity obtained (%)	49.6 50.2 49.0 48.6 49.0	44.9 45.6 46.2 46.4	41.3 42.7 42.0
σ_b (after ~90 minutes) (MPa)	0.13 0.12 0.13 0.09 0.13	0.23 0.12 0.12 0.25	0.29 0.23 0.28

Table 3.

Final confinement pressure(MPa): : 20
Cross-head speed(mm/s) : 0.1

Recipe, RC-ES-QS-FA (weight-%)	100/0/0/0	90/10/0/0	90/0/10/0	90/0/0/10
Vol-% of Krenit fibre(6mm spe. fine)	1.93	1.85	1.86	1.85
Vol-% of Crack-stop fibre(3mm)	1.69	1.62	1.63	1.62
Length of specimens (mm)	75.7 60.9 72.4 68.0 66.6 70.9	67.5 92 81.5 69 101 90 93	74 78 77 83 81.5 80	78 73.5 66 83 80 82
Vol-% obtained of Krenit fibre	3.61 3.98 3.56 4.14 4.31 4.09	2.90 2.91 3.05 3.07 2.82 2.98 3.03	3.64 3.37 3.42 3.56 3.68 3.48	2.99 3.19 3.15 2.98 3.04 3.04
Vol-% obtained of Crack-Stop fibre	3.16 3.48 3.11 3.62 3.77 3.58	2.53 2.54 2.67 2.69 2.46 2.60 2.64	3.18 2.95 2.99 3.11 3.22 3.04	2.62 2.79 2.75 2.60 2.66 2.65
Porosity obtained (%)	39.5 40.2 40.5 42.9 42.2 43.8	40.2 40.2 37.8 38.0 45.6 43.3 41.9	38.6 38.3 37.4 41.4 41.6 41.3	40.1 39.5 38.0 44.5 43.5 43.9
σ_b (after 7 days) (MPa)	6.77 5.08 3.49	8.87 8.53 10.31 7.42	6.38 3.35 4.64	7.01 5.48 5.79
σ_b (after ~90 minutes) (MPa)	0.15 0.18 0.14	0.28 0.39 0.23	0.20 0.18 0.16	0.23 0.22 0.13

Table 4.

Final confinement pressure(MPa): : 20
Cross-head speed(mm/s) : 0.1

Recipe, RC-ES-QS-FA-BS (weight-%)	76/8/8/8/0	61/13/13/13/0	40/20/20/20/0	65/7/7/7/14
Vol-% of Krenit fibre(6mm spe. fine)	1.71	1.23	0.85	1.40
Vol-% of Crack-Stop fibre(3mm)	1.50	1.07	0.74	1.23
Length of specimens (mm)	91 88 69 79 69 79	90 93.5 88.5 98 70.5 84	93.5 76 69 73.5 82 85	87.5 79.5 81 71 85 93.5
Vol-% obtained of Krenit fibre	2.39 2.56 2.62 2.60 2.74 2.59	1.90 1.83 1.86 1.81 1.78 1.83	1.21 1.23 1.27 1.38 1.19 1.30	2.22 2.26 2.16 2.20 2.16 2.10
Vol-% obtained of Crack-Stop fibre	2.09 2.24 2.29 2.27 2.40 2.26	1.66 1.60 1.63 1.58 1.55 1.60	1.06 1.08 1.11 1.20 1.04 1.14	1.95 1.98 1.90 1.93 1.90 1.84
Porosity obtained (%)	43.0 38.7 37.0 42.0 39.2 41.6	34.2 36.6 35.4 40.5 43.0 38.6	38.7 38.3 - 37.1 41.8 38.1	35.5 34.6 37.0 39.8 40.2 41.8
σ_b (after 7 days) (MPa)	6.49 6.72 7.89	11.48 10.74 8.76	4.75 5.38 7.52	5.22 5.53 4.56
σ_b (after ~90 minutes) (MPa)	0.50 0.57 0.40	0.57 0.43 0.70	0.47 0.36 0.47	0.29 0.30 0.27

Table 5.

Fibre	L_f [mm]	d_f [µm]	γ_f [kg/l]	E_f [GPa]
Krenit fine(quality:special)	6	40x250[a)]	1.01	12
Krenit extra fine, WEFF(quality:special)	6	40x100[a)]	1.01	12
Crack-Stop	3,6,12	18	0.91	4

a):rectangular cross-section

Table 6.

Recipe, RC-ES-QS-FA-BS (weight-%) : 100/0/0/0/0
Vol-% of Crack-Stop fibre(3mm) : 2.3
Assumption, β : 0.3

Content of Tylose [% of cement weight]	0.00	0.05	0.10	0.20	0.40
ds/dt [mm/s]	0.218	0.117	0.0792	0.0542	0.0292
α [mm^4/Ns]	1.9	0.55	0.25	0.12	0.034
Length of specimens, test [mm]	-	100	40	20	8
Length of specimens, predicted by equations (4)and(5) [mm]	-	57	39	27	14

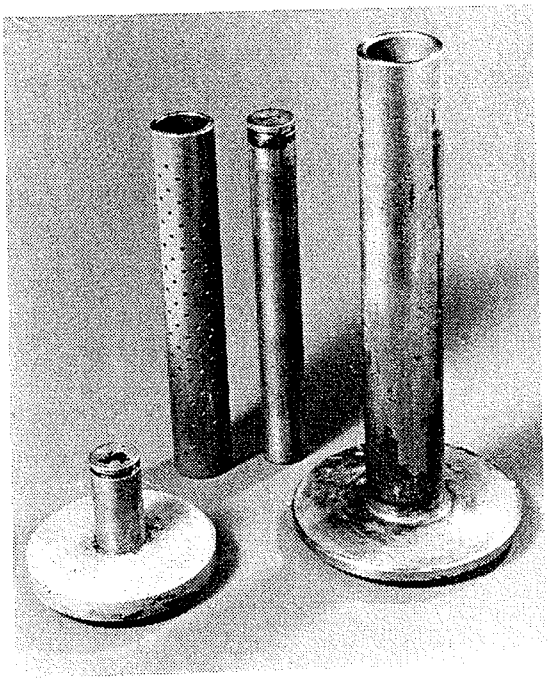

Figure 1

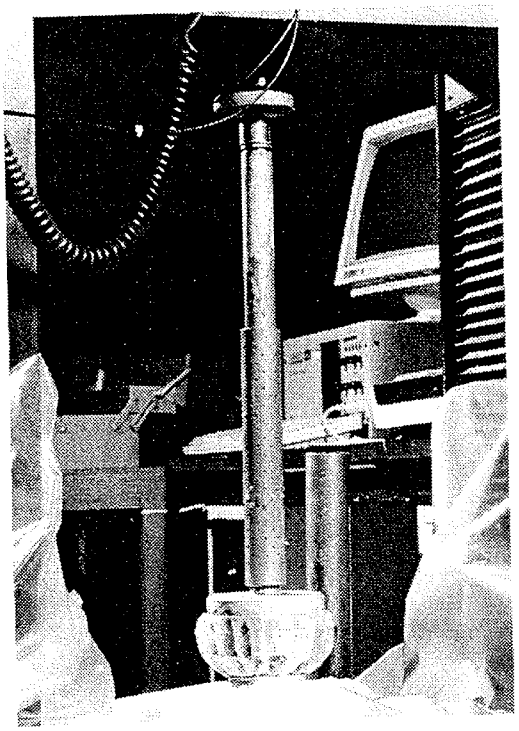

Figure 2

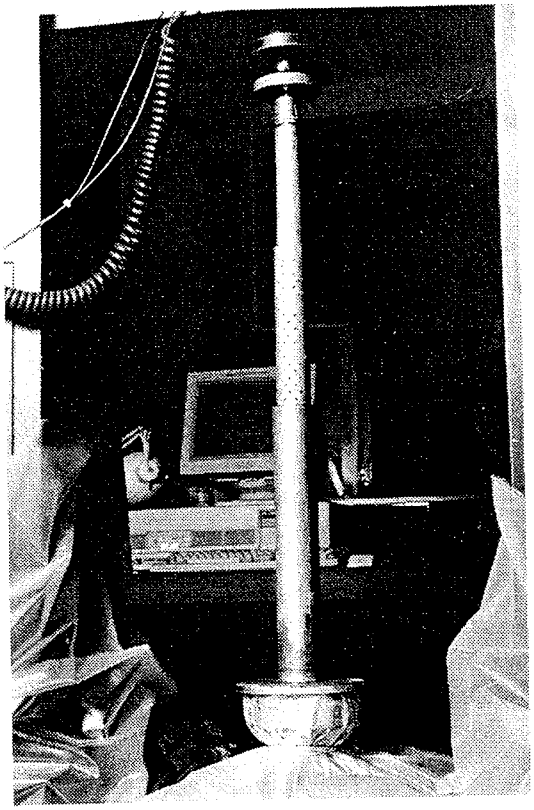

Figure 3

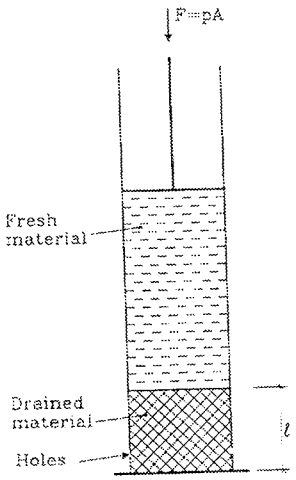

Figure 4

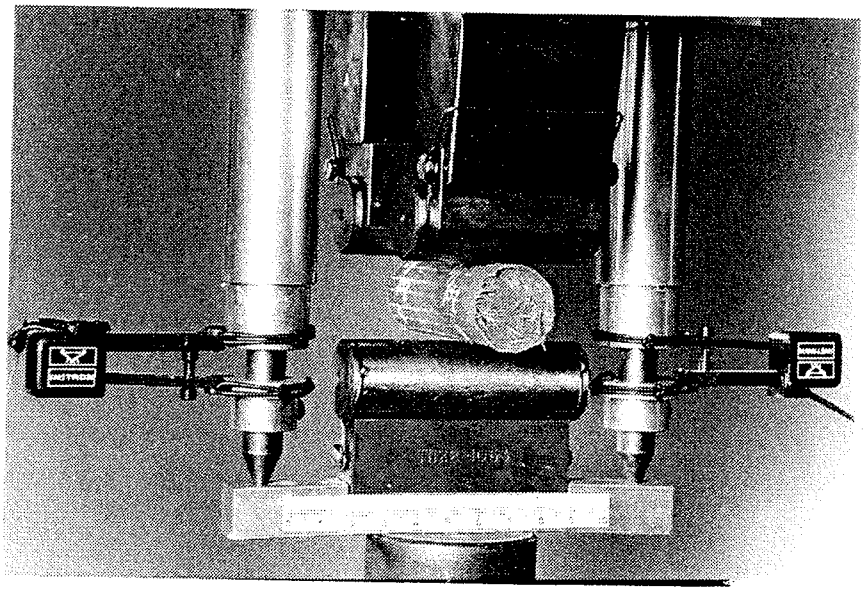

Figure 5

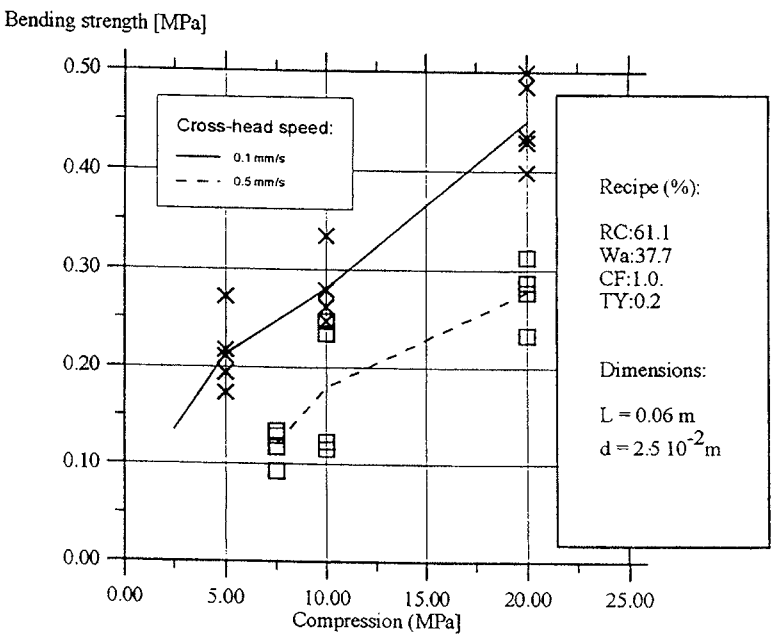

Figure 6

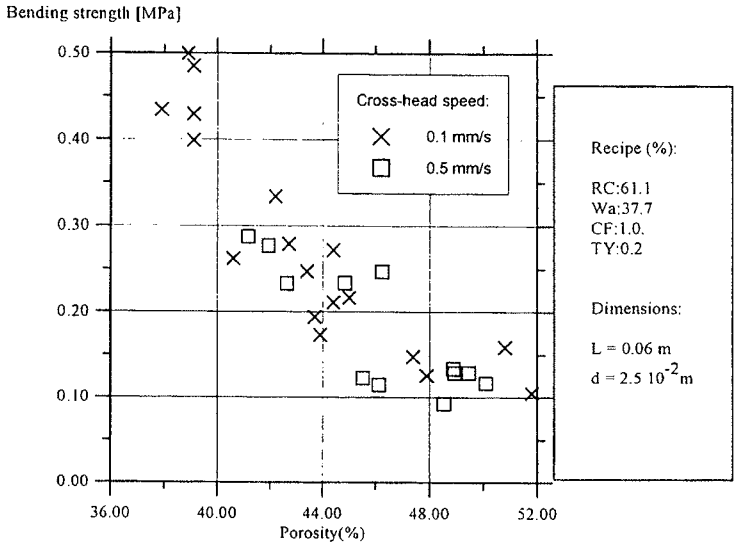

Figure 7

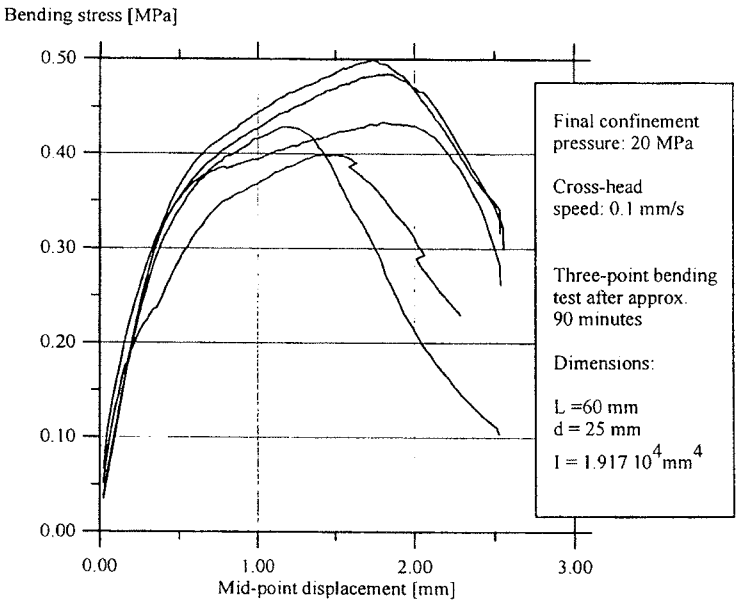

Figure 8

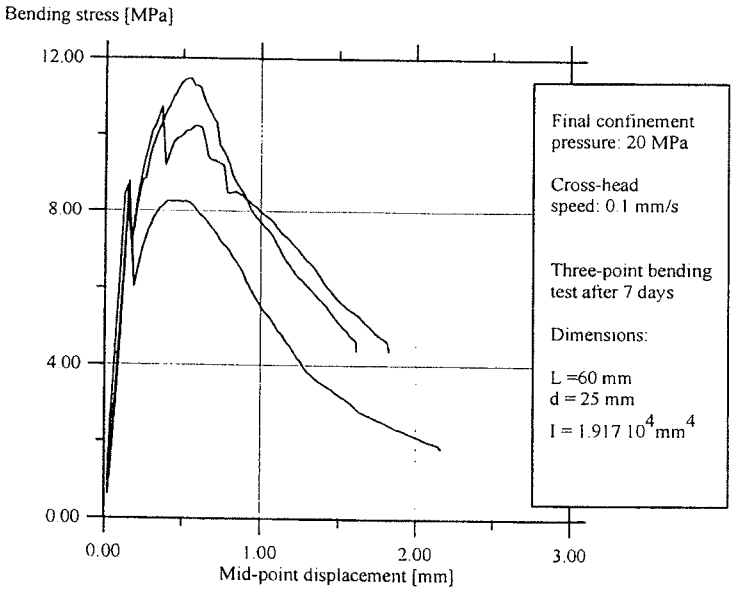

Figure 9

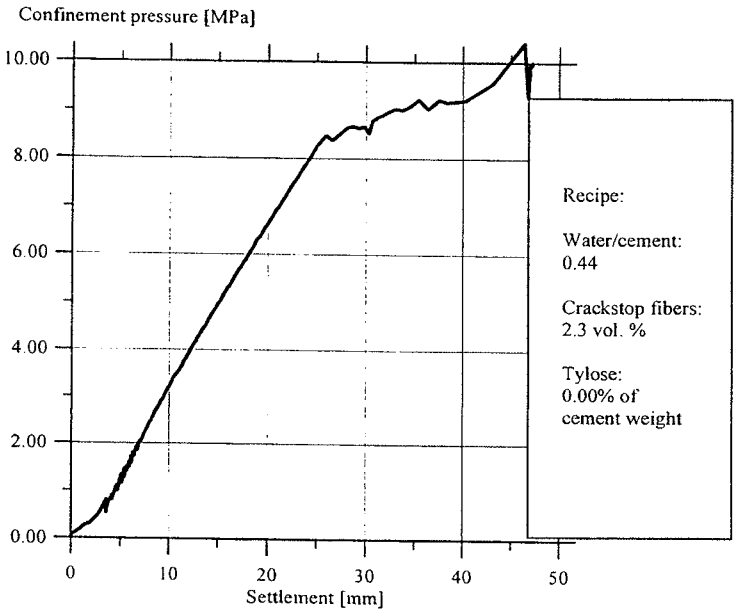

Figure 10

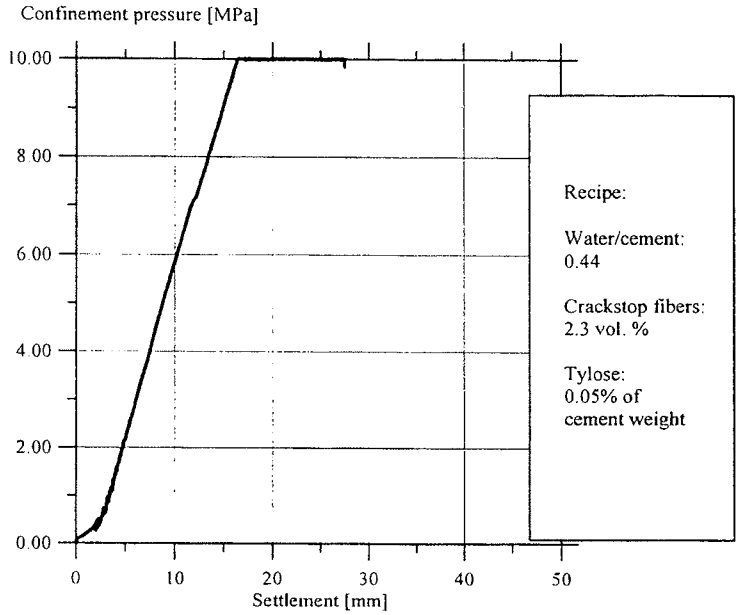

Figure 11

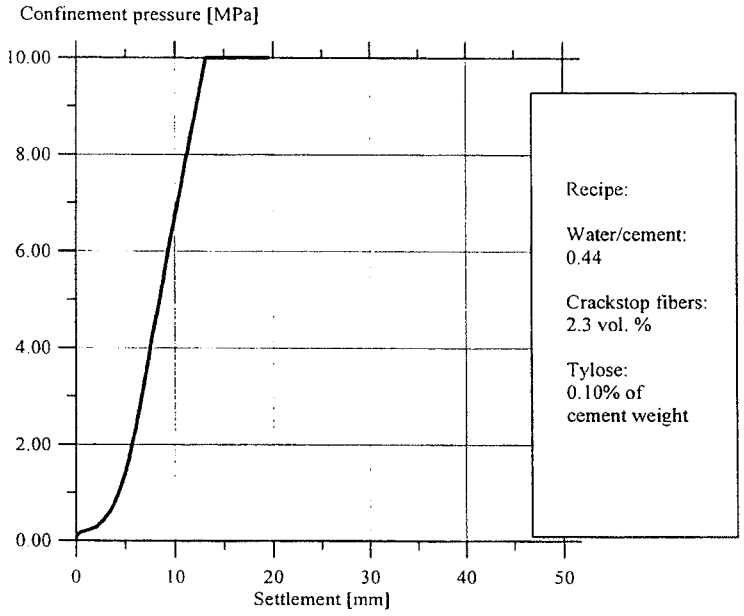

Figure 12

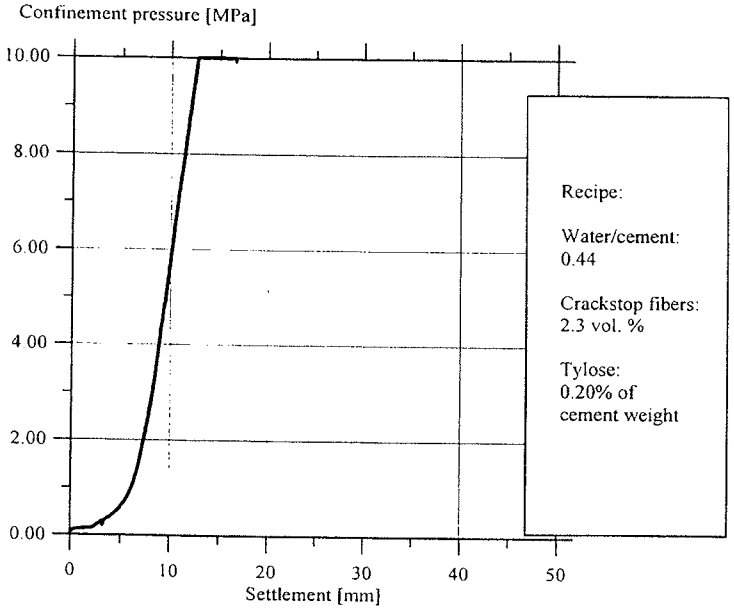

Figure 13

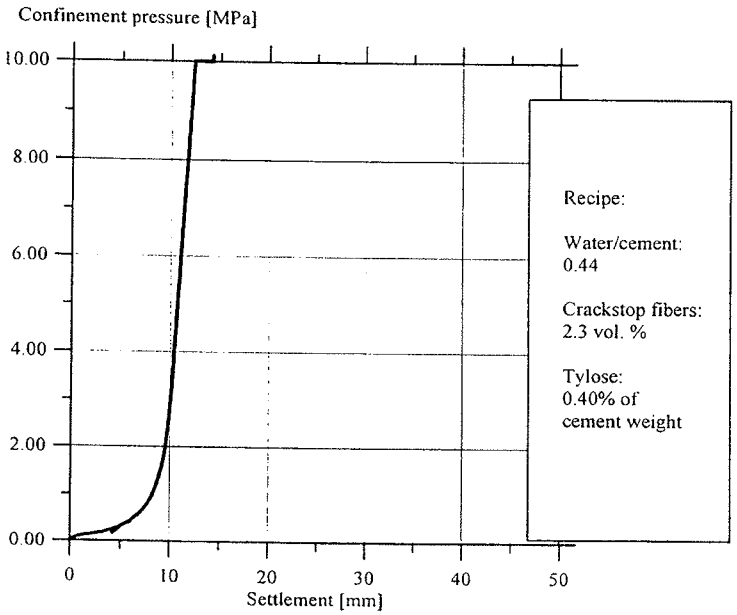

Figure 14

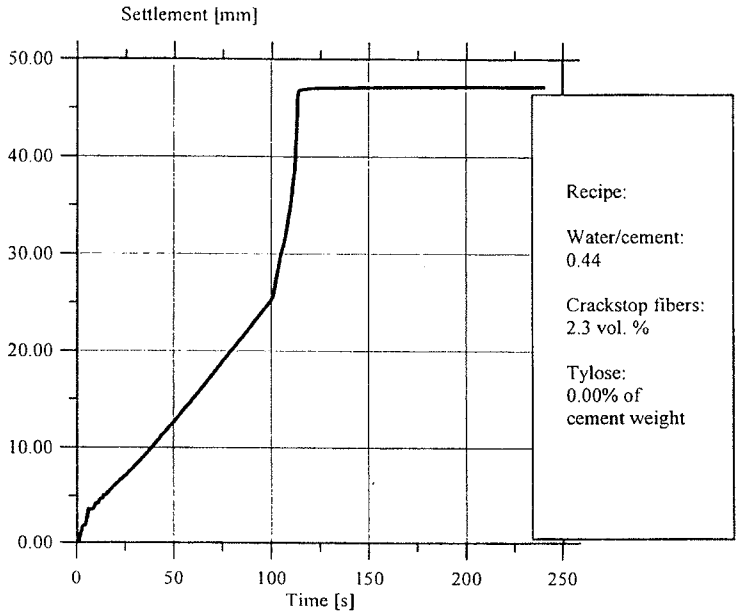

Figure 15

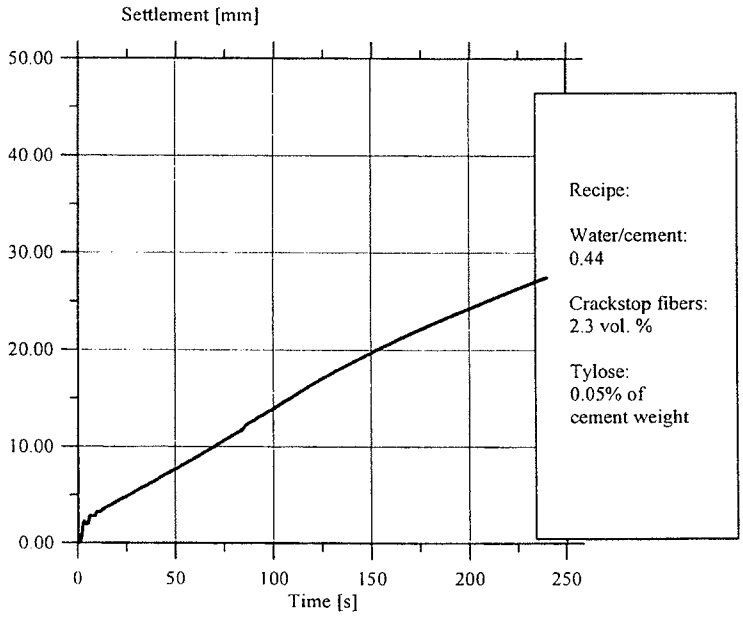

Figure 16

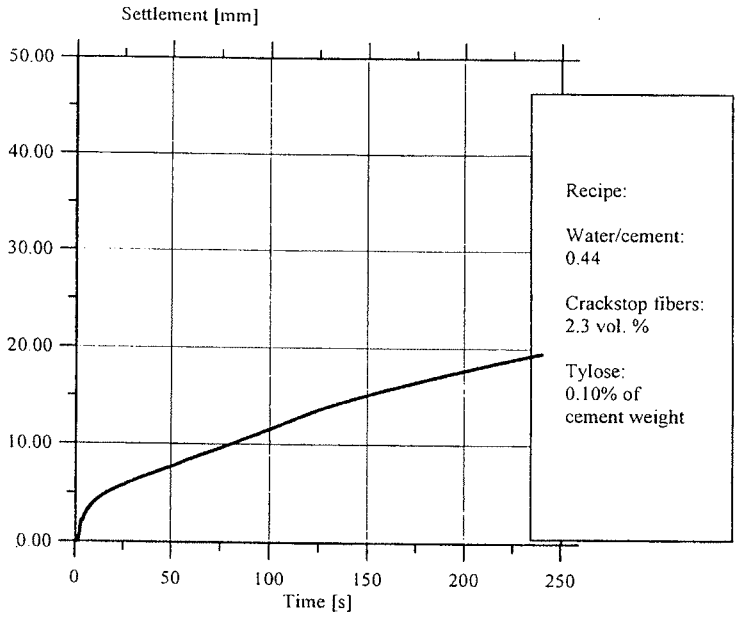

Figure 17

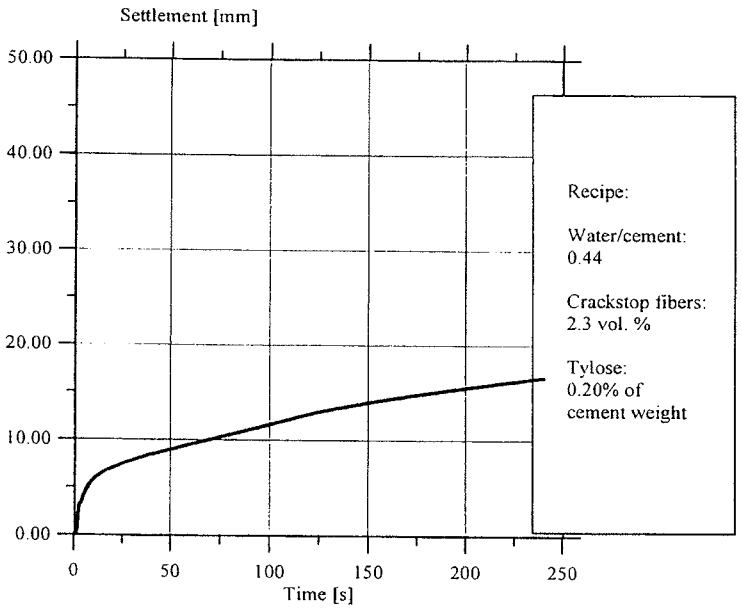

Figure 18

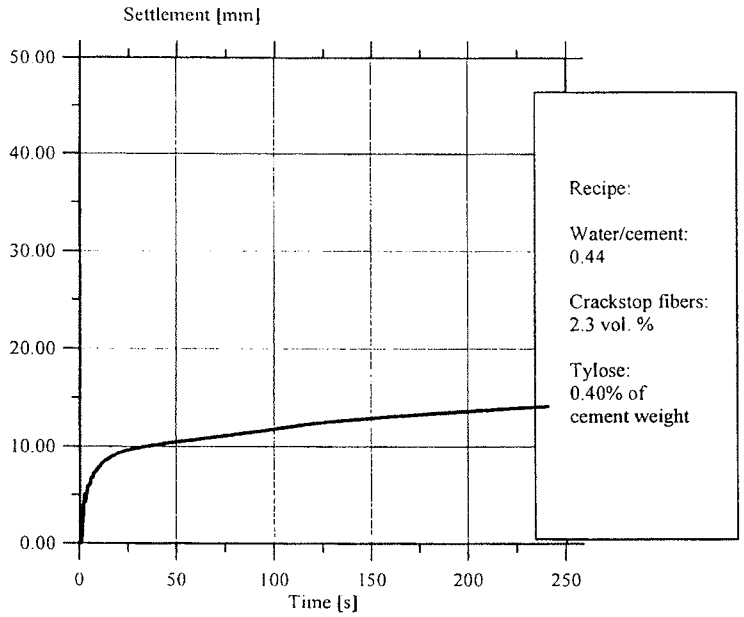
Settlement [mm]
50.00
40.00
30.00
20.00
10.00
0.00
0
50
100
150
200
250
Time [s]
Recipe:
Water/cement:
0.44
Crackstop fibers:
2.3 vol. %
Tylose:
0.40% of
cement weight

Figure 19

BKM REPORT NO. I7

EXTRUDED FIBER REINFORCED PIPES

By Carsten Pedersen[1]

ABSTRACT

The present paper describes a new technique for extrusion of fiber reinforced concrete (FRC). This technique is similar to the traditional extrusion technique but eliminates the problems related to the limitation in the design of mixtures for traditional extrusion. This paper presents the new technology and points out some advantages and possibilities of the process compared to traditional extrusion. In the present study the technique is applied to manufacture FRC pipes with an inner and outer diameter of 100 mm and 120 mm respectively. The mechanical properties of these testspecimens are investigated. The mechanical properties of the test specimens are significantly improved when applying the new technique compared to the properties of poured specimens with the same degree of fiber reinforcement.

INTRODUCTION

One of the advantages of applying the well-known extrusion technique for the processing of cement products is that the material is formed under high shear and high compressive forces. The interface bond between the fiber and the matrix is strengthened. With properly designed dies and controlled material mixes the matrix and fiber packing can be densified to achieve a low porosity. Extrusion is a potential candidate for low-cost commercial products, such as roofing tiles, corrugated sheets, building panels and pipes, see e.g. Shao, Marikunte and Shah(1).
However, the success of traditional extrusion make severe requirements to the mixture, see e.g. Thygesen(2) and Strabo et al.(3). The liquid phase and the cementitious constituents must not separate under application of pressure. When subjected to pressure the mixture must be plastic enough to flow into the die cross section, yet rigid enough to resist deformation after it exits the die. The mixture must not stick to the die and must yield a smooth surface after extrusion. These requirements make severe limitation in the design of mixtures for extrusion.

During the past two years, a new technique for the production of FRC profiles has been in the process of development in Denmark at VTB-beton a/s, the Department of Structural Engineering, Technical University of Denmark and the Institute for Product Development. This manufacturing process is similar to the well-known extrusion technique although the process eliminates the problems related to the limitation in the design of mixtures. Fibers and powder

---

[1] Industrial Ph.D. student, VTB-beton a/s, Dandyvej 11, DK-7100 Vejle, Denmark

material are mixed with an appropriate amounts of water so that cement and fibers are fully homogenized. Water is then drained out by using the new technique, which is based on a simple mechanical operation. Hence the degree of fiber reinforcement is increased and improvement in the bond between fibre and matrix in the hardened composite can be obtained. The driving force which causes dewatering is an applied pressure. By applying pressure the fresh material instantaneously builds up into a stable mass with the required profile.

This paper presents the new technique developed in this research program. We have applied the technique for production of FRC pipes with an inner diameter of 100mm and an outer diameter of 120mm. The extrudates are cut up into test specimens. The test specimens are then subjected to line load and the corresponding values of load and vertical and horizontal deflections are registered. The paper describes the mechanical behaviour observed in terms of load-deflection curves. The paper discusses how the mechanical properties of the extrudates and the output rate of the process are influenced by the content of admixtures for various recipes.

DESCRIPTION OF EXTRUTION PRINCIPLE

The extrusion technique principle developed in this study is illustrated in figure 1. Confinement pressure is applied to the material by the piston. In the draining section the core and the extruder pipe contain pores, so that surplus liquid can pass through and be led away. The confinement pressure causes dewatering of the fresh material in the zone close to the draining section, where the pipe of stable FRC material constitutes a filter which permits only water to pass. The length of the stable FRC pipe is increased as a function of time as the water is squeezed out. To move the stable FRC pipe forwards the core is moved backwards and immediately thereafter the core is moved forwards. When the core is moved backwards, the production pressure on the cross-section of the FRC pipe from the fresh material, combined with the frictional resistance between the FRC pipe and the extruder pipe, exceeds the frictional resistance between the FRC pipe and the core. Therefore the pipe of consolidated material will not be moved backwards with the core. When the core is moved forwards, the production pressure on the cross-section of the FRC pipe from the fresh material, combined with the frictional resistance between the FRC pipe and the core, exceeds the frictional resistance between the FRC pipe and the extruder pipe. Therefore the pipe of consolidated material will be moved forwards with the core. Hence this simple mechanical operation will cause the pipe of consolidated material to move one stroke length forwards. In that way more fresh material will be pressed forwards to the zone near the draining section. The production pressure causes dewatering of this material as described above. By moving the core one stroke length at adequate intervals a pipe of stable material will exit the section in front of the draining section. The procedure of moving the stable material by moving the extruder core as described was invented by H. Fredslund-Hansen[2] in 1994.

---

[2] Formerly at the Department of Structural Engineering, Technical University of Denmark

By applying the production pressure and by moving the core one stroke at adequate intervals the semi-continuous production process has been initiated.

FILLING OF THE EXTRUDER

The plan for the type of extruder used in this investigation is shown in figure 2. Component 018 is the feed pipe, which contains the piston (component 019), which is fitted with a scraper ring (not shown). The fresh premixed material is fed into the feed pipe through a hole (with a diameter of 1.5'') in the centre block (component 021). At the beginning of the filling process the piston is in the bottom position, nearest to the centre block (as shown). Through the hole in the centre block the mixed material is filled into the zone around the core of the extruder (component 020) and into the centre block. The fresh material is stopped near the extrusion head by the retaining pipe (component 026). When the zone around the core has been filled, more material is sucked into the feed pipe while the piston is moved slowly to the top position nearest to the main hydraulic cylinder (component 001). The material is sucked into the feed pipe through the hole in the centre block via a funnel (not shown). When the extruder is full, the funnel is removed and the hole is sealed by means of a plug (component 009).

The filling process described above requires that the mixture is liquid enough to flow into the feed pipe. If the mixture is not liquid enough, the extruder has to be fed from the top of the feed pipe, by the plate (component 029). The main hydraulic cylinder (component 001) is removed and the material is placed in the feed pipe. The hydraulic cylinder is fixed by means of the four screw bolts (component 013). This filling process results in more excess air in the mixture.

After filling the extrusion of a 100mm FRC pipe can begin.

EXTRUSION OF FRC-PIPES

Extrusion of a 100mm FRC pipe is performed according to the following procedure:
The extruder is filled as described above so that the fresh material is enclosed inside the extruder by the retaining pipe. Confinement pressure is applied to the material by the main hydraulic cylinder (component 001). The confinement pressure is named the production pressure. This pressure causes dewatering of the material in the zone close to the draining rings (components 024 and 028). This section is named the draining section. The success of this process depends on the separation of the liquid phase and the cementitious constituents taking place only in this section. The dewatering of the mixture results in a ring of stable material positioned near the draining rings and the retaining pipe. The ring of stable material now constitutes a filter which permits only water to pass. The production pressure causes the length of the ring to increase as a function of time as the water is squeezed out. When the ring of stable material has obtained an adequate length, the retaining plate (component 030) is moved forwards. The retaining pipe and the ring of stable material move forwards with the

plate, forced by the production pressure on the cross-section of the ring. In that way more fresh material will be pressed forwards to the zone near the draining section. The retaining plate is moved this way until the ring of stable material exceeds a length where the frictional resistance on the ring exceeds the force on the cross-section of the ring. In this case the ring of stable material will not move forwards under application of the production pressure. The retaining plate and the retaining pipe are removed. The core is moved backwards and immediately after this forwards. The core is moved with the hydraulic cylinder (component 002). When the core is moved backwards, the production pressure on the cross-section of the ring from the fresh material combined with the frictional resistance between the ring and the extruder pipe (component 017) exceeds the frictional resistance between the ring and the core. Therefore the ring of consolidated material will not be moved backwards with the core. When the core is moved forwards, the production pressure on the cross-section of the ring from the fresh material combined with the frictional resistance between the ring and the core exceeds the frictional resistance between the ring and the extruder pipe. Therefore the ring of consolidated material will be moved forwards with the core. Hence this simple mechanical operation will cause the ring of consolidated material to move one stoke length forwards. In that way more fresh material will be pressed forwards to the zone near the draining section. The production pressure causes dewatering of this material as described above. By moving the core one stroke at adequate intervals a pipe of stable material will exit the section in front of the draining section. This section is named the friction section (components 022 and 025). The stable FRC pipe is cut off when adequate lengths have been obtained.

Throughout this study, the prototype extruder was used to investigate the new manufacturing process. FRC pipes with an inside diameter of 100mm and a wall thickness of 10mm were extruded.

DETERMINATION OF THE LENGHT OF THE FRICTION SECTION

The frictional force at the inside of the pipe of stable material F_i can be obtained by:

$$F_i = \pi d_i l_f \tau \tag{1}$$

where d_i is the inside diameter of the pipe, l_f is the length of the friction section and τ is the frictional resistance between the stable material and the extruder material.
The frictional force at the outside of the pipe of stable material F_y can be obtained by:

$$F_y = \pi d_y l_f \tau \tag{2}$$

where d_y is the outside diameter of the pipe.
The force S caused by the production pressure P on the cross-section of the pipe from the fresh material can be obtained from:

$$S = \frac{\pi}{4}(d_y^2 - d_i^2)P \tag{3}$$

When the core is moved forwards, the force caused by the production pressure on the cross-

section of the pipe from the fresh material combined with the frictional resistance between the pipe and the core has to exceed the frictional resistance between the ring and the extruder pipe:

$$S + F_i > F_y \tag{4}$$

The frictional resistance between the pipe and the core combined with the frictional resistance between the pipe and the extruder pipe has to exceed the force caused by the production pressure of the fresh material on the cross-section of the pipe:

$$F_i + F_y \geq S \tag{5}$$

Given d_i, d_y, P and τ, equations (1)-(5) determine the possible range of l_f:

$$\frac{P}{4\tau}(d_y - d_i) \leq l_f < \frac{P}{4\tau}(d_y + d_i) \tag{6}$$

Preliminary results indicate that τ is approx. 0.20 MPa for the production pressure used in this study. See Pedersen(4). For the extruder used in this investigation (d_y = 120mm, d_i = 100mm) equation (6) gives the minimum value l_f = 125mm for the production pressure P = 5MPa.

MATRIX

The basic powder material was ordinary Danish rapid-hardening Portland cement (RC, grain density: γ_k = 3.15, median particle size: $d_{50/50}$ ~ 14 μm). This cement was combined with five different types of material: Silica powder (Elkem Silica: ES, γ_k = 2.17, $d_{50/50}$ ~ 1-5 μm), Silica fume (SI, Elkem silica slurry, W/SI = 1.0, γ_k = 2.17, $d_{50/50}$ ~ 1 μm), quartz powder(QP, γ_k = 2.62, $d_{50/50}$ ~ 24 μm), quartz sand (QS, γ_k = 2.62, $d_{50/50}$ ~ 180 μm) and ordinary Danish fly ash (FA, γ_k = 2.20, $d_{50/50}$ ~ 50 μm)

In the present study methylhydroxyethylcellulose (MHEC) is used to increase the viscosity of the mixing water. The MHEC used in this study is produced by the German company Hoechst under the name Tylose FL15002, see ref(5). Tylose was also used by Thygesen(2) and Strabo et al.(3), who worked with traditional extrusion of fiber reinforced concrete.

The content of Tylose FL15002 was based on tests aimed at optimizing the amount of Tylose in the actual mix. The Tylose-water-ratio by weight was typically: 0.20 - 0.53%.

FIBERS

The fibers used were polypropylene Crack-Stop fibers, polypropylene Krenit fibers and pitch-based carbon fibers. The polypropylene fibers are produced in Denmark by Cemfiber, see references(6) and (7). The polypropylene Krenit fibers were of a special type, with improved bonding. The carbon fibers are produced in Japan by Kureha, see ref(8). The properties of the fibers are listed in Table 1.

TESTING FRC PIPES

Some of the extrudates were sealed with plastic aluminum foil until the time of testing (20^0C). Other extrudates were sealed with plastic aluminum foil for 24 hours and immersed in water (20^0C) for further curing until the time of testing. These two different curing systems gave no significant difference in the material properties of the hardened pipes.

After hardening, each extrudate was cut into test specimens by means of a rotating diamond cutter. The inner and outer diameters of all specimens were 100 and 120mm respectively and their length was 30mm.

The specimens were subjected to line load at a cross-head speed of 0.1mm/sec. All tests were carried out in a 10 kN Instron closed-loop testing machine (type: 6022). Corresponding values of line load and vertical and horizontal deflections were registered until a total vertical deflection of 8mm was reached. The deflections were measured on the interior of the specimens, using special fittings and two transducers. The fittings were attached directly to the inside of the specimens. The vertical deflection must be measured this way in order to make sure that the true load-deflection curve is obtained, eliminating any imperfect contact between the specimens and the loading fixture.

The complete testing arrangement is shown in figure 3.

MECHANICAL PROPERTIES

In this section the experimentally determined load-deflection curves are compared with predicted load-deflection curves for poured specimens with the same type and degree of fiber reinforcement as the extrudates. The prediction of the load-deflection curves for the poured specimens are based on the stress-crack width relationship. The stress-crack width relationships for the poured material are determined by the model prediction, and the stress-crack width expression to be adopted in the model for prediction of load-deflection curves for poured specimens are then determined by fitting. The load-deflection curves are predicted by using a semi-analytical model presented in previous work(9). This model is based on the fictious crack model (FCM) by using fit for the softening curve of concrete as proposed by Stang and Aarre(10). It is assumed that four cracks develop in the pipe cross-section. Independently of pipe geometry and degree of fibre reinforcement very good agreement has been observed between the model prediction and the experimental data. See Pedersen(9) for full details. The stress-crack width relationships for the poured material are predicted by using an analytical model developed by Stang, Li and Krenchel(11). This model takes into account a series of micromechanical parameters to determine the fiber bridging stress. In the present study the interfacial frictional resistance, the snubbing coefficient and the Cook-Gordon parameter (length of fibre-matrix debonded zone) were fixed in accordance with ref(11). A snubbing coefficient of 0.05, Cook-Gordon parameters of 0.72mm and 0.27mm for Krenit fibres and Crack-Stop fibers, respectively and interfacial frictional resistances of 0.8 MPa and

0.4 MPa for Krenit fibres and Crack-Stop fibers, respectively have been used in the present study. The aggregate bridging stress is expressed as a function which fits a wide range of experimental data very well. In the present study a tensile strength of 3MPa, a characteristic crack opening of 0.02mm and a shape factor of 1.0 are used in the function for describtion of the aggregate bridging stress. All parameters are in accordance with ref(11), which is based on previous experience. See ref(11) for full details.

In figures 4 and 5 the experimentally determined curves are shown for mixtures of cement paste containing 0.5 vol. % of 3mm Crack-Stop fibers combined with 2.0 and 3.0 vol. % of 3mm Krenit fibers respectively. This results in approx. 0.75 vol. % of Crack-Stop fibers combined with approx. 3.0 or 4.5 vol. % of Krenit fibers in the extruded material. Figures 4 and 5 also show the theoretical load-deflection curves predicted for poured specimens with the same type and degree of fiber reinforcement as the extrudates (i.e. 0.75 vol. % of Crack-Stop fibers combined with 3.0 and 4.5 vol. % of Krenit fibers respectively). Furthermore, figures 4 and 5 also show the predicted load-deflection curves, assuming improved bonding (x3) between fiber and matrix.

Figure 6 shows the predicted stress-crack width relationships together with the curves, assuming improved bonding (x3). Furthermore, figure 6 show the fitted curves (thin lines) together with the material constants related to the pre-peak behavior of the material (characteristic crack opening w_0 and shape factor p) to be adopted in the model for prediction of load-deflection behavior of poured specimens.

These test results indicate that the mechanical properties are significantly improved by application of the extrusion process. The improvement of properties is caused by lower porosity and by improved bonding between matrix and fibers. A similar conclusion was made by Krenchel and Hansen(12), who worked with Krenit fiber reinforced plate material produced by means of the Magnani process, and by Shao et al.(1), who worked with traditional extrusion of FRC profiles.

Figures 7 and 8 show the experimentally determined curves for mixtures containing 0.5 vol. % of 3mm Crack-Stop fibers combined with 1.0 and 2.0 vol. % of 3mm Krenit fibers respectively. This results in approx. 0.75 vol. % of Crack-Stop fibers combined with approx. 1.5 or 3.0 vol. % of Krenit fibers in the extruded material. The matrix contains 70 weight-% of cement combined with 10 weight-% of quartz sand and 20 weight-% of quartz powder (RC-QS-QP:70-10-20).

It is observed that a peak load of 5.8-16.3 kN/m is obtained, corresponding to 5.8-17.1 MPa of ultimate bending strength although only 3mm fibers have been used as reinforcement in this study. Krenchel and Hansen(12) measured a bending strength of 20.5 MPa and Shao et al.(1) measured a bending strength of 28 MPa for material reinforced with 4 vol. % of polypropylen fibers and 4 vol. % of polyvinyl alcohol fibers respectively. Therefore higher strength can be obtained by optimizing the material composition and the design of the extruder.

RESULTS AND DISCUSSION

A total of 26 extrusion tests were performed to cover this program. Information of test date, recipe, water-powder-ratio by weight, Tylose-water-ratio by weight, production pressure, type of fibre and fibre volume concentration are summarized in Tables 2 and 3.
The results of the unsuccessful and the successful extrusion tests are shown in Tables 2 and 3 respectively.

Observations indicate that soft, fine fibers constitute a filter, which permits only water to pass the draining section. Throughout this study, soft 3mm Crack-Stop fibers were used as "process fibers". Measurements indicate that less than 1% cement is lost during the dewatering of cement paste containing more than 0.4 vol. % Crack-Stop fibers.

Tylose was used for adjusting the viscosity of the mixing water. The speed of the dewatering process is decreased as a function of the viscosity. By adjusting the content of tylose an appropriate output rate is determined. Based on Darcy's law a simple model for the dewatering process has been presented in previous work. Based on some simple tests the model predicts the output rate of the extrusion process. See Pedersen(13) for full details. Table 3 lists the predicted output rates along with the output rates observed from the full-scale extrusion tests. Good agreement is obtained. However, much more research is needed to confirm the model prediction.

No mixtures containing carbon fibres have been successfully extruded in this study. A matrix containing only 1/4 vol. % of 3mm carbon fibres combined with 2 vol. % of Crack-Stop fibres was not extrudable (Table 2, 190396) although the same matrix containing only 2 vol % Crack-Stop fibres was extrudable (Table 3, 110196 and 130396). The test results indicate that the use of carbon fibres causes inappropriate separation of the liquid phase and the cementitious constituents under the applied pressure. Observations made during the tests indicate that the separation is initiated in the zone where the feed pipe is connected with the centre block. At this connecting point the cross-sectional area is decreased to approx. 30%. Observations indicate that fibers are caught in this section and that the separation is probably caused by the stiffness of the carbon fibre system.
When using high concentrations of Krenit fibres a similar separation effect is observed. A plain cement matrix containing 4 vol. % of 3mm carbon fibres in combined with 1/2 vol. % of Crack-Stop fibres was not extrudable (Table 2, 020496) although the same matrix containing 3 vol. % of Krenit fibres combined with 1/2 vol. % Crack-Stop fibres was extrudable (Table 3, 010496). A matrix consisting of RC/QS/QP = 70/10/20(weight %) with 3 vol. % of 3mm Krenit fibres combined with 1/2 vol. % of Crack-Stop fibres was not extrudable (Table 2, 150496) although the same matrix containing 2 vol. % Krenit fibres combined with 1/2 vol. % of Crack-Stop fibres was extrudable (Table 3, 110496 and 180496). The failed attempt to extrude mixtures containing high volume concentrations of Krenit fibres is caused by the stiffness of the fiber system as described above and by the fact that the fibers constitut a draining system which causes separation not only in the draining section. When

using long fibres a similar separation effect is observed. A plain cement matrix containing 2 vol. % of 6mm Krenit fibres combined with 1/2 vol. % of 3mm Crack-Stop fibres was not extrudable (Table 2, 250396) although the same matrix containing 2 vol. % of 3mm Krenit fibres combined with 1/2 vol. % of 3mm Crack-Stop fibres was extrudable (Table 3, 270396).

CONCLUSION

Based on the work described here the following conclusion can be drawn:

A new extrusion process has been presented. Powder material and fibers are mixed with an adequate amount of water of water. As an effect of the dewatering caused by application of pressure, the material builds up into a stable mass with the required profile. Therefore the process eliminates the problems related to the limitation in design of mixtures for traditional extrusion. As with traditional extrusion the mechanical properties of the extrudates are improved by application of the process.
Inappropriate separation of the liquid phase and the powder material has been observed when using mixtures containing carbon fibers or high concentration of polypropylene fibers. More work is needed to investigate how this separation effect is influenced by the mixture and by the design of the extruder.

The dewatering process is significantly influenced by the viscosity of the mixing water. The speed of the process is decreases as the viscosity increases. Therefore, the addition of agents is a key parameter to achieving a suitable output rate of the process.
The highest output rate observed in this study was 4 meters/hour. In industrial application of the extrusion process higher output rates can be obtained through integrated optimization of material and extruder.

ACKNOWLEDGEMENTS

The work presented in this paper has been carried out at the Department of Structural Engineering (ABK), Technical University of Denmark.
Carsten Pedersen's work has been carried out as an Industrial Research Study, Ph.D. supported by grants from the Danish Academy of Technical Sciences (ATV), VTB-beton a/s, Eurotest aps and the Institute for Product Development (IPU). The study is supervised by Dr. Henrik Stang (ABK), Manager Jens Peter Andreasen (VTB), Manager Poul Rasmussen (Eurotest) and M.Sc. Johan Christian Gregersen (IPU), whom Carsten Pedersen thanks for their inspiring instruction.
The author want to thank the staff at the Department of Structural Engineering for their help during the work.

REFERENCES

1. Shao, Y., Marikunte, S., and Shah, S.P. Extruded Fiber Reinforced Composites.

Concrete International, April 1995.

2. Thygesen, E. Design of FRC-materials in structures. Ph.D. thesis, Department of Structural Engineering, Technical University of Denmark, 1993. In Danish.

3. Strabo, F., Clauson-Kaas, N.F., Just Andersen, P. and Thaulow, N. Extrusion of Fiber reinforced Concrete. Technological Institute, Denmark. 1987. In Danish.

4. Pedersen, C. Notat vedr. forsøg med ABK-ekstruder med bevægelig kerne. Department of Structural Engineering, Technical University of Denmark, 1994. In Danish.

5. Tylose. Hoechst Limited Company, D-6230 Frankfurt am Main 80. 1995. In German.

6. Specification paper. Crack-Stop fibers. Cemfiber A/S, DK-8800 Varde, Denmark. November 1994.

7. Specification paper. Krenit fibers. Cemfiber A/S, DK-8800 Varde, Denmark. November 1994.

8. Akihama, S., Suenaga, T., and Tadashi, B. Mechanical Properties of Carbon Fiber Reinforced Cement Composite and The Application to Large Domes. Kajima Institute of Construction Technology. July, 1984.

9. Pedersen, C. Calculation of FRC pipes based on the fictitious crack model. Department of Structural Engineering, Technical University of Denmark, 1995.

10. Stang, H., and Aarre, T. Evaluation of Crack Width in FRC with Conventional Reinforcement. 'Cem. Concr. Comp.', 14, 143-154, (1992).

11. Stang, H., Li, V.C. and Krenchel, H. Design and Structural Applications of Stress-Crack Width Relations in Fiber Reinforced Concrete. 1993. Accepted for publication Mat and Struc.

12. Krenchel, H., and Hansen, S. New Recipes and New Production Techniques For High Performance FRC-Materials. Rilem Proceedings 15, 65-83. E & FN Spon, 1991.

13. Pedersen, C. New Production Technique and Recipes For FRC Materials. Department of Structural Engineering, Technical University of Denmark, 1996.

NOTATION

The following symbols are used in this paper

d_i	inside pipe diameter
d_y	outside pipe diameter
F_i	frictional force at the inside of the pipe of stable material
F_y	frictional force at the outside of the pipe of stable material
l_f	lenght of the friction section
p	shape factor
P	production pressure
S	force caused by the production pressure on the cross-section of the pipe
w	crack mouth opening
w_0	characteristic crack mouth opening
τ	frictional resistance

TABLE CAPTIONS

Table 1 Properties of fibers

Table 2 Unsuccessful extrusion tests

Table 3 Successful extrusion tests

FIGURE CAPTIONS

Figure 1 Plan for the extrusion principle developed in this study

Figure 2 Plan for the type of extruder used in this investigation

Figure 3 Testing arrangement

Figure 4 Load-deflection curves. Extruded FRC pipes. Mixtures of cement paste containing approx. 0.75 vol. % of 3mm Crack-Stop fibers combined with approx. 3.0 vol. % of 3mm Krenit fibers

Figure 5 Load-deflection curves. Extruded FRC pipes. Mixtures of cement paste containing approx. 0.75 vol. % of 3mm Crack-Stop fibers combined with approx. 4.5 vol. % of 3mm Krenit fibers

Figure 6 Predicted stress-crack width relationships together with the fitted curves (thin lines) to be used in the model for prediction of the load-deflection behavior of poured specimens

Figure 7 Load-deflection curves. Extruded FRC pipes. Mixtures of RC-QS-QP:70-10-20 containing approx. 0.75 vol. % of 3mm Crack-Stop fibers combined with approx. 1.5 vol. % of 3mm Krenit fibers

Figure 8 Load-deflection curves. Extruded FRC pipes. Mixtures of RC-QS-QP:70-10-20 containing approx. 0.75 vol. % of 3mm Crack-Stop fibers combined with approx. 3.0 vol. % of 3mm Krenit fibers

Table 1

Fibre	L_f[mm]	d_f[µm]	γ_f[kg/l]	E_f[GPa]
Krenit extra fine, WEFF(quality:special)	3,6	40x100[a)]	1.01	12
Crack-stop	3,6	18	0.91	4
Carbon	3,6	14.5	1.63	38

a):rectangular cross-section

Table 2

Date	RC/QS/QP/ES/SI/FA (weight-%)	Water/powder	Tylose/water (%)	p (MPa)	Fibers (vol-%)
291195[3]	100/0/0/0/0/0	0.45	0.67	5	Crack-stop(3mm):1.9
201295[3]	100/0/0/0/0/0	0.33	0.00	5	Crack-stop(3mm):2.2
100196[3]	100/0/0/0/0/0	0.45	0.00	5	Crack-stop(3mm):1.9
240196[3]	64/0/12/12/0/12	0.49	0.11	3.5	Crack-stop(3mm):2.5, Krenit(6mm):2.3
250196[3]	64/0/12/12/0/12	0.48	0.22	3.5	Crack-stop(3mm):2.0, Krenit(3mm):1.0
160296[3]	76/0/8/0/16/0	0.60	0.04	10	Crack-stop(6mm):1.8, Carbon(6mm):1.3
210296[3]	76/0/8/0/16/0	0.51	0.08	10	Crack-stop(6mm):2.0, Carbon(6mm):1.5
270296[3]	76/0/8/0/16/0	0.60	0.08	15	Crack-stop(6mm):1.8, Carbon(6mm):1.3
060396[3]	76/0/8/0/16/0	0.71	0.08	15	Crack-stop(6mm):1.6, Carbon(6mm):1.2
070396[3]	100/0/0/0/0/0	0.41	0.24	5	Crack-stop(3mm):1.0, Carbon(3mm):1.0
190396[3]	100/0/0/0/0/0	0.41	0.24	5	Crack-stop(3mm):2.0, Carbon(3mm):0.25
250396[4]	100/0/0/0/0/0	0.56	0.48	15	Crack-stop(3mm):0.5, Krenit(6mm):2.0
020496[3]	100/0/0/0/0/0	0.54	0.50	5	Crack-stop(3mm):0.5, Krenit(3mm):4.0
150496[3]	70/10/20/0/0/0	0.4	0.25	5	Crack-stop(3mm):0.5, Krenit(3mm):3.0

[3]Dewatering inside the centre block and/or inside the feed pipe

[4]The fibers were not dispersed satisfactorly

Table 3.

Date	RC/QS/QP/ES/SI/FA (weight-%)	Water/powder	Tylose/water (%)	p (MPa)	Fibers (vol-%)	Output rate	Predicted output rate[5]
211295	100/0/0/0/0/0	0.45	0.67	3.5	Crack-stop(3mm):1.9	11mm/3 min.	11mm/4.5 min.
110196	100/0/0/0/0/0	0.41	0.24	5	Crack-stop(3mm):2.0	11mm/40 sec.	11mm/58 sec.
130396	100/0/0/0/0/0	0.41	0.24	5	Crack-stop(3mm):2.0	11mm/60 sec.	11mm/58 sec.
210396	100/0/0/0/0/0	0.41	0.24	5	Krenit(3mm):2.0	11mm/60 sec.	no prediction
270396	100/0/0/0/0/0	0.41	0.48	5	Crack-stop(3mm):0.5 Krenit(3mm):2.0	7mm/60 sec.	no prediction
010496	100/0/0/0/0/0	0.54	0.50	5 15	Crack-stop(3mm):0.5 Krenit(3mm):3.0	5mm/60 sec. 5mm/30 sec.	no prediction no prediction
110496	70/10/20/0/0/0	0.40	0.25	5 14	Crack-stop(3mm):0.5 Krenit(3mm):2.0	6mm/30 sec. 11mm/30 sec.	no prediction no prediction
160496	70/10/20/0/0/0	0.40	0.25	5 14	Crack-stop(3mm):0.5 Krenit(3mm):1.0	11mm/30 sec. 11mm/10 sec.	no prediction no prediction
180496	70/10/20/0/0/0	0.40	0.25	14	Crack-stop(3mm):0.5 Krenit(3mm):2.0	11mm/10 sec.	no prediction

[5]See Pedersen(13) for full details

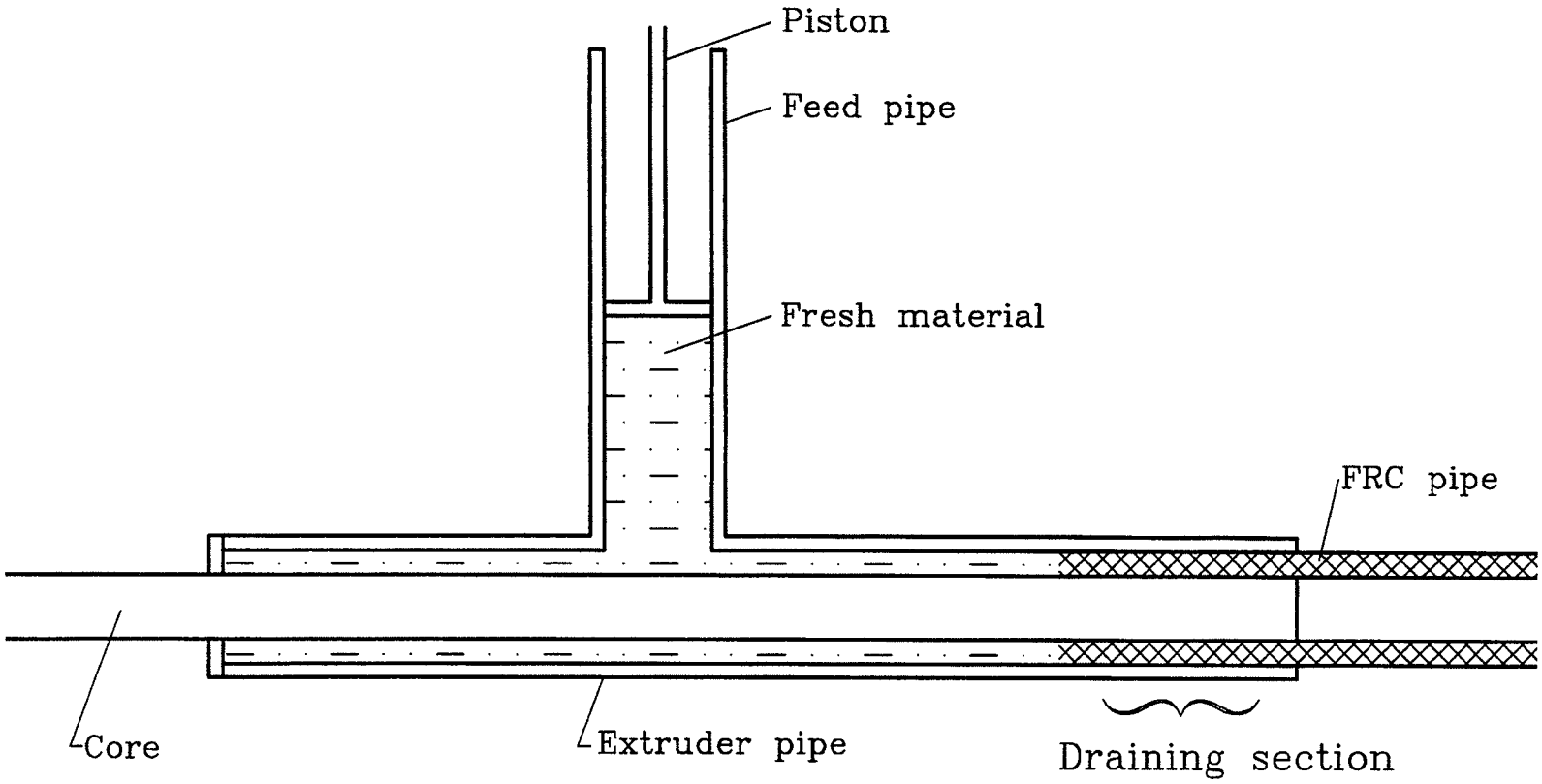
Piston
Feed pipe
Fresh material
FRC pipe
Core
Extruder pipe
Draining section

Figure 1

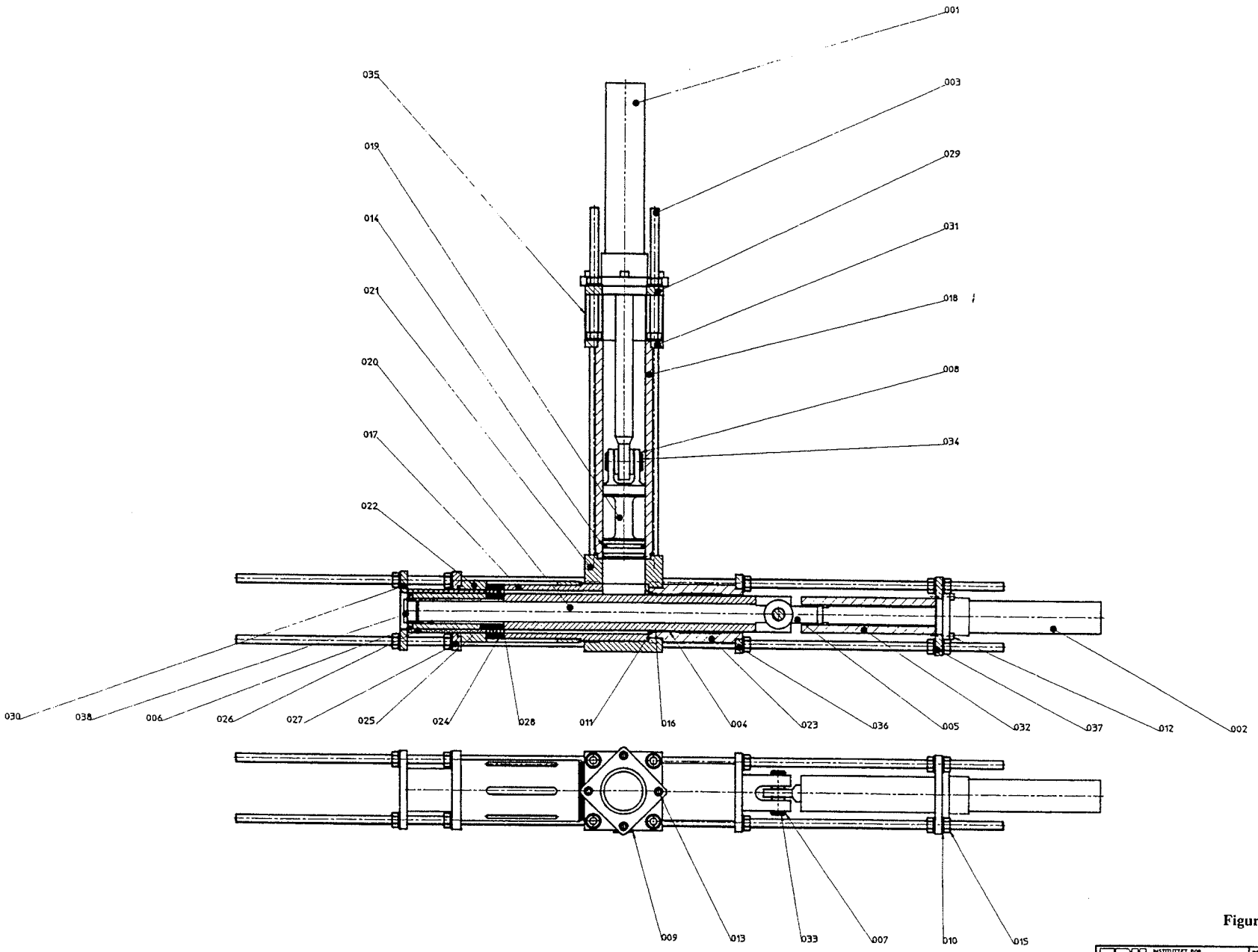

Figure 2

INSTITUTTET FOR PRODUKTUDVIKLING DTH, Bygning 423 2800 Lyngby. 45934411 Telefax 42882325		Mål 1:5	Dato/sign Sep 29 94/lm
Rekvirent VTB beton A/S		Titel Betonextruder	
Projekt Beton II		Tegn.nr. 10018872	Blad nr./ant. 1/1

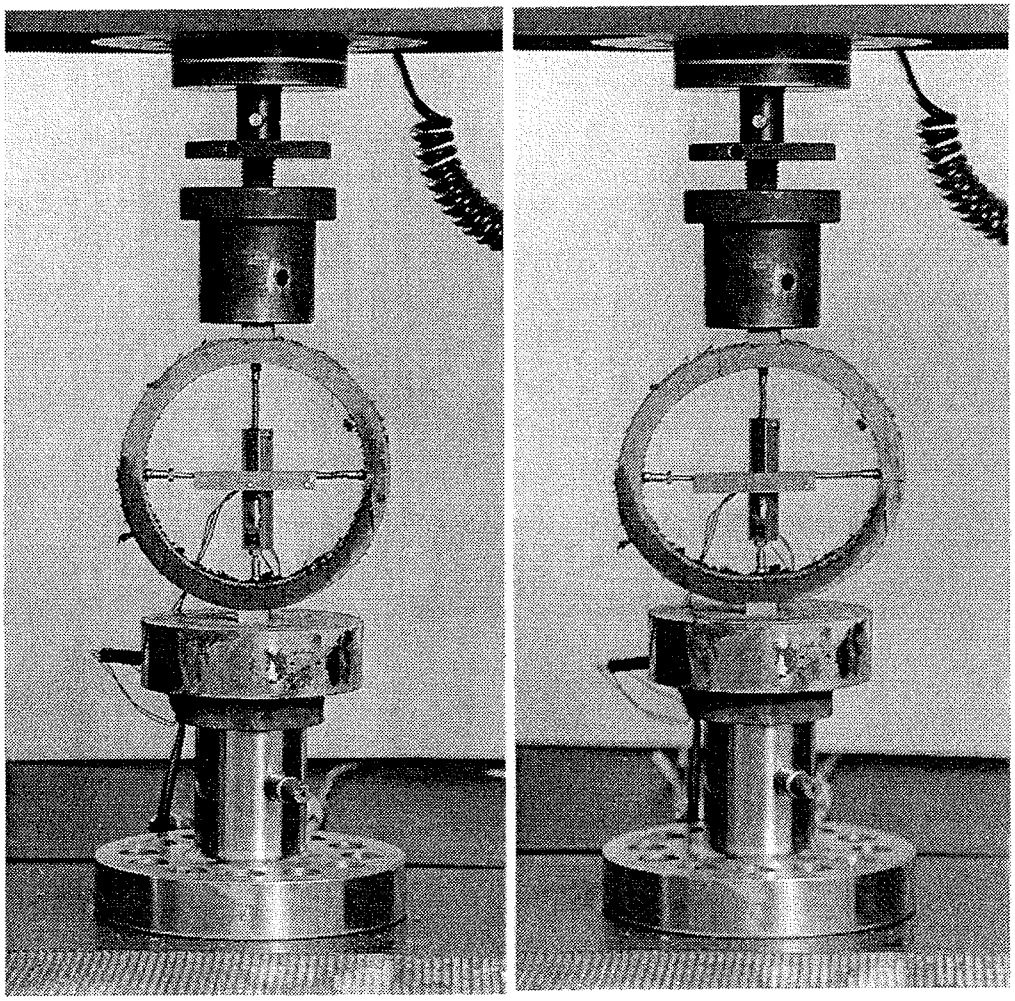

Figure 3

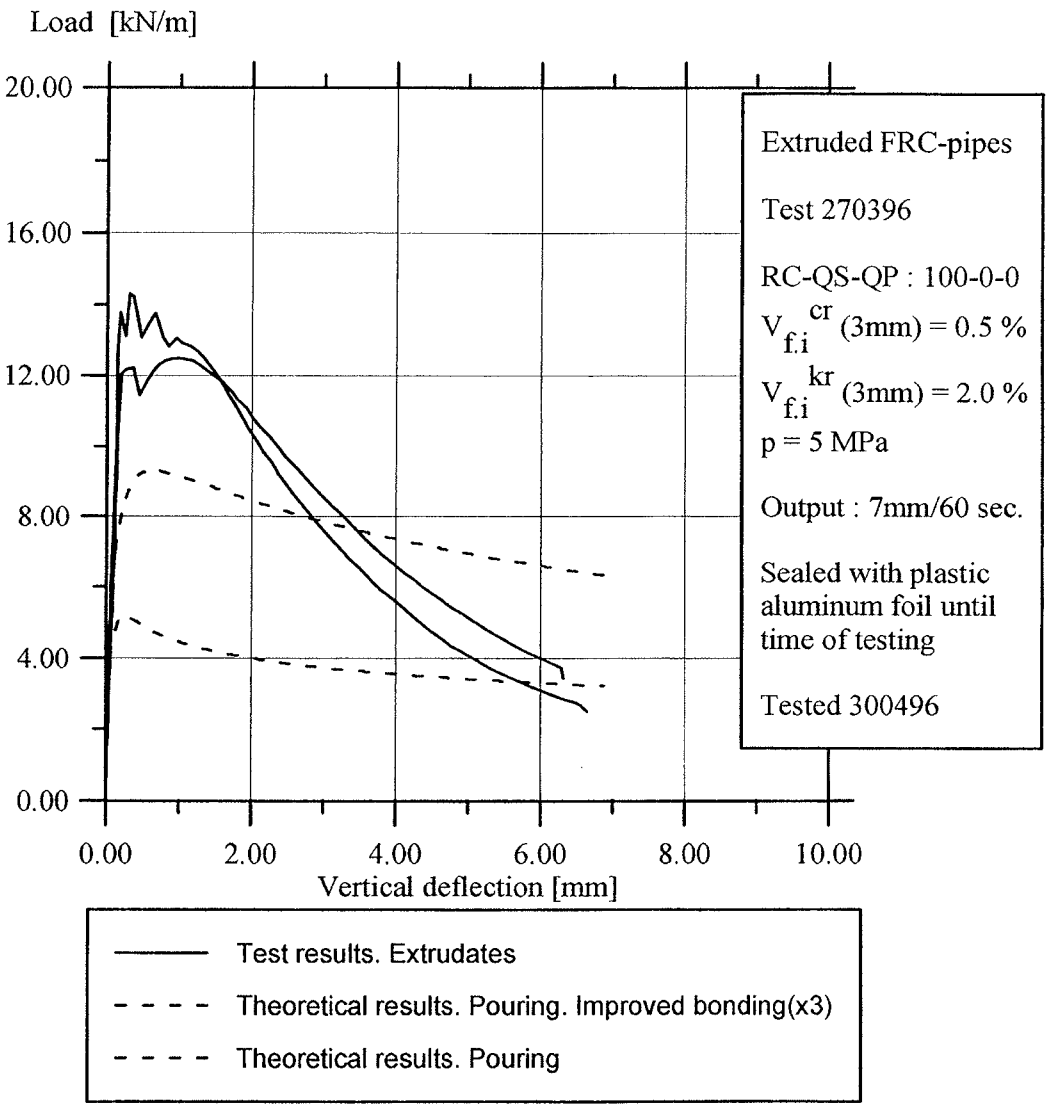
Load [kN/m]
20.00
16.00
12.00
8.00
4.00
0.00
0.00
2.00
4.00
6.00
8.00
10.00
Vertical deflection [mm]
Extruded FRC-pipes
Test 270396
RC-QS-QP : 100-0-0
$V_{f.i}^{cr}$ (3mm) = 0.5 %
$V_{f.i}^{kr}$ (3mm) = 2.0 %
p = 5 MPa
Output : 7mm/60 sec.
Sealed with plastic aluminum foil until time of testing
Tested 300496
Test results. Extrudates
Theoretical results. Pouring. Improved bonding(x3)
Theoretical results. Pouring

Figure 4

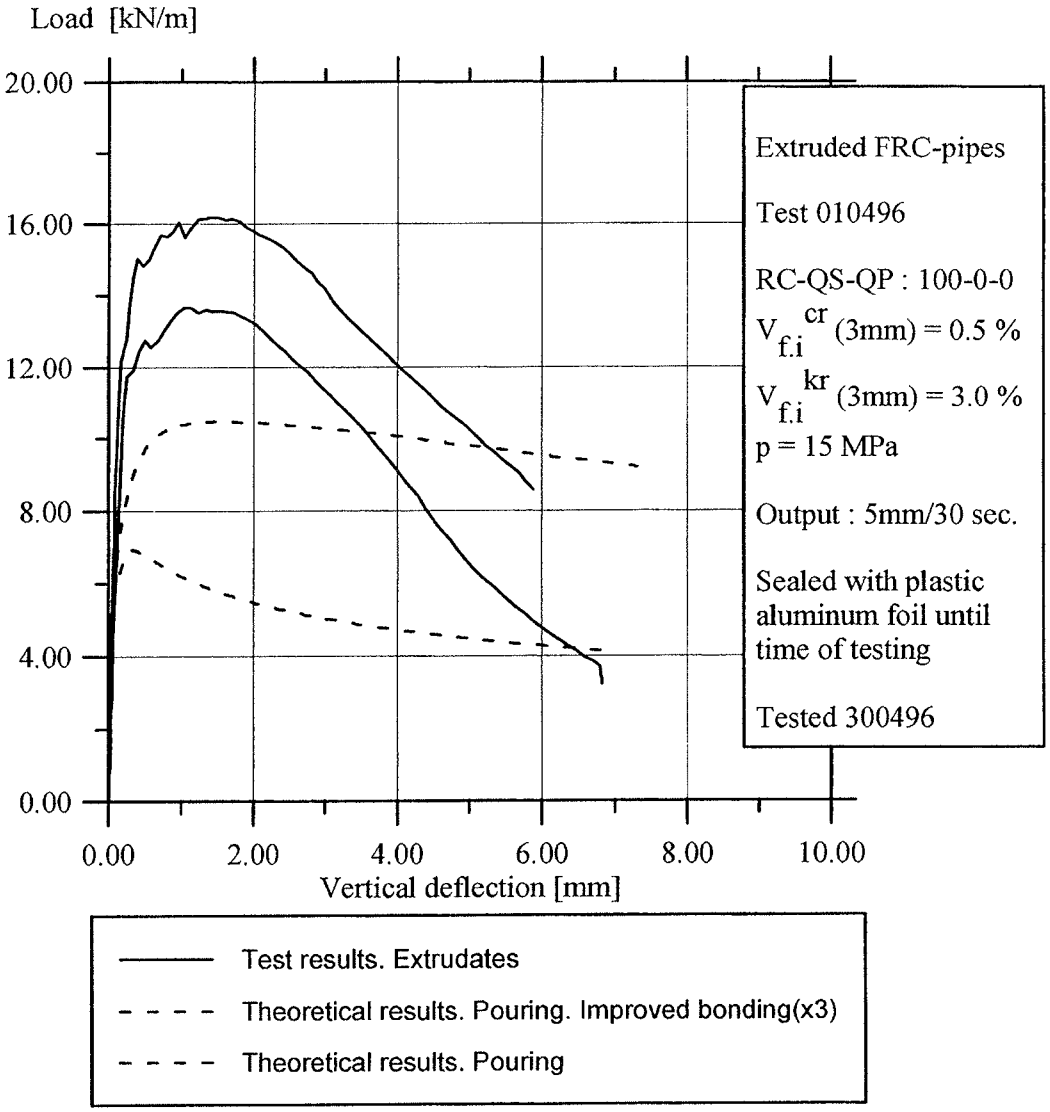
Load [kN/m]
20.00
16.00
12.00
8.00
4.00
0.00
0.00
2.00
4.00
6.00
8.00
10.00
Vertical deflection [mm]
Extruded FRC-pipes
Test 010496
RC-QS-QP : 100-0-0
$V_{f.i}^{cr}$ (3mm) = 0.5 %
$V_{f.i}^{kr}$ (3mm) = 3.0 %
p = 15 MPa
Output : 5mm/30 sec.
Sealed with plastic aluminum foil until time of testing
Tested 300496
Test results. Extrudates
Theoretical results. Pouring. Improved bonding(x3)
Theoretical results. Pouring

Figure 5

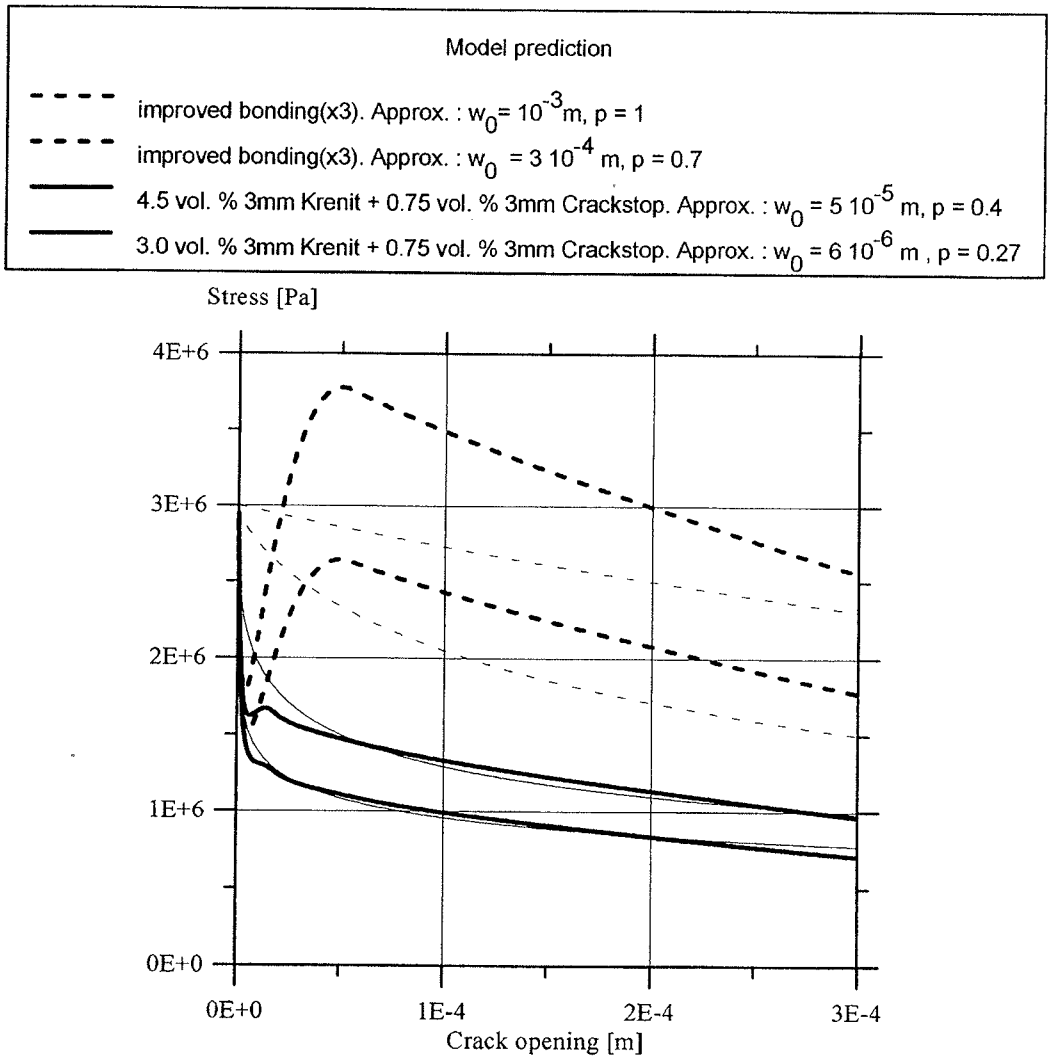
Model prediction
improved bonding(x3). Approx. : $w_0 = 10^{-3}$ m, p = 1
improved bonding(x3). Approx. : $w_0 = 3\ 10^{-4}$ m, p = 0.7
4.5 vol. % 3mm Krenit + 0.75 vol. % 3mm Crackstop. Approx. : $w_0 = 5\ 10^{-5}$ m, p = 0.4
3.0 vol. % 3mm Krenit + 0.75 vol. % 3mm Crackstop. Approx. : $w_0 = 6\ 10^{-6}$ m , p = 0.27
Stress [Pa]
4E+6
3E+6
2E+6
1E+6
0E+0
0E+0
1E-4
2E-4
3E-4
Crack opening [m]

Figure 6

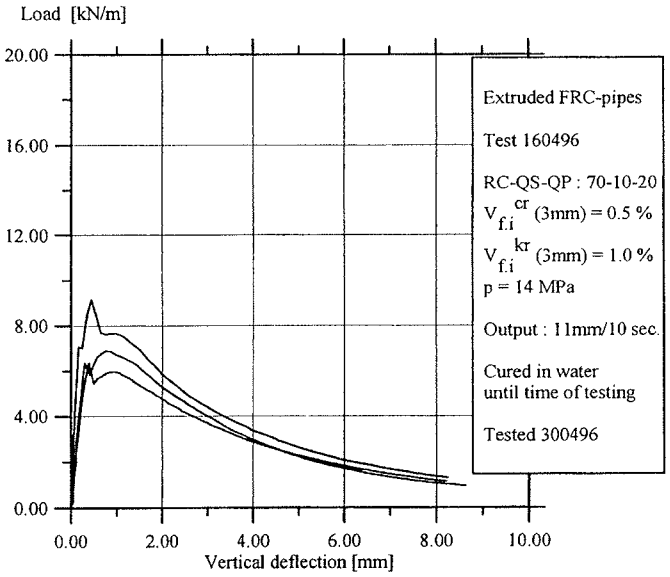

Figure 7

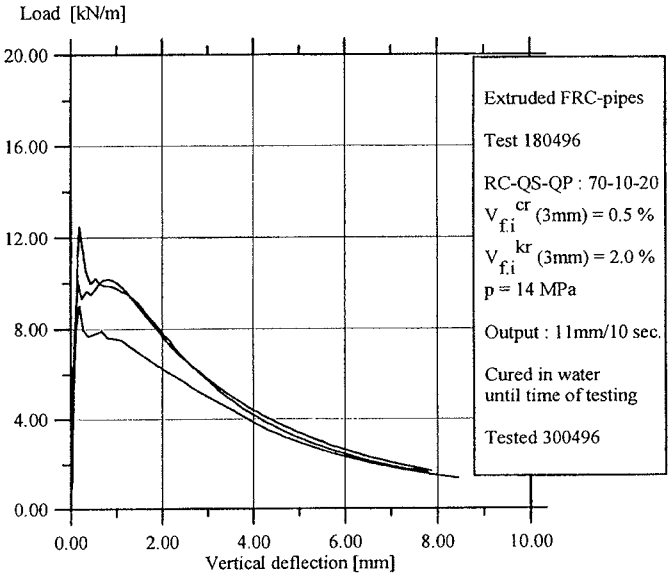

Figure 8